The Pennsylvania State University

The Graduate School

Department of Mechanical and Nuclear Engineering

IMPACT OF ADAPTIVE CRUISE CONTROL ON THE FORMATION OF SELF-ORGANIZED TRAFFIC JAMS ON HIGHWAYS

A Thesis in

Mechanical Engineering

by

Kshitij Jerath

Submitted in Partial Fulfillment

of the Requirements

for the Degree of

Master of Science

May 2010

The thesis of Kshitij Jerath was reviewed and approved* by the following:

Sean N. Brennan
Assistant Professor of Mechanical Engineering
Thesis Advisor

Asok Ray
Distinguished Professor of Mechanical Engineering

Karen A. Thole
Professor of Mechanical Engineering
Department Head of Mechanical and Nuclear Engineering

*Signatures are on file in the Graduate School

ABSTRACT

This thesis describes the analysis of a potential control mechanism for self-organizing systems by studying the specific problem of self-organizing traffic jams. Self-organizing traffic jams are known to occur in medium-to-high density traffic flows. Various techniques for modeling traffic flow are discussed and their advantages and limitations are considered. The master equation approach is selected for developing a model that describes the self-organizing behavior of traffic flow at a mesoscopic scale. The master equation approach is further developed to incorporate driver (or agent) behavior. Control of the self-organizing system is presented via introduction of similar agents with slightly varying interaction properties. The introduction of such agents into a self-organizing system is considered to be analogous to the introduction of vehicles with adaptive cruise control (ACC) into traffic flow. The behavior for both human-driven and ACC vehicles is modeled using the same driver model but with slightly different model parameters. It is found that introduction of a small percentage of agents with slightly different interaction behavior has the potential to affect the dynamics of the self-organizing system. Specifically, it is found that while introduction of ACC vehicles into traffic may enable higher traffic flows, it also results in disproportionately higher susceptibility of the traffic flow to congestion.

Table of Contents

LIST OF FIGURES

ACKNOWLEDGEMENTS

I am grateful to my advisor, Dr. Sean Brennan, for providing me with the opportunity and requisite intellectual freedom to pursue my research. I would also like thank him for pushing me in the right direction when I appeared to be all but lost in my endeavors. I am also grateful to all my colleagues and lab mates, especially Pramod and Sittikorn, for listening to my theories and explanations when I needed someone to provide an unprejudiced perspective to the problem at hand. I would like to thank the Department of Mechanical and Nuclear Engineering, the Thomas D. Larson Transportation Institute, and The Pennsylvania State University for providing me with the opportunity to pursue my goals. I would also like to thank all my teachers to date who have helped in providing an atmosphere of scientific and philosophical inquiry.

Finally, I would like to thank my parents and my sister, whose support and prodding have kept a mischievous child focused on his path of discovery.

> ***Ford**: Don't you think it was strange I was trying to shake hands with a car?*
>
> ***Arthur**: I assumed you were drunk.*
>
> ***Ford**: I thought cars were the dominant life form. I was trying to introduce myself.*

From, "The Hitchiker's Guide to the Galaxy" (2005)

Based on a novel by Douglas Adams

CHAPTER 1
INTRODUCTION

This thesis describes a methodology for analyzing and controlling the dynamics of self-organizing systems. The methodology is developed by focusing specifically on the problem of formation of self-organizing traffic jams in highway traffic. The motivation for the research was provided in part by the apparent lack of a general methodology to control the behavior of self-organizing systems. Further, and with direct practical implications, the research was motivated by the lack of a clear mandate on the effect of Adaptive Cruise Control (ACC) technologies on highway capacities and flows (Zwaneveld, et al., 1997).

In the following discussion, human-driven vehicles on a highway are viewed as independent, but interacting, agents. ACC vehicles may also be viewed as independent agents, but whose interaction effects may differ slightly from those of human-driven vehicles. The introduction of ACC vehicles on the highway can then be considered as a factor that may possibly modify the dynamics of the system. The thesis builds on this idea and analyzes how the introduction of ACC vehicles in highway traffic affects the formation of self-organizing traffic jams. The results may then be extended to other self-organizing systems, whose dynamics may be similarly modified by the introduction of agents with slightly different interaction effects.

Some of the goals of this thesis are as follows:

- To develop a methodology to control the dynamics of self-organizing systems by introduction of a small set of agents whose interaction effects are intentionally different from the rest of the agent population,
- To develop the methodology specifically to study the effects of introduction of ACC vehicles on the formation of self-organizing traffic jams,
- To validate the results using computer simulations of the self-organizing traffic jams.

1.1 Motivation

The concept of self-organization is not new. Descartes referred to the ability of matter to *arrange itself* into various physical entities, such as in planets and stars (Descartes, 1637). The term self-organization itself was supposedly coined after World War II by W. Ross Ashby (Ashby, 1947).

Though many systems are known to self-organize and exhibit emergent phenomena, the concepts and definitions of self-organization and emergence themselves have continued to remain vague. Further, little attention has been paid towards developing formal methodologies to control the behavior of self-organizing systems.

On the other hand, adaptive cruise control has been an area of intensive research over the past few decades. Active research has been performed by the likes of Herman, Gazis and Potts (Gazis, et al., 1959), Greenshields (Greenshields, et al., 1935), and Greenberg (Greenberg, 1959), and more recently by Seiler and Hedrick (Seiler, et al., 2004), Darbha (Darbha, et al., 1998), Zhou and Peng (Zhou, et al., 2004) and Ioannou (Ioannou, et al., 1993). However, while many studies show that ACC may improve highway traffic flows, the jury is still out on whether their impact is positive or not.

The following subsections elaborate on the motivation behind the research into analyzing the impact of ACC on self-organizing traffic jams.

1.1.1 Self-organization and Emergence

The process of self-organization has been described by Haken as the "spontaneous often seemingly purposeful formation of spatial, temporal, spatio-temporal structures or functions in systems composed of few or many components" (Haken, 2008). Systems that display the phenomenon of self-organization and/or emergence typically consist of multiple interacting components or *agents*. Self-organization has been observed in systems as diverse as ant colonies, growth of cities, the nervous system (Johnson, 2001), chemical reactions (Prigogine, 1984), lasers (Haken, 2007) , and communication networks (Prehofer, et al., 2005). Figure 1 and Figure 2 show the spontaneous structure formation characteristic of emergence in chemical reactions and biological entities, respectively.

By their very definition, self-organizing systems evolve without any external control. However, in certain cases, it is desirable that the system evolves towards one state rather than another. For example, consider snow on mountains (Birkeland, et al., 2002), or sand in sandpiles (Bak, et al., 1988). Both systems tend to self-organize to a critical slope. A tiny perturbation to this self-organized critical state is enough to trigger an avalanche, which may lead to physical and financial losses. In such a scenario, it is desirable to know the dynamics of the system that enables it to reach the critical state, and the parameters that affect the system evolution. Such knowledge

may enable one to modify the dynamics to a more favorable outcome that results in fewer avalanches. The modifications may be introduced by inclusion of a small percentage of agents with slightly different interaction effects. For example, boulders with favorable characteristics, such as larger size, may be positioned in favorable positions on unstable mountain slopes to possibly reduce the size or frequency of avalanches.

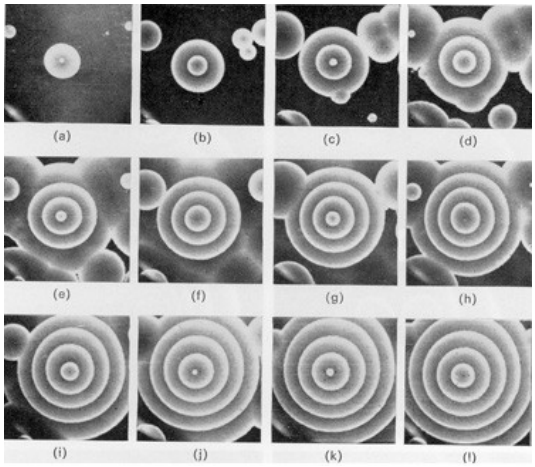

Figure 1: Emergence of concentric waves in a BZ reaction-diffusion system (Zhabotinsky, 2007)

Figure 2: Flocking behavior in starlings over Tøndermarsken, Denmark (Hansen, 2006)

A similar argument may be offered for self-organizing traffic jams. It is known that in medium-to-high density traffic conditions, traffic flow self-organizes into clusters (Kerner, et al., 1993). This phenomenon is also referred to as “stop-and-go” traffic, owing to the formation of several clusters of stationary and moving traffic, and as “phantom” traffic jams, because the jam forms without any known extenuating circumstances such as accidents or bottlenecks. Once a certain critical vehicular density is reached, cluster formation can be initiated by a small perturbation, such as a small braking effort applied on a single vehicle. Due to typical human driving behavior, the driver in a following vehicle tends to apply a slightly larger braking effort to accommodate for the fact that the leading vehicle may be stopping. This results in an even larger braking effort by other following vehicles, till a cluster of slow moving or stationary vehicles is formed. This process is comparable to the avalanches formed in snow or sandpiles. The formation of clusters results in adverse effects on the environment (in terms of excessive emissions), financial losses (in terms fuel wastage) and losses in productivity (in terms of lost man hours due to traffic jams). If the dynamics of the self-organizing traffic jams are known, it may be possible to modify the behavior to enable the traffic to flow at higher densities without cluster formation. As in the

avalanche example, modifications to the system dynamics may be introduced by inclusion of a small set of ACC vehicles with slightly different interaction effects. More importantly, knowledge of how traffic dynamics may be modified in presence of ACC vehicles may provide insights to designers to devise better ACC algorithms.

Apart from these strong arguments outlining the advantages of controlling self-organizing behavior in the specific systems mentioned, another reason that motivates this research is the relative ubiquity of such systems in the world around us. Wherever we find a population of independent, but interacting agents, we may usually find some form of self-organizing behavior resulting in emergent phenomena. It is sometimes desirable to be able to manipulate a small subset of the agent population to enable the system to self-organize to a certain state. In the near future, such form of control may be applied to self-organizing systems such as traffic jams, forest fires, avalanches, and chemical reactions. In the not-so-distant future, we may see such control being introduced to control the flocking behavior in birds, and the growth of cities. Much further into the future, opportunities may arise to use such a methodology in biological projects to control seizures in the human brain, and in geo-engineering projects to control earthquakes, or even in bulk modeling and influencing societal trends, as made famous in Asimov's "Foundation" series .

1.1.2 Traffic jams and Adaptive cruise control

The US Department of Transportation mentioned in a recent report that "between 1985 and 2006, vehicle miles traveled increased by nearly 100 percent, while highway lane miles only increased 5 percent during the same period" (FHWA, 2008). Another report from the Texas Transportation Institute stated that "between 1982 and 2005, the percentage of the major road system that is congested grew from 29 percent to 48 percent" (Shrank, et al., 2007). With growing vehicular population and reducing opportunities for infrastructure expansion, new avenues for improving traffic flow on our highways must be explored.

Traffic jams and congestion result mainly due the one or more of the following three reasons:

(a) *Design issues* – The presence of ramps and traffic lights can result in reduction of road capacity causing a traffic jam.

(b) *Operational issues* – Construction work or accidents can create bottlenecks in traffic flow resulting in congestion.

(c) *Inherent tendencies* – The presence of too many vehicles on a highway may cause a traffic jam in the case where a tiny perturbation occurs. In other words, by the inherent nature of the system, a tiny perturbation beyond critical density may result in a self-organized traffic jam.

This thesis focuses on this third cause: the inherent tendencies of the system to self-organize.

While research thrust has been maintained towards improving highway capacity and reducing congestion, such efforts were, until recently, focused on developing and demonstrating the concept of advanced highway systems (AHS). However, with increasing financial constraints, and the obvious need for a massive infrastructure overhaul to implement such systems, the focus has shifted to intelligent vehicle initiatives (IVI) (Vahidi, et al., 2003). Intelligent vehicle initiatives include various driver-assist technologies such as collision avoidance, driver alert systems and cruise control, and are primarily developed keeping in mind the needs of individual drivers. These technologies have now begun to appear in mainstream vehicle models on our highways. However, there is still no clear mandate on how these IVI technologies impact highway capacity (Kesting, et al., 2005) (Nagel, et al., 1995). This thesis will attempt to establish a relationship between adaptive cruise control laws and their impact on highway capacity and the formation of “phantom” jams.

1.2 Problem Statement

The following problem statement summarizes the central theme of this thesis:

This project aims to study the interactions between driver algorithms, some representing human-driven vehicles, and others representing computer algorithm-driven automated (ACC) vehicles. As a goal of the study, it is sought to determine how changes in driver algorithm parameters and different mixtures of driver algorithms affect the overall macroscopic behavior of traffic flow, especially in medium-to-high-density regimes wherein complex emergent behavior such as "phantom" jams is observed. The desired result of the study is to determine if and under what conditions a mixture of driver algorithms can achieve traffic flow flows higher than when vehicles using only human-driver algorithms populate the road.

From a broader perspective, a framework for a general methodology is sought to analyze how the self-organizing behavior of a group of agents can be modified or even controlled. The control action may be brought about by introduction of slightly dissimilar agents with interaction responses that differ from the rest of the agent population.

1.3 Outline of Remaining Chapters

The remaining chapters of this thesis are organized as follows:

Chapter 2 gives a literature review of existing methodologies for analyzing traffic flow. It also discusses the existing state-of-the-art in adaptive cruise control technologies and provides a brief overview of how previous traffic modeling approaches handled self-organizing traffic jams.

Chapter 3 describes the system under consideration and details the master equation approach towards traffic flow modeling.

Chapter 4 describes how the master equation approach applied to the given system yields a deterministic equation for stochastic dynamics of the self-organizing traffic jam or vehicle cluster. The chapter also details the derivation of a set of transition rates for defining the cluster dynamics.

Chapter 5 extends the approach of Chapter 4 to a multiple species environment wherein the traffic flow consists of human-driven vehicles and ACC vehicles. It also predicts how the emergent system behavior is modified by introduction of a set of slightly dissimilar agents.

Chapter 6 summarizes the results of this thesis and discusses future directions and how this methodology may be applicable to other self-organizing systems.

CHAPTER 2
LITERATURE REVIEW

This chapter attempts to provide a survey of the existing literature and an overview of how problems in the field of traffic flow have been dealt with in the past. The chapter traces the history of vehicular traffic flow research from its beginnings in the early 1930's to the state-of-the-art techniques used today. It also describes the advent of driver assist technologies and how they have begun to permeate into mainstream vehicles. Further, literature pertaining to various systems that exhibit self-organization and emergence is also reviewed, with special emphasis on self-organizing traffic jams. The aim of this chapter is to establish the scope of the problem of traffic flow with a mixture of human-driven and ACC vehicles and its application to the evolution of self-organizing traffic jams.

2.1 Fundamental Diagram of Traffic Flow

The field of automotive technology is a vibrant one, and has seen periods of stupendous growth. In 1895, only four automobiles had been produced in the United States. By 1901, there were 8,000 registered vehicles in the United States, and by 1910 there were over 450,000 (Garber, et al., 2009). Since then the industry has seldom looked back.

In the early years of the growth of the automobile industry, an increase in vehicle population was counterbalanced by a corresponding increase in highway mileage. However, it was soon realized that highway mileage growth could not keep pace with the growing societal demand for automotive transportation. In order to better understand methods for highway design, it was necessary to establish a relationship between traffic demand and highway capacity. In 1935, B N Greenshields proposed what was perhaps the first traffic flow model. According to his observations made using photographic methods, Greenshields postulated that there existed a linear relationship between speed and density (Greenshields, et al., 1935):

$$v_s = v_{max} - \frac{v_{max}}{\rho_j}\rho \tag{2.1}$$

where, v_s = space mean speed, i.e. the average speed of a traffic stream,

v_{max} = free flow speed or maximum permissible speed,

ρ = traffic density (in vehicles per unit distance)

ρ_j = jammed traffic density, i.e. the density at which traffic stops moving

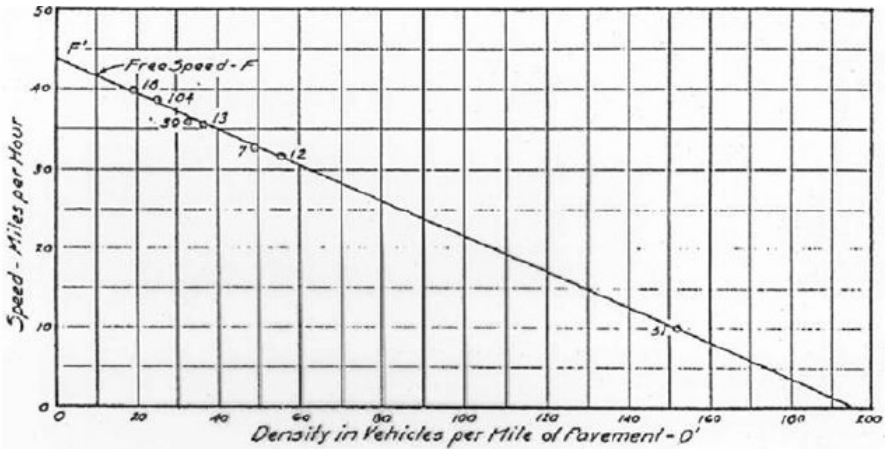

Figure 3: Observations made by Greenshields using photographic equipment depict the linear relationship between speed and density (Greenshields, et al., 1935)

Figure 3 depicts the linear relationship obtained by Greenshields. Further, traffic flow (q) is defined as the product of space mean speed and density, i.e.

$$q = v_s \rho \tag{2.2}$$

Substituting (2.2) into (2.1), we obtain equation (2.3)

$$q = v_{max}\,\rho - \frac{v_{max}}{\rho_j}\rho^2 \tag{2.3}$$

Thus, Greenshields was able to show that a quadratic relationship exists between traffic flow and density. Figure 4 depicts this relationship, which, over the years, has come to be known as the fundamental diagram of traffic flow (Kuhne, 2008). At zero density, the flow is obviously zero, because there are no vehicles on the road. As the density begins to rise, so does the flow, until a maximum flow is achieved at a critical density. Up to this point the movement of vehicles is relatively free and there is little interaction between the vehicles. Beyond this critical point, the vehicle behavior is affected by other vehicles around it. An increase in density results in a decrease of vehicle speed and vehicle flow; this continues up to jam density, when traffic comes to a standstill.

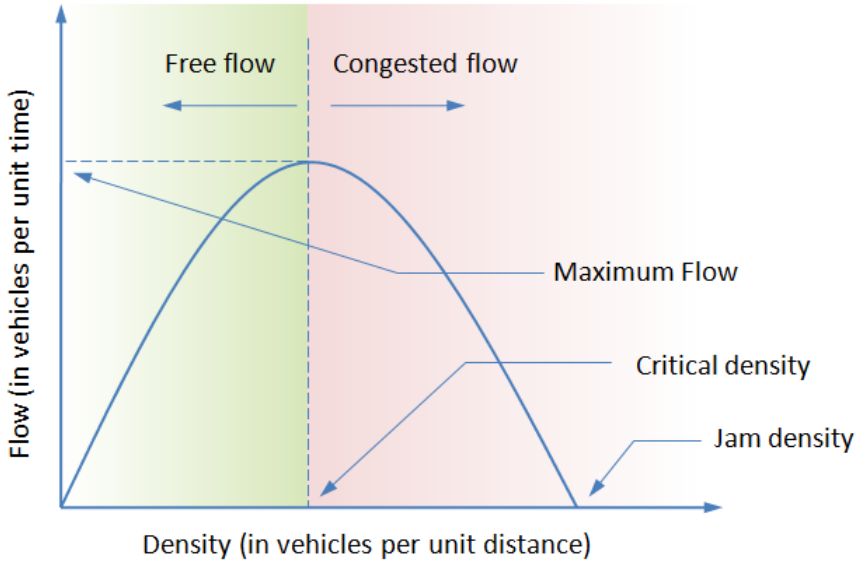

Figure 4: Fundamental diagram of traffic flow (as proposed by Greenshields)

The next major advances in traffic flow research came in the 1950's, when Lighthill, Whitham, Greenberg, Herman, Montroll, Pipes and Richards began developing models for traffic flow and other phenomena observed on highways. In 1958, R E Chandler, R Herman and E W Montroll, who were part of the research staff at General Motors, put forward a theory of traffic flow based on car following studies (Chandler, et al., 1958). In their paper, they discussed the manner in which individual vehicles follow each other on a highway. They also discussed how disturbances propagate through these vehicles within the traffic stream. Along with some other publications during the same period (Herman, et al., 1958) (Gazis, et al., 1959), these theories established the foundations for stability analysis procedures for traffic flow.

Harold Greenberg in his 1959 paper titled "An analysis of traffic flow" (Greenberg, 1959), put forth a different perspective to the same problem. He analyzed the traffic stream as a continuous fluid, and used fluid dynamic principles to derive relations between speed, density and flow. Lighthill and Whitham (Lighthill, et al., 1955), analyzed the phenomenon of a 'hump', or an area of increased density, formed on highways. This was perhaps one of the first attempts at analyzing the nature of shock waves observed in traffic flow.

As the years have progressed, traffic flow modeling techniques have come to be classified into a few distinct categories. These modeling techniques and categories are discussed in the next section.

2.2 Existing Modeling Techniques

Models for traffic flow can be classified into one of the following three categories, viz. microscopic models, macroscopic models or mesoscopic models. In *microscopic* models, the traffic is treated as a system of interacting particles, and the behavior of individual vehicles is explicitly defined using ordinary differential equations. In *macroscopic* models, the traffic is viewed as a compressible fluid and its bulk properties are analyzed (Nagatani, 2002). However, traffic flow often exhibits phenomena that occur at a scale between those described by either microscopic or macroscopic modeling techniques. Emergent traffic jams are an example of such phenomena, because fluctuations at a microscopic level (disturbances in speeds of individual vehicles) eventually lead to a macroscopic behavior ("phantom traffic jam" or "slinky effect"). In such phenomena, both microscopic fluctuations and macroscopic analyses are required to describe the system. Such phenomenon can be described using mesoscopic models. In *mesoscopic* models ('mesos', Greek for middle), traffic flow is analyzed using a stochastic description of groups or clusters of vehicles, or probability distributions of vehicle densities. A brief overview of each of these modeling techniques is given below.

2.2.1 Microscopic Modeling

Microscopic models are based on the premise that the response of a driver-vehicle unit is dependent on its neighboring vehicles. The velocity of the j^{th} vehicle depends on the vehicle $(j-1)^{th}$ vehicle, or the leading vehicle ahead of it (Nagatani, 2002) (Helbing, 2001). Microscopic models describing vehicular traffic flow generally fall into two subcategories, viz. car following models and cellular automata models. The first microscopic traffic models were proposed by Pipes (Pipes, 1953). Later, Newell (Newell, 1961) proposed car-following models with non-linear effects. **Car-following models** are described by equations of motion for the individual vehicles, such as:

$$\frac{dx_j(t+\tau)}{dt} = V(\Delta x_j(t)) \tag{2.4}$$

where, $x_j(t)$ = position of vehicle *j* at time *t*,

τ = delay time,

$\Delta x_j(t)$ = $x_{j-1}(t) - x_j(t)$ = headway of vehicle *j* at time t

$V(\Delta x_j(t))$ = desired velocity

Equation (2.4) models how a driver may adjust his/her vehicle velocity according to the vehicle headway. Further, it also shows that there is a time delay between when the driver perceives headway (or a change in headway) and when the vehicle velocity is adjusted according to the perceived headway. This time delay corresponds to various components including human reaction time and actuator response time, and is usually of the order of 1 second (Del Castillo, et al., 1994). Several modifications to this simple model are possible, including the following:

- Obtaining a simplified differential equation model by removing the dependence of position x_i on delay time τ (using Taylor's expansion) (Bando, et al., 1995)
- Using an Intelligent Driver Model (IDM) that takes into account the relative velocity between the two vehicles, to avoid possible collisions (Treiber, et al., 1999)

While car-following models describe the behavior of individual vehicles very well, they do not provide an analytical means to extend this description of behavior to the macroscopic scale. In other words, car-following models cannot be used to analyze the behavior of large groups of vehicles, such as found in traffic jams. Attempts at such a description are limited to the use of numerical simulation of a group of vehicles (Kesting, et al., 2005). Numerical simulations limit the possibility of analytically predicting changes in behavior, if certain parameters in the system are changed.

Cellular automata (CA) models are used for traffic flow modeling because often they are the simplest models that can describe the phenomena observed in real traffic situations. Cellular automata are essentially a class of "spatially and temporally discrete, deterministic mathematical systems characterized by local interaction and an inherently parallel form of evolution" (Ilachinski, 2001). In the present context, a cellular automata model would describe the roadway as a set of discrete sites which can exist in a finite number of states, such being occupied by a vehicle or being vacant. The state of each of these sites is then updated according to an evolution rule that operates in discrete time. The efficiency and speed of cellular automata models can be attributed to the following properties, which make them ideal for parallel computing environments (Helbing, 2001):

(a) Discretization of space into identical cells (lattice sites),

(b) Finite number of possible states,

(c) Parallel updates at regular time intervals, and

(d) Globally applied update rules, based on short-range interactions with a finite number of neighboring sites.

The earliest traffic flow research using CA models was done by Cremer (Cremer, et al., 1986), and later by Nagel and Schreckenberg (Nagel, et al., 1992). CA microscopic models for traffic flow are less descriptive of vehicle dynamics than their car-following counterparts, but they make up in terms of their simplicity and ease of numerical implementation. According to the CA model proposed by Nagel and Schreckenberg in (Nagel, et al., 1992), the road is defined as a one-dimensional array of L sites. Each site may be occupied by at most one vehicle, or it may be empty. Further, the vehicles may have integer velocities between 0 and v_{max} . Once the system is initialized to a random state, the following steps are performed in parallel on all vehicles:

(a) **Acceleration**: If velocity v of a vehicle is less than v_{max} , and the distance to the next vehicle ahead is greater than $v + 1$, then the velocity is incremented by 1.

(b) **Deceleration**: If the distance to the next vehicle ahead is less than v, then velocity is reduced to $v - 1$.

(c) **Randomization**: The velocity of a vehicle is reduced to $v - 1$, with probability p.

(d) **Car motion**: Each vehicle is advanced v sites.

Like the car-following model, several modifications have been proposed to this model, such as including a slow-to-start rule for the vehicles to model inertia (Schadschneider, et al., 1997).

Despite their remarkable simplicity, the very definition of cellular automata implies that the behavior of CA models cannot be predicted. Thus, while CA models may mimic the real-life behavior of a certain traffic pattern, the only way the same traffic pattern can be analyzed for a different set of parameters is by running the CA algorithm again. As with car-following models, this type of numerical simulation approach limits the possibility of predicting changes in behavior, if certain parameters in the system are changed.

2.2.2 Macroscopic Modeling

Macroscopic modeling techniques treat traffic as a one-dimensional compressible fluid. The traffic states at position x and time t are defined by the spatial vehicle density $\rho(x, t)$ and average vehicle velocity $v(x, t)$ (Nagatani, 2002). The oldest continuum or macroscopic model was proposed by Lighthill and Whitham (Lighthill, et al., 1955), and is based on the assumption that in

absence of any on- and off-ramps, the number of vehicles on a highway is conserved (Helbing, 2001). This conservation law leads to a model that describes vehicular flow using the continuity equation of fluids:

$$\frac{\partial \rho(x,t)}{\partial t} + \frac{\partial q(x,t)}{\partial x} = 0 \tag{2.5}$$

where, $q(x,t) = \rho(x,t)v(x,t)$ is the traffic flow. Lighthill and Whitham assumed that the traffic flow is a function of only the density, as postulated by the fundamental diagram of traffic flow, i.e. $q(x,t) = Q\big(\rho(x,t)\big) = \rho V(\rho(x,t))$. Substituting this expression for flow into equation (2.5), and using it to model traffic flow results in formation of shock-fronts (discontinuities in vehicular density) because the velocity of propagation in dense traffic is less than the velocity of propagation in free traffic. Whitham (Whitham, 1990) later suggested adding a small diffusion term to the Lighthill-Whitham model to avoid the development of shock-fronts, according to:

$$q(x,t) = Q\big(\rho(x,t)\big) - D\frac{\partial \rho(x,t)}{\partial t} \tag{2.6}$$

Using the fundamental traffic flow diagram, $Q\big(\rho(x,t)\big) = v_{max}\,\rho(x,t)(1-\rho(x,t))$ and substituting into equation (2.6) , the Burgers equation is obtained. The Burgers equation describes the nonlinear propagation and diffusion in traffic flow. Several modifications to this simple model have been proposed by Payne (Payne, 1979), Philips (Philips, 1979) and others (Lee, et al., 1999) (Berg, et al., 2000). These models are closely related and can be seen as special cases of the following model (Nagatani, 2002):

$$\frac{\partial \rho}{\partial t} + \frac{\partial (\rho v)}{\partial x} = 0 \tag{2.7}$$

$$\rho\frac{\partial v}{\partial t} + \rho v\frac{\partial v}{\partial x} = \frac{\rho}{\tau}[V(\rho) - v] - c_0^2\frac{\partial \rho}{\partial x} + \mu\frac{\partial^2 v}{\partial x^2} \tag{2.8}$$

where τ, c_0^2, and μ are phenomenological constants. The phenomenological function $V(\rho)$ represents the desired velocity achieved in steady state. The constant τ is the relaxation time to

steady state. The desired velocity $V(\rho)$ corresponds to the optimal velocity, and relaxation time τ corresponds to the delay time in the microscopic model.

While macroscopic models provide an excellent description of the macroscopic behavior of traffic flow, they are unable to incorporate the dynamics of individual vehicles. When considering a system of mixed traffic, such as human-driven and ACC vehicles on the same roadway, the driver models and dynamics of individual vehicles play an important role in determining overall behavior. Consequently, it is difficult to use these models to analyze the impact of ACC vehicles on macroscopic behavior, such as in self-organizing traffic jams.

2.2.3 Mesoscopic Modeling

Mesoscopic modeling techniques are based on gas-kinetic models (Prigogine, et al., 1960), or aggregation models (Mahnke, et al., 1997). The kinetic theory treats vehicles as a gas of interacting particles (Nagatani, 2002). One of the first gas-kinetic models was proposed by Prigogine and Andrews (Prigogine, et al., 1960), and was later improved upon by Paveri-Fontana (Paveri-Fontana, 1975). Prigogine and Herman (Prigogine, et al., 1971) (Nagatani, 2002) have proposed that traffic flow can be modeled using a velocity distribution function $f(x,v,t)$ considered over an element $dxdv$. The traffic flow is described by the variation of the velocity distribution function over time. Prigogine and Andrews (Prigogine, et al., 1960) postulated that the velocity distribution function can change by only one of two processes:

(a) Relaxation process: A vehicle accelerates to achieve its desired velocity, and
(b) Collision process: A vehicle is forced to decelerate in order to avoid a collision with a preceding vehicle.

The following equation can then be used to model traffic flow in a Boltzmann-like fashion:

$$\frac{df(x,v,t)}{dt} = -\left(\frac{\partial f(x,v,t)}{\partial t}\right)_{rel.} + \left(\frac{\partial f(x,v,t)}{\partial t}\right)_{coll.} \tag{2.9}$$

$$\left(\frac{\partial f(x,v,t)}{\partial t}\right)_{rel.} = \frac{f(x,v,t) - \rho(x,t)F_{des}(v)}{\tau_{rel}};\ \left(\frac{\partial f(x,v,t)}{\partial t}\right)_{coll.} = (\Gamma^{+} - \Gamma^{-})(1-P)$$

where, $f(x,v,t)$ = velocity distribution function for each vehicle

$\rho(x,t)F_{des}(v)$ = desired velocity distribution function

τ_{rel} = relaxation time

Γ^{+} = Collision term causing addition of vehicles to element $dxdv$

Γ^{-} = Collision term causing removal of vehicles from element $dxdv$

P = Probability of being unable to pass a vehicle

The velocity distribution function determines the probability that a vehicle is present in an element dx of the road, with a velocity that lies within an element dv at time t. Integrating $f(x,v,t)$ over the length of the road, and over all non-negative velocities, yields the total number of vehicles (N) on the road at a given time t.

The first term in the right-hand side of equation (2.9) represents the relaxation of the velocity distribution function $f(x,v,t)$ to the desired velocity distribution $\rho(x,t)F_{des}(v)$ with the relaxation time τ_{rel} in the absence of interactions. The relaxation term further consists of two sub-processes (Figure 5):

(a) A vehicle originally inside $dxdv$ accelerates to move out of the element, and
(b) A slow moving vehicle originally outside $dxdv$ accelerates to enter the element.

The second-term represents the changes in the velocity distribution of a vehicle due to "collisions" or interactions with other vehicles. It too is further represented by two sub-processes (Figure 5):

(a) A vehicle originally inside $dxdv$ leaves the element because it collides with a slower moving vehicle, thus reducing it speed, and
(b) A fast moving vehicle originally outside $dxdv$ enters the element because it collides with slow moving vehicles inside the element.

The aggregation approach (Mahnke, et al., 1997) is loosely developed around the same concept as discussed above, and is based on the use of the master equation. The master equation describes the time evolution of the probability distribution of the system states. In other words, the master equation describes how the probability that a system is in a particular state evolves over time (similar to the evolution of the vehicle distribution function) based on the manner in which the system transitions between various states (similar to the four sub-processes mentioned above). For

example, one may use the master equation to determine how the number of vehicles in a particular state (say vehicles in traffic jam) changes with time, based on the transitions a vehicle makes either from a jammed state to a free state or vice versa. The master equation approach is described in detail in chapters 3 and 4.

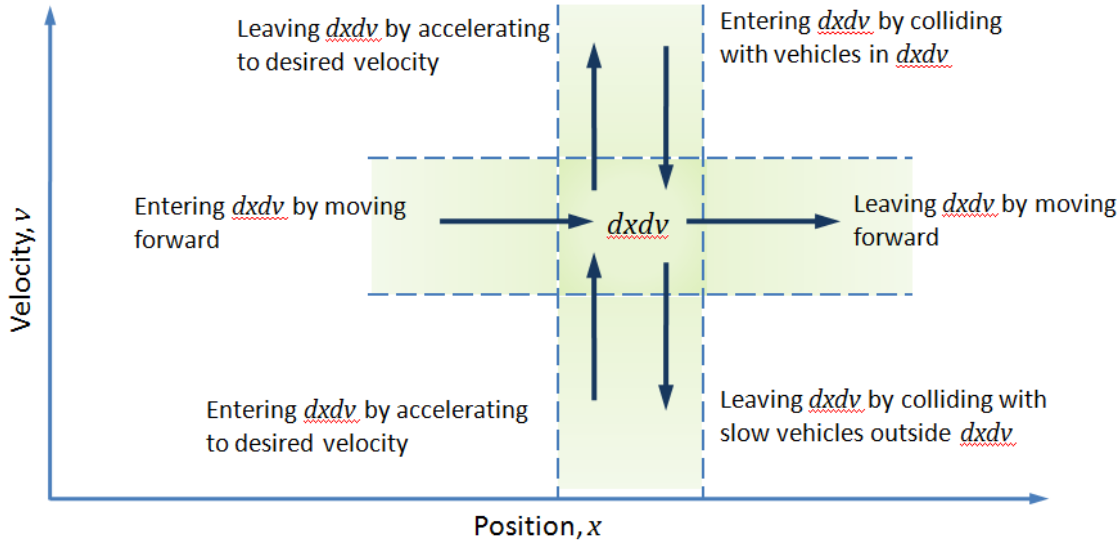

Figure 5: Various processes involved in describing the time evolution of the vehicle distribution function $f(x,v,t)$ for traffic flow modeling using Boltzmann approach

2.2.4 Selection of a Traffic Flow Modeling Technique

Traffic flow models are expected to accurately describe the flow of traffic across all possible scenarios. This function generally encompasses an accurate description of traffic across the entire range of observed flow and density values, as well as a reasonable depiction of other phenomena observed in traffic such as stop-and-go traffic or self-organized traffic jams.

All modeling techniques described in the previous sub-sections perform these functions reasonably well with minor modifications. However, they differ in the scale at which these problems are addressed. While microscopic modeling techniques work at the scale of individual vehicles, macroscopic techniques work on a much larger "bird's-eye view" scale. However, both the microscopic and macroscopic approaches have certain shortcomings. In microscopic techniques, the large number of interacting elements requires a large number of descriptive equations, which generates complexity problems, both analytically and computationally (Bellomo, et al., 2007). On the other hand, macroscopic techniques reduce the computational complexity by dealing with quantities that are averaged, at each time, locally in space. However, the macroscopic approach

only performs well in high density regimes (congested traffic). Further, it is not feasible to use a macroscopic approach for the analysis of a meso-scale effect such as a “phantom” traffic jam, with the additional complexity of accounting for multiple driver models (human and ACC).

In this situation, mesoscopic techniques provide a practical micro-macro link (Nagatani, 2002), and the use of the master-equation approach enables a description at a vehicular level that can be scaled up to analyze the traffic flow behavior at a macroscopic scale. In other words, the mesoscopic approach using the master-equation enables a description of the system at the vehicular level, while simultaneously allowing an analysis of the system behavior occurring at the macroscopic scale, such as with the formation of self-organizing traffic jams. Since the master equation approach includes microscopic description of vehicles to determine their macroscopic behavior, it is an ideal tool for analyzing the traffic flow dynamics of a mixture of human-driven and ACC vehicles.

2.3 Adaptive cruise control

The concept of controlling the speed of a vehicle dates back to 1788, when James Watt and Matthew Boulton built the first centrifugal governor to control the speed of a steam engine. One of the earliest cruise control systems for automobiles was invented by Ralph Teetor in 1945. These early automotive cruise control technologies required the driver to manually bring the vehicle to a desired speed, after which the cruise control system would maintain the desired speed for the driver.

In modern times, the goal of adaptive cruise control has been primarily to reduce driver effort by controlling the speed of the vehicle according to a specific driver model or control law. Adaptive cruise control is different from previous cruise control technologies in that it controls the vehicle acceleration based on a several variables, the most important ones being the distance to the leading vehicle (or headway), the velocity of the following vehicle, and the relative velocity between the two vehicles. These variables are determined by the equipment (such as radar- or laser-based systems) installed on the vehicle. Radar-based systems usually offer better performance in terms of detecting vehicles and obstacles ahead, as compared to laser-based systems. However, radar-based systems are also more expensive than their laser counterparts.

Adaptive cruise control technologies are now available in numerous mainstream passenger vehicles, and are offered by most major automobile brands such as Audi, BMW, Ford, Honda, Hyundai, Jaguar, Lexus, , Mercedes-Benz, Nissan, Toyota, Volkswagen and Volvo.

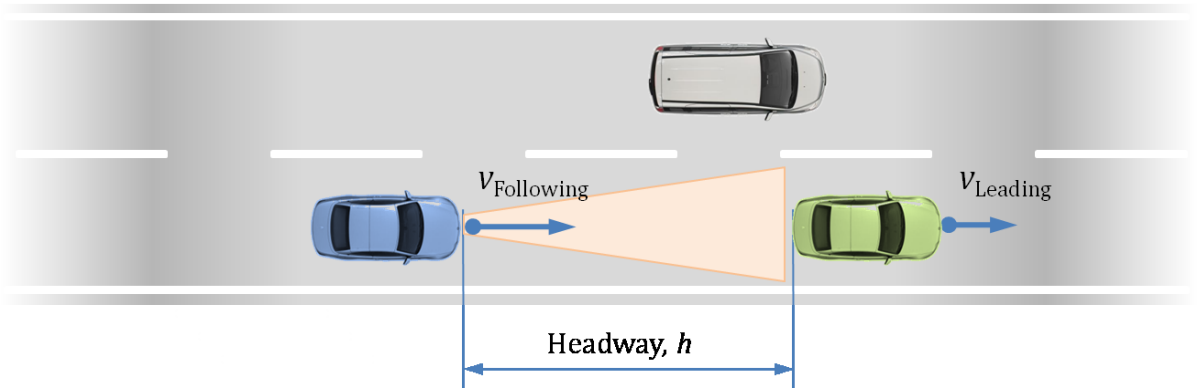

Figure 6: Variables required for adaptive cruise control algorithms

2.3.1 Adaptive cruise control algorithms

The process behind driving a vehicle can be defined as consisting of two conflicting tasks:

(a) Driving at the maximum possible velocity, and

(b) Avoiding a collision with a preceding vehicle.

Under most traffic conditions, human driver effort is geared towards finding a trade-off between these two tasks, which results in following a preceding vehicle at a safe distance. The basic idea underlying the concept of adaptive cruise control is to reduce the driver effort by taking these tasks away from the human and allowing them to be performed by a computer. The computer performs these tasks using an adaptive cruise control algorithm that seeks to closely mimic the driving abilities of an ideal human driver. Thus, by using adaptive cruise control systems in a vehicle the human driver depicted in Figure 7, is replaced by a computer-based controller such as the Pipes model depicted in Figure 8 (Ioannou, et al., 1993).

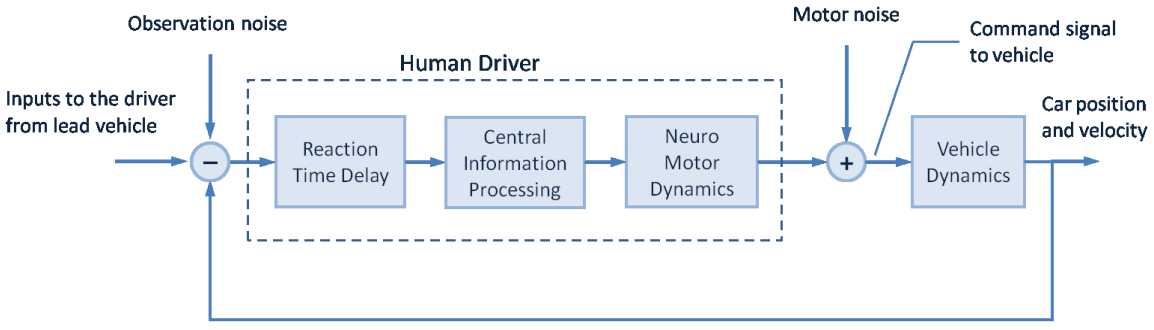

Figure 7: Human driver model

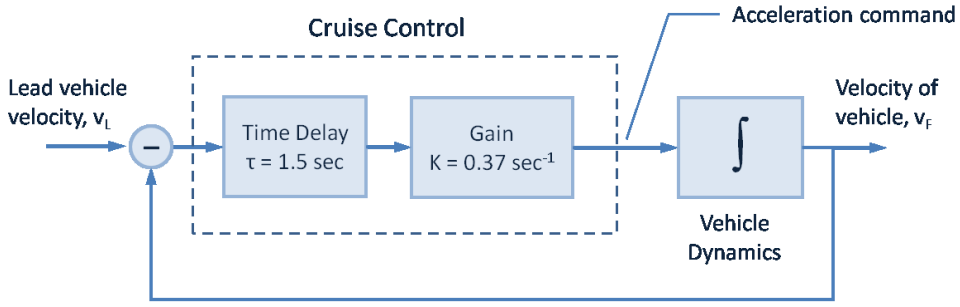

Figure 8: Adaptive cruise control (Pipes Model)

Typically, an adaptive cruise control algorithm has the general form given by:

$$\alpha = f(\lambda, h, v, \Delta v) \tag{2.10}$$

where, α = Desired acceleration (control effort)

λ = Control gain(s)

h = Headway between vehicles

v = Velocity of following vehicle

Δv = Relative velocity between vehicles

Since the basic premise behind developing an adaptive cruise control is to be able to safely follow a vehicle ahead, the corresponding algorithms are usually based on car-following models discussed in Section 2.2. Some of the prominent works on car following theories are described below. These form the foundations of adaptive cruise control algorithms.

Constant time headway (CTH) policy

The constant time headway (CTH) policy is a common safe practice suggested to human drivers (Zhou, et al., 2004). According to the policy, the following vehicle must always maintain constant time headway from the leading vehicle. The time headway is usually recommended to be 2 seconds. In terms of distance headway or range, this translates to maintaining headway proportional to the velocity of the vehicle. The desired distance headway can be calculated as follows:

$$h = d_0 + T \cdot v \tag{2.11}$$

where, h = Desired distance headway, or simply headway

d_0 = Minimum distance between vehicles at zero velocity

T = Constant time headway

v = Velocity of the following vehicle

A sliding mode controller can be developed based in the above policy (Zhou, et al., 2004). Since the desired range is given by equation (2.11), the headway error signal is $e_i = R_i - Tv_i$, where R_i is the actual headway. The appropriate acceleration (control effort) may then be determined as a function of the error signal and the relative velocity.

General Motors' Car-following Models

The research group at General Motors labs in Detroit performed extensive work in trying to determine a descriptive car-following model. The GM car-following models use the following general form (May, 1990):

$$response = func(sensitivity, stimuli) \tag{2.12}$$

where, $response$ = Acceleration (or deceleration) of the following vehicle

$sensitivity$ = synonymous to control gain

$stimuli$ = Relative velocity of the lead and following vehicle

The difference between the various models proposed by GM's research labs is in terms of the expressions for sensitivity. In all, the GM research group proposed five car-following models, with each model providing an improvement over the previous one. The fifth model from GM is the most general and has the largest number of parameters. The control law for the fifth model is presented here.

$$\ddot{x}_{n+1}(t + \Delta t) = \frac{a_0\,[\dot{x}_{n+1}(t + \Delta t)]^l}{[x_{n+1}(t) - x_n(t)]^m}\left(\dot{x}_{n+1}(t) - \dot{x}_n(t)\right) \tag{2.13}$$

where, x_{n+1} = Position of the (n+1)th, or following, vehicle

x_n = Position of the nth, or leading vehicle

a_0 = Dimensionless sensitivity coefficient

l, m = Constants

As can be seen from equation (2.13), the acceleration of the vehicle is dependent on the *sensitivity*, comprising the vehicle velocity, vehicle headway and constants l and m, and the *stimulus*, comprising the relative velocity between the following and the preceding vehicles. If the relative velocity between the vehicles is large, such as when a vehicle is rapidly approaching a stationary vehicle, a large deceleration effort is required in order to avoid a collision. Similarly, the sensitivity term is adjusted according to the vehicle velocity and headway. If the vehicle is travelling at a high velocity or at very small headways, it must decelerate quickly in response to even small changes in relative velocity in order to avoid a collision. Thus the velocity of the vehicle is in the numerator and the headway is in the denominator of the sensitivity term. Different values of the constants l and m have been proposed to match experimental data.

Intelligent driver model

The Intelligent Driver Model (IDM) guarantees crash free driving, It maintains the speed of the vehicle based on an acceleration control effort that is a continuous function of vehicle velocity, the headway, and the velocity difference (approaching rate) to the lead vehicle (Kesting, et al., 2005):

$$\alpha = \dot{v}_i = a\left\{1 - \left(\frac{v_i}{v_0}\right)^4 - \left(\frac{s^*(v_i, \Delta v_i)}{s_i}\right)^2\right\} \tag{2.14}$$

where, v_i = Velocity of the i^{th} vehicle

v_0 = Desired velocity of the i^{th} vehicle

s_i = Headway to the lead vehicle

$s^*(v_i, \Delta v_i)$ = Desired minimum headway

The control law for the intelligent driver model can be thought of as consisting of two terms, viz. the *relaxation term* and the *interaction term*. The relaxation term, $(1 - (v_i/v_0)^4)$, is dominant at low vehicle densities, or large headways. As vehicle velocity v_i approaches the desired velocity v_0, the acceleration effort approaches zero. The interaction term is a function of the ratio of the 'desired minimum gap' $s^*(v_i, \Delta v_i)$, and the actual headway s_i, where the desired minimum gap is given by:

$$s^*(v_i, \Delta v_i) = s_0 + vT + \frac{v\Delta v}{2\sqrt{ab}} \tag{2.15}$$

where, s_0 = Minimum distance in congested traffic vehicle

T = Constant safe time headway

a = Constant acceleration term

b = Comfortable braking deceleration

The interaction term can be dominant in two scenarios. First, if the relative velocity between the following and preceding vehicles is large, or if the velocity of the following vehicle is large, the desired minimum headway is also large, resulting in a dominant interaction term and a correspondingly large deceleration effort. Second, the interaction term is also dominant if the actual headway is small, resulting in a large deceleration contribution in the control law.

2.3.2 Studies on impact of ACC on traffic flow

Since the introduction of adaptive cruise control, numerous studies have been conducted to ascertain its impact on traffic flow. These studies can be considered to have been conducted in three different stages, which progressed as automated vehicle guidance technologies evolved (Zwaneveld, et al., 1997). The three stages are:

(a) Stage 1: Introduction of automated vehicles with ACC in mixed traffic

(b) Stage 2: Introduction of dedicated lanes for automated vehicles

(c) Stage 3: Introduction of intelligent infrastructure and communication networks

Each of these stages attempted to introduce technologies that would help improve traffic flow. Analyses for each of the stages comprised of a mixed approach of both simulation studies and real traffic data analysis. It may be observed that the infrastructure requirement for each stage was higher than that for the previous one.

Results from the **first stage** were mixed, with some studies indicating that addition of vehicles with adaptive cruise control resulted in decreased flow (van Arem, et al., 1995), whereas others indicated an increase in traffic flow (Ludmann, 1995). One of the most prominent studies in this stage was the PROMETHEUS program, which suggested that addition of ACC would not degrade highway efficiency, while simultaneously improving driver comfort (Morell, et al., 1994).

Results from the **second and third stages**, which involved additional infrastructure deployments such as dedicated lanes for automated vehicles, and vehicle-to-vehicle and vehicle-to-roadway communications, indicated a marked improvement in capacity. Many of the studies conducted during these stages were initiated by the National Automated Highway Systems Consortium (NAHSC) in the United States. Research indicated that formation of platoons or strings

of cars (which required inter-vehicle communication) could greatly increase highway capacity (Varaiya, 1993). The California PATH program demonstrated the usage of such platoons. Other studies also indicated similarly impressive results of increased highway capacities (Kraaslan, et al., 1991) (Shladover, 1991) (Chien, et al., 1997).

While recent studies on AHS indicate remarkable improvements in highway capacities, it remains a reality that these systems require a massive infrastructure overhaul and investment. Bringing such systems into practice would require a paradigm shift by both the industry and the average consumer. In the present financial climate, this approach doesn't seem feasible. Quite the contrary, the adaptive cruise control technologies already being introduced into the market today indicate a shift to an approach similar to the one that defined Stage 1. In other words, it is a more realistic goal to expect that highways in the near future will be populated with a mix of ACC and human-driven vehicles. Further, as previously mentioned, there is no clear mandate on how highway capacity is impacted when a mixture of human-driven and ACC vehicles coexist on a highway. Thus an urgent need exists to evaluate the effects of such mixed traffic flow on highway capacities in order to better design ACC algorithms. Better designed ACC algorithms may help improve highway capacity in mixed traffic and may also help avoid highway capacity reduction resulting from self-organizing traffic jams.

2.4 Self-organization and traffic jams

2.4.1 Analysis of self-organizing systems

As mentioned previously in Section 1.1, several systems, such as cities, traffic and animal herds, exhibit self-organizing and emergent behavior. Traditionally, there have been four schools of study which have developed the theory of emergent behavior in complex systems (De Wolf, et al., 2004), viz.

- Complex adaptive systems theory (furthered by the Santa Fe Institute),
- Nonlinear dynamical systems theory,
- Synergetics school (introduced by Herman Haken), and
- Far-from-equilibrium thermodynamics (influenced greatly by Ilya Prigogine).

In addition, some critically self organizing systems may be viewed as statistical mechanics problems with critical phase transitions. Each of these approaches has its own set of analysis techniques. Some common numerical techniques include agent-based modeling and use of cellular

automata (both from complex adaptive systems theory). Some common theoretical techniques employ limit cycles and attractors (from dynamical systems theory), and equations of time evolution of probability density functions of system states such as master- and Fokker-Planck equations (from far-from-equilibrium thermodynamics).

In many such systems it is desirable to control the evolution of the self-organization process. However, until recently, most research had been directed towards analyzing the behavior of various self-organizing systems, whereas very little effort has been directed towards control or manipulation of such systems (Gershenson, 2007). Earlier attempts at modifying the dynamics of self-organizing systems have mostly been based on trial-and-error or numerical simulations rather than development of an analytical approach. For example, the emergent behavior of human crowds in panic situations has been analyzed to identify exit strategies employed by them. Numerical simulations and evolutionary algorithm approaches have indicated how to better design exits to reduce casualties in such panic situations (Helbing, 2001). Figure 9 and Figure 10 depict the trial-and-error and evolutionary optimization approaches for designing better exits for panicking human crowds. However, no general approach exists to determine how the system behavior can be modified to produce predictable results.

(a) Fewer people can exit a room in traditionally designed exits

(b) More people can exit a room when a column is introduced near the exit

Figure 9: Trial-and-error reveals a counter-intuitive result for improving exit strategies for panicking human crowds (Helbing, 2001)

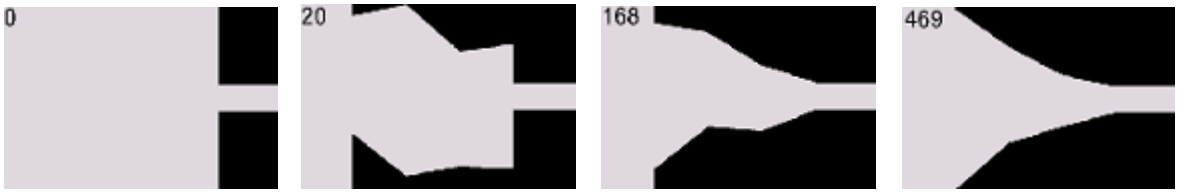

Figure 10: Evolutionary algorithms help better design exits for panic situations. Images indicate stages in evolution. (Helbing, 2001)

2.4.2 Self-organizing traffic jams

It is apparent that each vehicle on a highway is driven by a driver who operates according to his or her own will. In other words, each vehicle on a highway may be considered an independent *agent*, which operates without any influence of other vehicles. However, in medium-to-high density traffic conditions, these vehicles are closely spaced and can no longer operate without the influence of neighboring agents. Under such circumstances, the interactions between the vehicles (or agents) result in a collective behavior that cannot be derived from observing the behavior of a single agent. This behavior was explained in Section 1.1 and usually takes the form of what is known as "slinky waves" or "phantom" traffic jams or "stop-and-go" traffic. In other words, the interactions between individual vehicles results in a behavior that *emerges* when a group of vehicles comes together.

One of the earliest recorded data of the formation of ***vehicle clusters*** (used henceforth in lieu of "slinky waves", "phantom" traffic jams or "stop-and-go" traffic) was provided by Treiterer using aerial photography techniques over German highways (Treiterer, et al., 1974). Figure 11 indicates the clustering of vehicles in traffic flow on a German highway. Nagel and Schreckenberg were perhaps the first to reproduce the phenomenon using a cellular automata model of traffic flow (Nagel, et al., 1992). Later, Kerner and Konhäuser showed that given an "initially homogeneous traffic flow, regions of high density and low average velocity can spontaneously appear, if the density of cars in the flow exceeds some critical value" (Kerner, et al., 1993). Experimental verification of the spontaneous formation of jams is provided in (Sugiyama, et al., 2008).

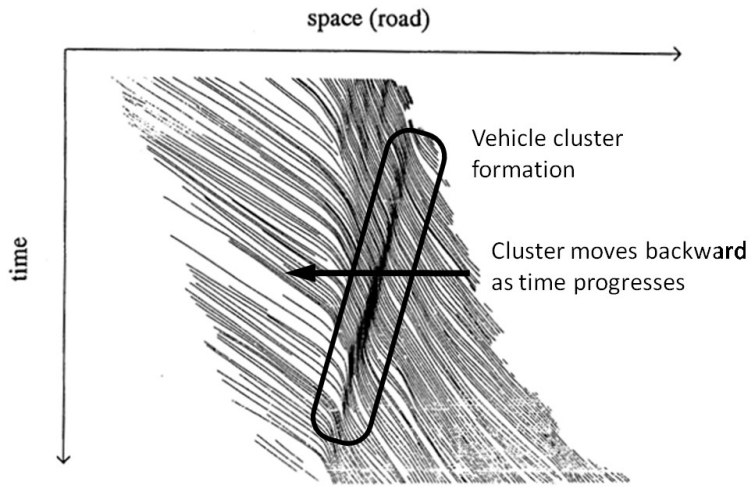

Figure 11: Space-time lines (trajectories) for individual vehicles from aerial photography by Treiterer. Reproduced and augmented from Nagel, et al., (1992).

The fact that the spontaneous structure formation occurs only beyond a certain critical density suggests that vehicle cluster formation in highway traffic may be an example of self-organized criticality. The process by which a system self-organizes itself into a critical state is known as ***self-organized criticality (SOC)***. The concept of self-organized criticality was first forwarded by Bak, Tang and Wiesenfeld as an explanation of 1/f noise (Bak, et al., 1988). The field of self-organized criticality is relatively nascent, and there is still no methodology to predict which systems will exhibit self-organized criticality and which will not. However, it has been found that self-organized criticality is usually observed in highly nonlinear, slowly-driven, non-equilibrium systems (Jensen, 1998). In absence of a general methodology to determine the conditions necessary for a system to exhibit SOC, researchers have been studying individual critically self-organizing systems such as sand piles, forest fires, earthquakes and brain activity. It has been found that systems which critically self-organize usually possess long-range spatio-temporal correlations and power law distributions.

Nagel and Paczuski have analyzed the emergent behavior of traffic flow using cellular automata models, and found power law distributions for survivability of traffic jams (or the frequency of traffic jam events versus the time for which they exist) (Nagel, et al., 1995). Figure 12 indicates the power law distribution for traffic jam survivability P(t). The evolution of traffic jams or growth of cluster size has been analyzed using a one-dimensional random walk argument. The results indicate that the size of the traffic jam is also related to the time for which it exists according to a power law distribution (Paczuski, et al., 1996). Paczuski and Nagel in the same paper have also developed a methodology to identify the critical state of the traffic jam using the Fokker-Planck equation, which is a continuous form of the master equation.

As has been previously mentioned, self-organization of vehicles in traffic flow into traffic jams can be described as a cluster formation process. Mahnke and Pieret have studied the emergence of traffic jams from a nucleation or aggregation perspective (Mahnke, et al., 1997). In their paper, Mahke and Pieret develop a deterministic analysis technique for the stochastic process of cluster formation to determine the time evolution of the average cluster size in a traffic jam. Their analysis consists of using the master equation to describe the stochastic process of vehicles joining or leaving a cluster. The master equation approach forms the basis of the present analysis of the impact of ACC vehicles on the formation of self-organizing traffic jams, or aggregation of vehicles into vehicle clusters, and has been discussed in Chapter 3.

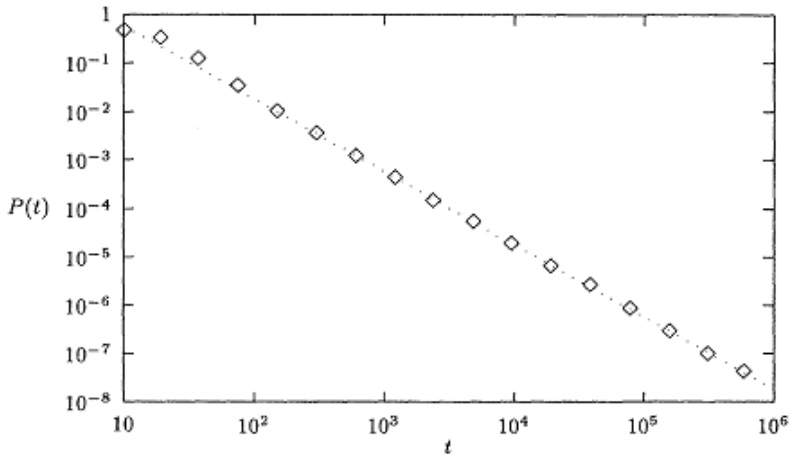

Figure 12: Survivability of emergent traffic jams (or lifetime distribution) P(t) in the outflow region: average over more than 65000 clusters (avalanches). (Paczuski, et al., 1996)

2.5 Summary

In this chapter, various existing methodologies for traffic flow modeling were introduced and their pros and cons were discussed. It was found that microscopic modeling techniques rely heavily on numerical simulations to describe overall traffic flow behavior, which is undesirable. On the other hand, macroscopic modeling techniques are unable to incorporate vehicle dynamics for individual vehicles, as required when modeling traffic with a mixture of human-driven and ACC vehicles. It was also determined that mesoscopic modeling techniques represent traffic flow at a scale between microscopic and macroscopic behavior and hence provide an ideal tool for analyzing the mesoscopic scale behavior found in self-organizing traffic jams.

Further, specific control laws for adaptive cruise control algorithms were discussed. The control laws will be used to model individual vehicle dynamics for both human-driven and ACC vehicles, with a slight difference in their parameters. The impact that the difference in parameters and the proportion of ACC vehicles will have on the cluster formation process characteristic of self-organizing traffic jams is the primary focus of the remainder of this thesis. The solution to the problem will be presented as a proof of concept for future development of methodologies concerning control of self-organizing systems. The presented methodology will hopefully provide a starting point for developing a framework for control of self-organizing systems.

CHAPTER 3
THE MASTER EQUATION APPROACH

This chapter provides a detailed description of the master equation approach for modeling traffic flow, as presented by Mahnke and Pieret (Mahnke, et al., 1997). The master equation finds widespread use in the modeling of system dynamics in areas of application as diverse as economics (Weidlich, et al., 1992), system reliability (Helbing, 1995), photon emissions (Agarwal, 1970) and string theory (Verlinde, 1992), to name a few. In general, the master equation provides an ideal modeling framework for stochastic processes. A stochastic (or non-deterministic) process is usually characterized by a probability distribution function that determines the probability that a system is in a certain state at a given time. The evolution of the probability distribution function is determined by a set of transition probabilities which describe the probability that the system changes from a given state to another. Thus, in order to model the dynamics of a given system, it is first necessary to have a clear understanding of the system itself. Specifically, it is necessary to know the possible states of the system and the manner in which the system may move from one state to another.

3.1 System description and behavior

The problem at hand consists of a set of vehicles or agents moving on a roadway. One would intuitively expect that the system under consideration should be a straight stretch of road with vehicles on it. Consider this system (Figure 13) comprising x miles of a single-lane highway, with no on- or off-ramps. To describe the system completely one would require two additional quantities, viz. the number of vehicles entering the roadway from the left (or inflow, Q_{in}) and the number of vehicle leaving the roadway on the right (or outflow, Q_{out}).

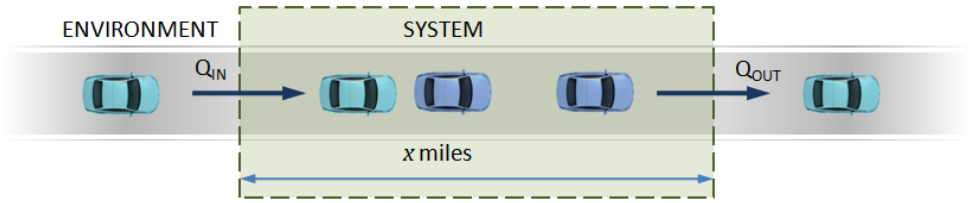

Figure 13: An open system description for traffic flow – straight highway

The system described above is an accurate representation of real-life traffic. However, though such a system resembles reality, a system *without* open boundary conditions (no inflows or

outflows) is much easier to analyze. From a purely thermodynamic point of view, the evolution of an isolated system, which has no energy or mass transfer with the environment, is easier to analyze as compared to an open system. Thus, in order to ease analysis, the realistic system description is traded in for a simplified system description, wherein the system is isolated from the environment. The simplified system (Figure 14) consists of a closed ring roadway, with no exit or entry points for vehicles. The elimination of the open boundary conditions results is conservation of the number of vehicles on the road, which eases analysis.

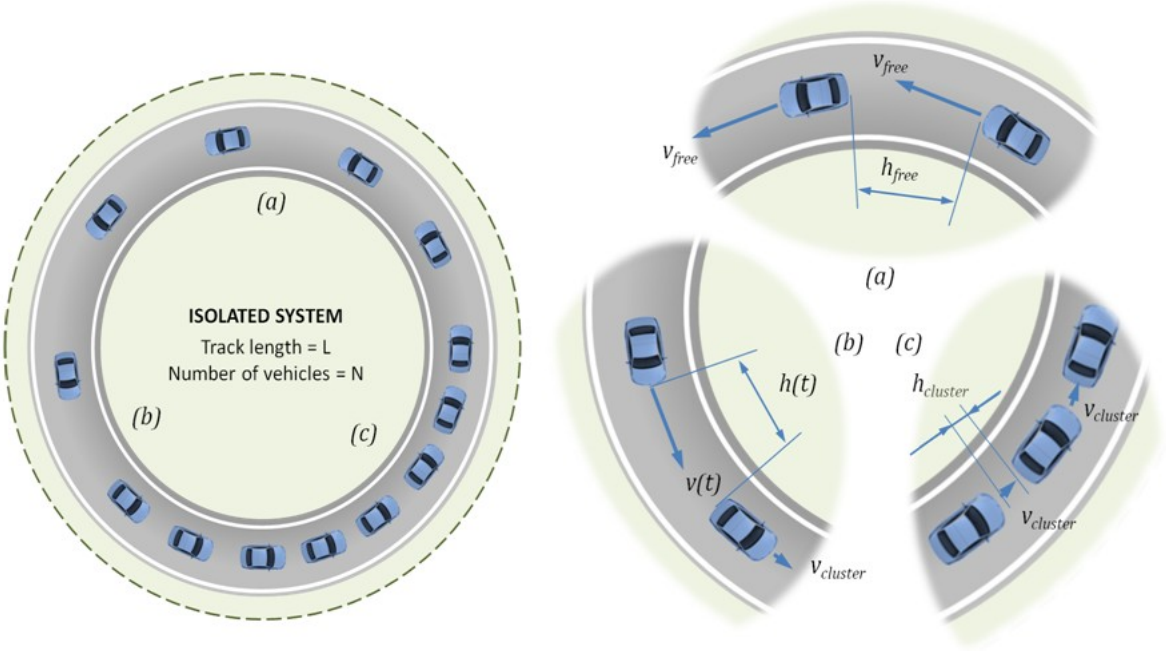

Figure 14: An isolated system description of traffic flow – closed ring road (a) vehicles in free flow, (b) vehicles transitioning from free flow to jammed state, and (c) vehicles in a traffic jam.

The vehicles shown in the system in Figure 14 can exist in one of two states:

(a) A vehicle can be moving freely with relatively little interaction with other vehicles, as shown in section (a) of the figure, or

(b) A vehicle can be stuck in a cluster, with a high degree of interaction with other vehicles, as shown in section (c) of the figure.

The evolution of clusters on the roadway is dependent on the manner in which vehicles transition from one state to another. The system state can then be defined as the number of vehicles present in a particular state at a given time. In view of the fact that a vehicle can only be in one of the two mentioned states, the number of vehicles in either state at a given time can provide a complete description of the system state at that instant of time. Since the problem of interest is

the formation of self-organizing traffic jam, the **system state** will be considered to be the *number of vehicles present inside a vehicle cluster at any given time* t. For the purposes of simplicity, a system with only one cluster will be considered.

At this point it would bode well to define a 'cluster'. In general, one may consider a cluster to be any group of vehicles with sufficient interactions between them. In other words, if the control effort on one vehicle produces an effect on a second vehicle, the two vehicles may be considered as belonging to the same cluster. For example, if a vehicle brakes suddenly and causes another vehicle somewhere behind it to brake, the two vehicles may be considered as belonging to the same cluster. This definition is open to question in various regards, such as "What constitutes 'sufficient' interaction?", "What metrics must be used to determine if two vehicles interact with each other?" and "Are groups of fast moving vehicles also to be considered as 'traffic jams' or 'clusters'?". While these questions are all relevant in a more general sense, the specific concern of this thesis is the formation of self-organizing traffic jams that cause congestion and reduce traffic flow. Thus, for the purposes of this thesis, a 'cluster' will be considered to be a group of vehicles that is in accordance with real-life observations of traffic jams on highways. Thus a group of vehicles is considered to be a cluster if:

(a) Traffic moves very slowly, or is stationary over a segment of the roadway containing that group of vehicles, and/or
(b) The vehicles in the group are very closely spaced, i.e. have very small headways.

Experimental data indicates that when vehicles come to a stop in a traffic jam on a highway, they usually maintain a minimum headway of about 1 m (Mahnke, et al., 1997). Thus, in the present analysis, a vehicle is considered to be in a cluster or jam, if its headway to the preceding vehicle is approximately 1 m.

Returning to the problem of system description, the system state has been defined as the number of vehicles present in a cluster at a given time. As a next step, a stochastic framework that describes how a vehicle cluster grows or diminishes in size is required. In other words, a set of equations that describes the evolution of the probability of the system being in a certain state is needed. Such a framework that describes the dynamics of evolution of the system is provided by the master equation.

3.2 The Master equation

The system state under consideration is the number of vehicles, n, present inside a cluster at a given time, t. Since the number of vehicles on the road is usually large, it is impossible to perform precise calculations of their states, and it is easier to handle the evolution of system states as a stochastic process. As has already been mentioned in section 2.4, the master equation modeling approach considers cluster aggregation as a stochastic process. In other words, the manner in which a cluster changes its size is considered to be random in nature. In order to describe this stochastic process, one requires a probability distribution function, say $p(x,t)$ that indicates the probability that the system is in a state x at time t. This section describes the derivation of the master equation from the fundamentals of probability theory, using concepts such as conditional probability and the Markov process assumption.

3.2.1 The Markov process assumption

Prior to discussing the Markov process assumption, the concept of conditional probability must be discussed. Consider the discrete case with two events A and B. Let the probability that the event A occurs be $P(A)$, and the probability that the event B occurs be $P(B)$. Then the joint probability $P(A,B)$ that both events A and B occur is given by:

$$P(A,B) = P(B|A) \cdot P(A) \tag{3.1}$$

where $P(B|A)$ is the *conditional probability* that event B occurs given that event A has already occurred. Extending this formulation to the continuous case, where a system state may go from state x_1 at time t_1, to state x_2 at time t_2, we find the corresponding joint probability $P_2(x_1,t_1;x_2,t_2)$. This joint probability, which represents the probability that the system was in state x_1 at time t_1 and state x_2 at time t_2, is given by:

$$P_2(x_1,t_1;x_2,t_2) = P_{1|1}(x_2,t_2|x_1,t_1) \cdot P_1(x_1,t_1) \tag{3.2}$$

where $P_{1|1}(x_2,t_2|x_1,t_1)$ is the *conditional probability* that the system is in state x_2 at time t_2, given that it was in state x_1 at time t_1. Now, according to the Markov process assumption the future states of a system are dependent only on the current state of the system, and are independent of any previous states that the system may have assumed. The Markov process assumption is stated mathematically as follows:

$$P_{1|n-1}(x_n, t_n|x_{n-1}, t_{n-1}; \dots x_2, t_2; x_1, t_1) = P_{1|1}(x_n, t_n|x_{n-1}, t_{n-1}) \quad for\ t_1 < t_2 < \cdots < t_n \tag{3.3}$$

This seems to be a reasonable assumption with regards to the evolution of the cluster size. For example, consider a cluster C_1 at time t_1 containing n_1 vehicles. Next, consider a cluster C_2 at time t_2 containing n_2 vehicles, none of which were present in cluster C_1. It seems logical to assume that any future state of the cluster will be dependent only on the current state $C_2(n_2, t_2)$, and not on any previous state because the information contained in the previous state is lost as vehicles in that state leave the cluster. The Markov assumption as stated above is utilized in the derivation of the Chapman-Kolmogorov equation (Doraiswamy, et al., 1987).

3.2.2 The Chapman-Kolomogorov equations

Consider a stochastic process that goes through the states (x_1, t_1), (x_2, t_2) and (x_3, t_3), where $t_1 < t_2 < t_3$. The joint probability of being in the given states at the respective times is given by:

$$P_3(x_3, t_3; x_2, t_2; x_1, t_1) = P_{1|1}(x_3, t_3|x_2, t_2) \cdot P_{1|1}(x_2, t_2|x_1, t_1) \cdot P_1(x_1, t_1) \tag{3.4}$$

The **Chapman-Kolmogorov (C-K) equations** describe the conditional probabilities for transitions through various states. Specifically the C-K equation shown in equation (3.5) describes the conditional probability for a process beginning from a state (say state 1, (x_1, t_1)) and going to another state (say state 3, (x_3, t_3)) via transitions through all possible intermediate states (states 2,(x_2, t_2)). The C-K equation is derived from equation (3.4), and the derivation is included in Appendix 1. The C-K equation is given by:

$$\boldsymbol{P_{1|1}(x_3, t_3|x_1, t_1) = \int P_{1|1}(x_3, t_3|x_2, t_2) \cdot P_{1|1}(x_2, t_2|x_1, t_1)\, dx_2} \tag{3.5}$$

The conditional probability on the left-hand side is also referred to as the *transition probability*, because it denotes the probability of the system transitioning from state x_1 at time t_1 to state x_3 at time t_3. In this particular equation, the conditional probability represents a *two-step transition probability*, since the system goes through two steps, viz. $x_1 \rightarrow x_2$, and $x_2 \rightarrow x_3$ before arriving at the final state x_3. In order to emphasize its use as a transition probability, the conditional probability is sometimes denoted mathematically as $T_\tau(x_2|x_1)$, where $\tau = t_2 - t_1$. It must be noted that this notation is applicable only for stationary Markov processes, where the conditional probability is independent of time, and homogeneous Markov processes, for which the

conditional probability depends only on the time difference $(t_2 - t_1)$. In accordance with this mathematical notation, the two-step transition probability described by the C-K equation in equation (3.5) can be expressed as:

$$\boldsymbol{T_{\tau+\tau'}(x_3|x_1) = \int T_{\tau'}(x_3|x_2) \cdot T_{\tau}(x_2|x_1)\, dx_2} \quad (3.6)$$
$$where, \tau = t_2 - t_1, and\ \tau' = t_3 - t_2$$

Since, the eventual goal of this development is to determine a set of equations to describe the evolution of system dynamics, it is necessary to obtain a differential form of the C-K equation. The first step in determining the differential form is to represent the transition probability using a Taylor series expansion. The expansion will provide an explicit dependence on time, which will aid the development of the differential form of the C-K equation. The differential form of the Chapman-Kolmogorov equation is known as the master equation.

3.2.3 Derivation of the master equation

The derivation of the master equation from the Chapman-Kolmogorov equation is included in this section. From equation (3.6), it is known that the transition probability $T_{\tau'}(x_3|x_2)$ is a function of the variables x_2, x_3 and τ'. The transition probability can then be expanded using Taylor series around time step $\tau' = 0$, i.e. for $t_3 = t_2$. The expansion is included below in equations (3.7) and (3.8), in both mathematical notations, in order to ease understanding:

$$P_{1|1}(x_3, t_3|x_2, t_2) = P_{1|1}(x_3, t_3 = t_2|x_2, t_2) + (\tau' - 0)\frac{d}{dt}P_1(x_3, t_3 = t_2|x_2, t_2) + O(\tau'^2) \quad (3.7)$$

or, $$T_{\tau'}(x_3|x_2) = T_{\tau'}(x_3|x_2; \tau' = 0) + (\tau' - 0)\, T'_{\tau'}(x_3|x_2; \tau' = 0) + O(\tau'^2) \quad (3.8)$$

In equation (3.7) t_2 represents any arbitrarily chosen moment in time. An explanation of the terms in the Taylor expansion is in order. There are four terms each in equations (3.7) and (3.8), and these have been described below:

(a) $\boldsymbol{T_{\tau'}(x_3|x_2)\ or\ P_{1|1}(x_3, t_3|x_2, t_2)}$ **– Term on left hand side**: As has been previously mentioned, this term refers to the conditional probability that the system is in state (x_3, t_3), given that it was in state (x_2, t_2). In other words, it represents the transition probability that a system goes from state x_2 to x_3 in time $(t_3 - t_2)$. The Taylor expansion is

required to express this transition probability explicitly in terms of the time step $\tau' = t_3 - t_2$. An explicit dependence on time will allow for the development of a differential form of the C-K equation.

(b) $\boldsymbol{T_{\tau'}(x_3|x_2;\tau'=0)\ or\ P_{1|1}(x_3,t_3=t_2|x_2,t_2)}$ **– First term on right hand side**: This term is the constant term in the Taylor series expansion. It represents the transition probability of a system transitioning from x_2 to x_3, at $\tau' = 0$. In other words, the term specifies that given that the system is in state x_2 at time t_2, what is the probability that the system is in state x_3 at time t_2 itself. Clearly, since the system cannot exist in two states at the same time, this component of the transition probability is given by the Krönecker delta function, i.e.

$$T_{\tau'}(x_3|x_2;\tau'=0) = \delta(x_2 - x_3) = \begin{cases} 1, if\ state\ x_3 = x_2 \\ 0, if\ state\ x_3 \neq x_2 \end{cases} \quad (3.9)$$

To state the concept more clearly, the first term specifies the probability that the system stays in state x_2, i.e. the system does not transition to another state x_3. If the system does transition to another state, the contribution of this term towards the transition probability will be zero. Thus, the first term is a measure of the probability that a transition does not occur. In order to satisfy the normalization property of probability (sum of probabilities of all outcomes must equal 1) the term is modified as follows:

$$T_{\tau'}(x_3|x_2;\tau'=0) = (1 - \alpha_0\tau')\delta(x_2 - x_3) \quad (3.10)$$

$$where\ \alpha_0(x_2) = \int W(x_3|x_2)dx_3,\ \ and\ W(x_3|x_2) = \frac{d}{dt}T_{\tau'}(x_3|x_2;\tau'=0)$$

In the above equation $W(x_3|x_2)$ indicates the transition probability rate at $\tau' = 0$. The transition probability rate describes the manner in which the transition probability changes with time. The integral of $W(x_3|x_2)$ over all possible final states x_3 yields the total transition probability rate of the system transitioning to a state other than x_2. Consequently, the expression for the probability that the system transitions from state x_2 to any other state x_3 is given by $\tau'\alpha_0(x_2)$. Thus, the probability that the system does *not* transition to a state other than x_2 is given by $(1 - \alpha_0\tau')\delta(x_2 - x_3)$.

(c) $(\boldsymbol{\tau' - 0})\, \boldsymbol{T'_{\tau'}(x_3|x_2; \tau' = 0)}$ $\boldsymbol{or}$ $(\boldsymbol{\tau' - 0})\frac{\boldsymbol{d}}{\boldsymbol{dt}}\boldsymbol{P_1(x_3, t_3 = t_2|x_2, t_2)}$ **– Second term on the right hand side**: As mentioned above, $W(x_3|x_2)$ or $T'_{\tau'}(x_3|x_2; \tau' = 0)$ represents the transition probability rate at $\tau' = 0$. This term is a measure of rate of change of probability and has the units of per unit time. The transition probability rate describes the rate of change for the probability that the system transitions from one state to another.

(d) $\boldsymbol{O(\tau'^2)}$ **– Last term on the right hand side**: This term represents higher order terms of τ'. Since τ' is considered to be small, these higher order terms can be neglected.

Thus, the Taylor series expansion presented in equation (3.8) can be re-written as follows:

$$T_{\tau'}(x_3|x_2) = (1 - \alpha_0\tau')\delta(x_2 - x_3) + \tau' W(x_3|x_2) \tag{3.11}$$

Substituting equation(3.11) into equation (3.6), dividing by τ' and taking the limit $\tau' \to 0$, we obtain the differential form of the Chapman-Kolmogorov equation, or the **Master equation** :

$$\frac{\partial}{\partial t}T_\tau(x_3|x_1) = \int [W(x_3|x_2)T_\tau(x_2|x_1) - W(x_2|x_3)T_\tau(x_3|x_1)]dx_2 \tag{3.12}$$

The intermediate steps between equation (3.11) and (3.12) are presented in Appendix 2. The form of the Master equation presented in equation (3.12) is rather unwieldy and more intuitive form is presented below by removing the redundant indices:

$$\frac{\partial}{\partial t}P(x,t) = \int [W(x|x')P(x',t) - W(x'|x)P(x,t)]\, dx' \tag{3.13}$$

In this form, the meaning of the master equation becomes apparent. It is clear that the master equation describes the rate of change of the probability distribution of a system. The first term under the integral sign is the product of two terms: the probability that the system is in a certain state x', and the transition probability rate that the system moves from that state into the state of interest, x. Similarly the second term is also a product of two terms: the probability that the system is currently in the state of interest, x, and the transition probability rate that the system moves out of this state to another state x'.

If the states are discrete, then the meaning of the master equation becomes even more obvious. The equation transforms into the **discrete form of the Master equation**:

$$\frac{d}{dt}P(n,t) = \sum_{n' \neq n} [w(n,n')P(n',t) - w(n',n)P(n,t)] \quad (3.14)$$

where, $w(n,n')$ = Transition probability rate of the system transitioning from state n' to state n

$P(n',t)$ = Probability that the system is in state n' at time t

$w(n',n)$ = Transition probability rate of the system transitioning from state n to state n'

$P(n,t)$ = Probability that the system is in state n at time t

The discrete form of the master equation makes the gain-loss nature of the equation more apparent, and is shown in Figure 15. In the context of the problem of cluster formation, given a cluster of n vehicles, it represents a measure of the difference between the rate at which the system leaves the state n to go to another state n', and the rate at which the system joins the state n from another state n', summed over all possible states n'. In other words, the master equation represents a difference between the inflow of the system into state n and the outflow of the system to states n'. It may also be observed that the transition probability rates $w(n,n')$ and $w(n',n)$, are greater than zero. The rates may also be greater than 1, since they only represent the rate at which the probability changes and not probabilities themselves.

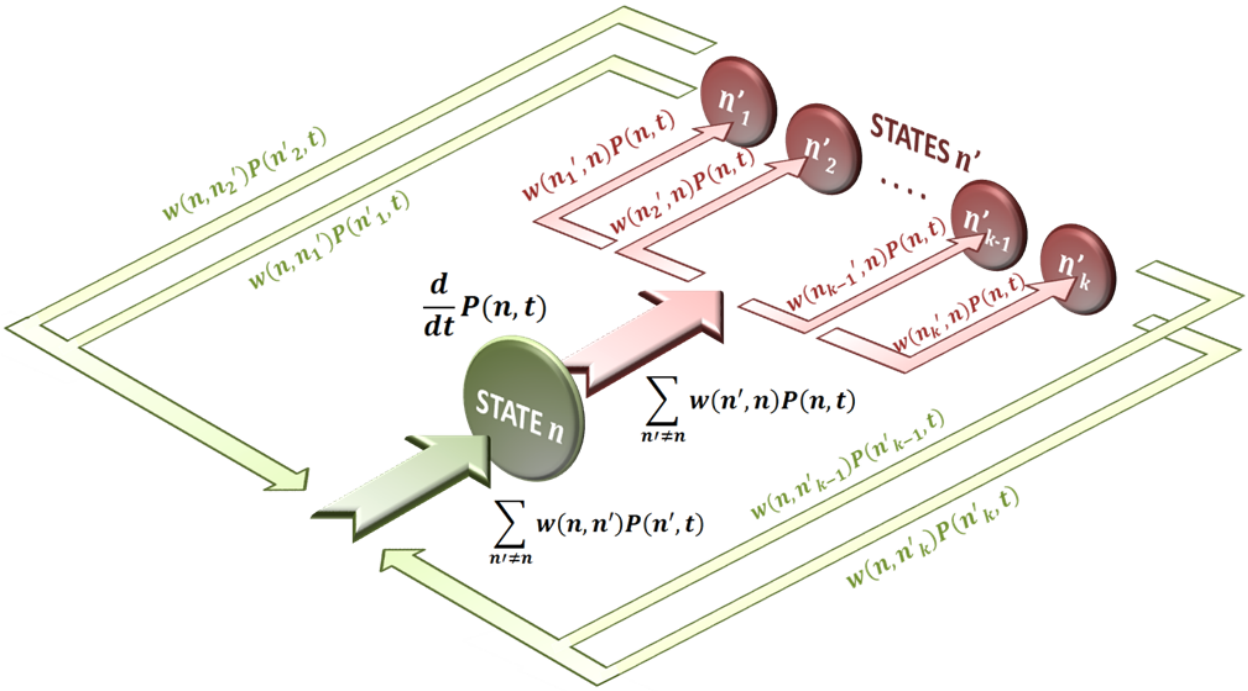

Figure 15: Rates of transition between various states describe the discrete form of the master equation

In this section, the master equation and its development was described. The study of the steady state is the next most intuitive step. The steady state is of interest because, left to its own, the system tends to self-organize itself and eventually reach this state (Nicolis, et al., 1977). The master equation is used to determine the steady state (or *stationarity* condition) of the system.

3.3 Stationarity and detailed balance

As mentioned before, the steady state is a result of the self-organization process inside the system. For example, after an avalanche has occurred, the system (in this case, the snow particles on the mountain slope) tends to self-organize itself back into a steady state (in this case, the critical slope). Similarly, it is of interest to observe the steady state that the self-organizing traffic jam or vehicle cluster eventually settles into. It must be pointed out here that the steady state must not be confused with equilibrium. Agents inside the system may continue to interact and transition between various states and the system may continue to operate far-from-equilibrium, even in steady state (Nicolis, et al., 1977). The concepts regarding steady state in equilibrium and non-equilibrium systems, specifically the concept of detailed balance, are discussed in this section.

3.3.1 Stationarity condition

The *stationarity* condition, or the steady state, is defined as the state of the system when the rate of change of probability $P(n,t)$ is zero. The stationary probability distribution, $P^{st}(n)$, corresponding to the steady state is then a time-independent distribution, such that:

$$\frac{d}{dt}P(n,t)|_{P=P^{st}} = 0$$

Consequently, the stationary master equation is given by:

$$0 = \sum_{n' \neq n} [w(n,n')P^{st}(n') - w(n',n)P^{st}(n)] \tag{3.15}$$

The significance of the stationary master equation is that it indicates that, in steady state, the sum of all transitions from state n to all other states n', must be balanced by the sum of all transitions from all other states n' to the state n. Note that the stationarity condition does not preclude the existence of a non-equilibrium process. In other words, the fact that the rate of

change of probability of a given state is zero does not imply that the system is in equilibrium. The stronger condition of detailed balance is discussed next.

3.3.2 Detailed balance

The stationarity condition discussed above puts a constraint on the manner in which a system may transition between states. The stationarity condition requires only that the sum of transitions from one state to all other states be equal to the sum of transitions from all other states to the one state. Detailed balance, on the other hand, places a much stronger condition on the system. Specifically, the condition of detailed balance states that the rate of transition from a first state to a second state must equal the rate of transition from the second state to the first state, for every pair of states. In fact, the condition of detailed balance can be used to describe a system in equilibrium. Mathematically, for each pair of states n and n':

$$0 = w(n, n')P(n', t) - w(n', n)P(n, t) \tag{3.16}$$

At this point, one may observe the difference between the stationarity and detailed balance conditions. It is obvious that the detailed balance condition also satisfies the stationarity condition. Consider an example of three states of a system; say states A, B and C. Under the detailed balance condition, i.e. in equilibrium, the proportion of the system in each of these states remains constant. The detailed balance condition is illustrated in Figure 16(a). On the other hand, the stationarity condition only requires that the sum of all transitions to and from a state remain the same. This weaker condition allows for changing proportions of the system in any given state. A stationarity condition that violates detailed balance is illustrated in Figure 16 (b).

(a) Detailed balance holds. Proportion of states remains constant and system is in thermal equilibrium.

(b) Detailed balance is violated. Constant flux of states is observed, even in steady state.

Figure 16: Difference between stationarity and detailed balance conditions. Length of arrows indicates transition rates.

It may seem odd to discuss the condition corresponding to thermal equilibrium when the system under consideration is essentially undergoing a non-equilibrium process (spontaneous pattern formation). In the yet-developing field of non-equilibrium thermodynamics, it is known that, in general, non-equilibrium processes violate the detailed balance condition (Ebeling, et al., 2005). However, in order to analyze non-equilibrium systems, usually one of two assumptions is made; the one of interest here being that the condition of detailed balance holds away from equilibrium (Evans, 2005). In the problem at hand, Mahnke suggests that though the probability distributions for different vehicle cluster states may initially be indicative of strong non-equilibrium, they eventually tend towards a final equilibrium state. Mahnke proposes analyzing the non-equilibrium behavior as a sequence of (quasi-) equilibrium states. Specifically, it is suggested that even "if the initial probability vector $P(n,0)$ is strongly nonequilibrium, many probabilities $P(n,t)$ change rapidly as soon as evolution starts (short-time regime), and then relax more slowly towards equilibrium (long-time behavior). The final thermodynamic equilibrium is reached in the limit $t \to \infty$" (Mahnke, et al., 2003). Such behavior has been studied by Miller (Miller, et al., 1999). The final equilibrium state referred to here is a stable cluster that neither increases nor diminishes in size.

Thus vehicle cluster formation may be analyzed as progressing through a series of equilibrium states and we may model the cluster formation as a one-dimensional random walk, with the one dimension being the cluster size. Further, it is assumed that a vehicle cluster only transitions between the nearest states at every time step, i.e. the system can only transition from $n \to n \pm 1$ in one time step, where n denotes the number of vehicles present in the cluster. Further, the cluster size may increase and decrease in the same time step so that the size remains unchanged. This would correspond to a transition of the form $n \to n$. In such a framework, the discrete master equation reduces to:

$$\frac{d}{dt}\boldsymbol{P}(\boldsymbol{n},\boldsymbol{t}) = \boldsymbol{w}_{+}(\boldsymbol{n}-\boldsymbol{1})\boldsymbol{P}(\boldsymbol{n}-\boldsymbol{1},\boldsymbol{t}) + \boldsymbol{w}_{-}(\boldsymbol{n}+\boldsymbol{1})\boldsymbol{P}(\boldsymbol{n}+\boldsymbol{1},\boldsymbol{t}) - [\boldsymbol{w}_{+}(\boldsymbol{n}) + \boldsymbol{w}_{-}(\boldsymbol{n})]\boldsymbol{P}(\boldsymbol{n},\boldsymbol{t}) \quad (3.17)$$

where, $w_{+}(n-1)$ = $w(n-1,n)$, corresponding to transition from state n to $n-1$

$w_{-}(n+1)$ = $w(n+1,n)$, corresponding to transition from state n to $n+1$

$w_{+}(n)$ = $w(n,n-1)$, corresponding to transition from state $n-1$ to n

$w_{-}(n)$ = $w(n,n+1)$, corresponding to transition from state $n+1$ to n

The system under consideration is a finite system, with $n = 0,1, \dots N$, where n denotes the number of vehicles present in a cluster and N denotes the total number of vehicles on the road. Thus, in addition to equation (3.17), two boundary conditions are required at the maximum and minimum cluster sizes. The boundary conditions are given by:

$$\frac{d}{dt}P(0,t) = w_{-}(1)P(1,t) - w_{+}(0)P(0,t)$$
$$\frac{d}{dt}P(N,t) = w_{+}(N-1)P(N-1,t) - w_{-}(N)P(N,t) \quad (3.18)$$

At this point it is realized that further analysis should be preceded by the determination of the expressions for the transition probability rates, viz. $w_{+}(n-1), w_{-}(n+1), w_{+}(n)$ and $w_{-}(n)$. The next chapter (Chapter 4) details how the transition rates for the discrete master equation were determined and also mentions the drawbacks of the transition rates employed by Mahnke in (Mahnke, et al., 1997). The determination of transition rates is followed up by the steady state solution for vehicle cluster dynamics. The steady state analysis serves to achieve the goal of determining a relation between vehicle density and average cluster size. Details about the steady state analysis and development of the relationship between vehicle density and average cluster size are included in chapter 5.

CHAPTER 4
TRANSITION PROBABILITY RATES

In the previous chapter the basic framework of the master equation approach was discussed and its application to the vehicle cluster formation phenomenon was introduced. In order to proceed further with the analysis of cluster dynamics, the transition probability rates need to be determined. In this chapter, the transition probability rates used by Mahnke (Mahnke, et al., 1997) for analyzing vehicle clusters on a road are discussed, and their limitations are mentioned. An alternative approach for determining the transition probability rates is then proposed, and expressions for the new rates are calculated.

4.1 Transition probability rates proposed by Mahnke

The transition probability rates, or simply transition rates, proposed by Mahnke are based upon the so-called Optimal Velocity Model (OVM) suggested by Bando (Bando, et al., 1995). This section discusses these transition rates and their limitations.

4.1.1 Optimal Velocity Model

The Optimal Velocity Model is a recent car-following model proposed by Bando (Bando, et al., 1995), and is described by the following equation:

$$\ddot{x}_n = a\{v_{opt}(h) - \dot{x}_n\} \tag{4.1}$$

where,

x_n	=	Position of the vehicle
h	=	$\Delta x_n = x_{n+1} - x_n$, headway to the preceding vehicle
$\dot{x}_n$	=	Current velocity of the vehicle
$\ddot{x}_n$	=	Control effort, or acceleration
a	=	Constant representing driver's sensitivity
$v_{opt}(h)$	=	"Optimal velocity" which is a function of headway

As can be seen, the two model parameters that define the control effort on the vehicle are the sensitivity of the driver, a, and the optimal velocity function, $V(h)$. It is evident that the control law proposed by this model is independent of the relative velocity between the following and

preceding vehicles. The absence of dependence on relative velocity causes vehicles to crash in traffic flow simulations (Nagatani, 2002). The presence of crashes in numerical simulations is a cause for concern because it limits the potential use of this control law in ACC vehicles. Further, the optimal velocity function is usually chosen to have an elegant mathematical form, and calibration is performed using real traffic flow data from highways to fit the function to the data. In other words, the function eventually represents an empirical relation fitted specifically to the data for a given segment of a highway (Bando, et al., 1995). The calibration required for fitting the model causes a loss of generality and reduces the portability of the model across various scenarios.

The optimal velocity function originally proposed by Bando was:

$$V(h) = \tanh(h - 2) + \tanh(2) \tag{4.2}$$

A fit for the above optimal velocity function for data obtained from the Chuo motorway, Japan is shown in Figure 17. Several limitations of the OVM have already been pointed out, and these limitations carry over when the model is used for calculating transition rates.

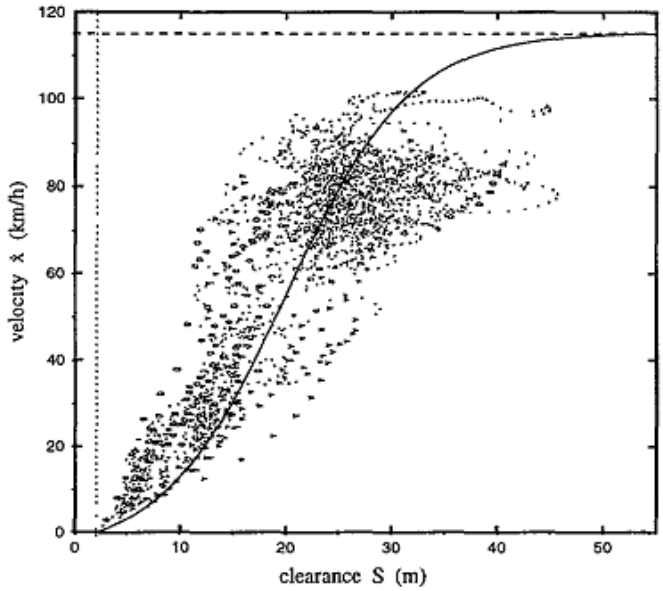

Figure 17: Velocity vs. headway data from a car-following experiment on the Chuo motorway (Koshi, et al., 1983), as presented in (Bando, et al., 1995)

4.1.2 Transition rates proposed by Mahnke

In (Mahnke, et al., 1997), Mahnke and Pieret have used the sigmoid function described below as the optimal velocity function.

$$V(h') = \frac{(h')^2}{d^2 + (h')^2} \tag{4.3}$$

where, h' = Normalized headway, h/l, where l = effective length of vehicle

d = Interaction distance, (D/l), where D = headway corresponding to $v_{max}/2$

$V(h')$ = Ratio of optimal velocity ($v_{opt}(h')$) to maximum free flow velocity v_{max}. i.e. $V(h') = v_{opt}/v_{max}$

The optimal velocity function can be re-written as follows without any normalizing factors:

$$v_{opt}(h) = \frac{(h)^2}{D^2 + (h)^2} v_{max} \tag{4.4}$$

The optimal velocity function is used to find the expression for the velocity of a vehicle at any point in the closed ring road, based on the headway to the preceding vehicle. The expression for velocity is then used to determine the transition rate. Two expressions for the transition probability rates are required in order to proceed with the steady state analysis of cluster dynamics. These are:

(a) $w_+(n)$, the transition rate of a system joining the state n. In the present context, this corresponds to a car in free flow joining a cluster of size n vehicles, i.e. a car entering a traffic jam.

(b) $w_-(n)$, the transition rate of a system leaving the state n. In the present context, this corresponds to a car leaving a cluster of size n vehicles and entering free flow, i.e. a car exiting a traffic jam.

Transition probability rate for joining a cluster, $w_+(n)$

Mahnke has proposed the following expression for the transition probability rate for joining a cluster of size n:

$$w_+(n) = \frac{bl}{\tau_{rel}} \frac{v_{opt}\left(h_{free}(n)\right) - v_{opt}(h_{clust})}{h_{free}(n) - h_{clust}} \tag{4.5}$$

where, $h_{free}(n)$ = Headway in free flow when n vehicles are present in cluster (in meters)

h_{clust} = Headway inside cluster (observed data indicates its value ≈ 1 m)

τ_{rel} = Relaxation time (in seconds)

b = Dimensionless constant = $v_{max}\,\tau_{rel}\,/l$

It may be observed that the transition rate has units of (1/s). Further, one may notice that the dependence of the transition rate on the cluster size is implicit. The transition rate depends on the free flow velocity, which in turn depends on the free headway. It is the free headway that is directly dependent on the cluster size. It is known that the total number of vehicles (N) on the closed ring is fixed, as is the headway inside a cluster $(h_{clust} = 1m)$. Thus, as the number of vehicles present in a cluster increases, there is more space available for the rest of the vehicles on the remaining stretch of the road. Consequently, as the cluster size increases, the free headway also increases.

The above expression for the transition rate may be expressed in a simpler fashion as follows, to truly express the idea behind its development:

$$w_+(n) = K\frac{v_{free}\,(n) - v_{clust}}{h_{free}\,(n) - h_{clust}} = Constant \times \frac{Relative\ velocity}{Distance\ traveled} \qquad (4.6)$$

where, $v_{free}\,(n)$ = Optimal velocity corresponding to free headway

The above simplification makes apparent the reasoning behind this expression for the transition rate. The expression is obtained from simple kinematic relations for time taken for one particle to collide with another particle. In other words, the time taken to join a cluster is given by the total distance traveled divided by the speed of the vehicle. With reference to Figure 18, the cluster joining process is considered as a collision between two particles, particles A and B. The time taken for particle A to cover the requisite distance to "collide" with particle B, or come within cluster distance (h_{clust}) of particle B is given by:

$$t_{join} = \frac{Distance}{Speed} = \frac{h_{free} - h_{clust}}{v_{free} - v_{clust}}$$

Consequently, the transition probability rate is given by the inverse of the time to join the cluster, and is of the same form as shown in equation (4.5):

$$w_+(n) = \frac{1}{t_{join}} = \frac{v_{free} - v_{clust}}{h_{free} - h_{clust}}$$

Thus, the situation of "joining" a cluster in fact refers to "colliding" with the tailing vehicle in the cluster. It is evident from the paraphrased equation that the velocity of the vehicle joining

the cluster is assumed to be constant till the vehicle reaches the cluster. However, it is known from car-following theory that as vehicles come closer to a preceding vehicle, some form of control effort is applied to regulate their motion, i.e. they tend to slow down and adjust for the decreased headway. In fact, this adjustment procedure forms the foundation of adaptive cruise control and general human driving behavior. One may observe that the OVM does suggest an adjustment procedure in the form of changing the acceleration based on a vehicle's headway and velocity. In fact, the OVM is a statement of the control effort that must be applied to a vehicle in order to follow a preceding vehicle at a desired speed. The control effort is proportional to the error signal $(v_{opt}(h) - \dot{x}_n)$. However, this approach has not been utilized in (Mahnke, et al., 1997), which uses a constant "optimal" speed approach instead. Thus, it is obvious that the assumption of constant speed used to determine the transition rate, which has been used by Mahnke, does not adequately capture car-following behavior. The observation suggests that the corresponding transition rates used to model the cluster joining or aggregation process do not represent that process accurately. This is an important observation since the aggregation process is central to the analysis of vehicle cluster dynamics.

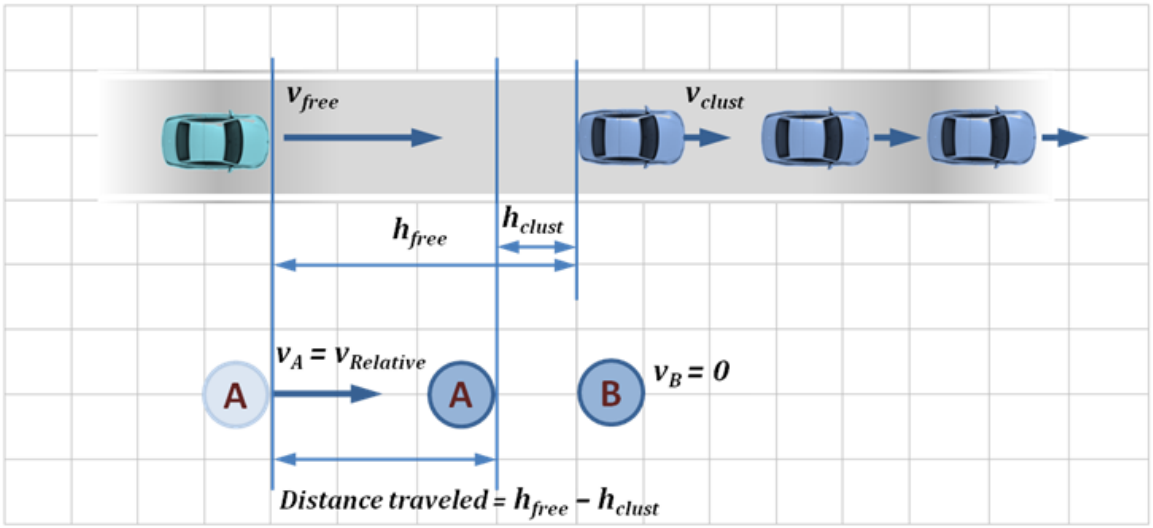

Figure 18: Cluster joining as a collision process. The equivalent particle collision problem assumes that particle A maintains a constant velocity till it collides with particle B.

Transition probability rate for leaving a cluster, $w_-(n)$

The transition probability rate for leaving the cluster is defined as a constant by Mahnke. This seems to be a reasonable assumption, because when a vehicle is leaving a cluster, there usually aren't any vehicles ahead of it. Even if vehicles are present, they are themselves accelerating away from the cluster and do not interact with the vehicle just leaving the cluster.

Consequently, the time it takes for a vehicle exiting a traffic jam to return to free flow is independent of other vehicles to quite an extent. Thus, the transition probability rate for leaving a cluster is given by:

$$w_{-}(n) = \frac{1}{\tau_{rel}} = constant \tag{4.7}$$

4.1.3 Limitations of transition rates proposed by Mahnke

The limitations of the transition rates employed by Mahnke and Pieret, and their lack of suitability for use in a problem concerning ACC vehicles have been mentioned at various points in this sub-section. These limitations are summarized below:

- **Transition rate $w_{+}(n)$ is not representative of true traffic behavior**: The transition rate for joining the cluster has been shown to be derived from an equivalent collision process. The collision process is not representative of true driver behavior, human or otherwise. In fact, the assumptions upon which the transition rate expression is based suggests that the vehicle deceleration is infinite when the headway of the vehicle becomes equal to the cluster headway. Clearly this assumption is not valid and a new expression for transition rate $w_{+}(n)$ must be determined.
- **Inappropriate use of Optimal Velocity Model**: The transition rate for joining the cluster is based on the inherent assumption that vehicles maintain an optimal velocity in traffic flow. The way in which the OVM has been used in determining the transition rate expression, does not include the true essence of the model. The OVM does not propose that the velocity of vehicles is equal to the "optimal" velocity function at all times, rather it states that vehicles try to attain the "optimal" velocity based on their current velocity and headway. On the contrary, the study of (Mahnke, et al., 1997) uses the optimal velocity function as the ground truth for vehicle velocity, and does not account for the dynamics of the control effort. Clearly this is an erroneous use of the model.
- **Limitations of the Optimal Velocity Model**: Even if the OVM is used appropriately, it is known that the model itself is prone to failure, in the sense that the model's lack of dependence on relative velocity causes vehicles to crash in simulations. Clearly this is undesirable. Another car-following model must be utilized to determine the correct expression for transition probability rate for joining a cluster.

4.2 New transition probability rates

Many limitations of the earlier approach have been discussed in the previous section. In this section it is sought to improve upon some of those limitations in order to obtain better expressions for transition rates. As a first step, a different car-following model is chosen that is known to well represent traffic flow behavior. Next, the car-following model is used to find the time taken to join a cluster for a set of typical traffic conditions. This is followed by the determination of an expression for transition probability rate that is better representative of true traffic behavior.

4.2.1 General Motors' fourth model

As was mentioned in section 2.3, the research group at General Motors proposed a set of five car-following models. The fourth GM model was representative of the car-following behavior to a good extent (Brackstone, et al., 1999), without containing added complexity and parameters, as in the fifth GM model. The fourth GM model is presented below:

$$\ddot{x}_{n+1}(t + \Delta t) = \frac{\alpha\,[\dot{x}_{n+1}(t + \Delta t)]}{[x_n(t) - x_{n+1}(t)]}\left(\dot{x}_n(t) - \dot{x}_{n+1}(t)\right) \tag{4.8}$$

where, x_{n+1} = Position of the $(n+1)^{th}$, or following, vehicle

x_n = Position of the n^{th}, or leading vehicle

α = Sensitivity coefficient, or driver's sensitivity (dimensionless)

The GM fourth model represents a second-order nonlinear ordinary differential equation (ODE). Assuming that the reaction time delay can be neglected, i.e. $\Delta t = 0$, the ODE can be written as:

$$\ddot{x}_{n+1}(x_n - x_{n+1}) + \alpha\dot{x}_{n+1}^2 - \alpha\dot{x}_{n+1}\dot{x}_n = 0,$$

where the dependence of the variables on time is implicit. In the present context, x_{n+1} denotes the position of the vehicle entering the cluster, and x_n denotes the position of the vehicle inside the cluster. Since it is assumed that the vehicle inside the cluster is either stationary or moving with a slow constant velocity, its velocity $\dot{x}_n$ is assumed to be a constant, v_c. Thus, the ODE describing the motion of a vehicle entering a cluster may be re-written as $\ddot{x}_{n+1}(x_{n+1} - x_n) + \alpha\dot{x}_{n+1}^2 - \alpha v_c\dot{x}_{n+1} = 0$, where v_c is the "cluster velocity". When applied to the situation of a vehicle joining a cluster, the solution to this differential equation has the potential to yield the time taken to join a

cluster. Once the time taken to join the cluster is obtained, it is a simple task to obtain the transition rate $w_+(n)$.

However, there is still a bone of contention in the model description. While the constant v_c may be determined from observation, or an intuitive sense of traffic jam behavior ($v_c \approx 0 - 2\ m/s$), the range of values for the driver sensitivities (α) aren't firmly established. In order to determine the necessary range, one must consider the scenarios which constrain the values that the driver sensitivity may attain. Looking deeper into equation (4.8), one observes that if $\alpha = 0$ there is no deceleration effort on the part of the driver, even as it approaches a stationary vehicle in the cluster. This scenario implies an imminent collision or the requirement of an infinite deceleration effort to avoid a collision. The situation is similar to the Mahnke approach, whose limitations were discussed in the previous approach. As driver sensitivity (α) begins to increase, the control effort also increases, implying an increasing amount of deceleration applied to the vehicle. However, it is obvious that there is a range of deceleration values that is considered acceptable for passenger vehicles. According to the AASHTO (American Association of State Highway and Transport Officials) standards, the maximum value of acceptable deceleration for passenger vehicles is $3.4\ m/s^2$ (Wang, et al.). Collision avoidance studies usually assume the maximum possible deceleration values to be $8\ m/s^2$ (Seiler, et al., 1998). However, since the problem at hand considers normal traffic flow and car-following behavior, and not any exigent circumstances, the values from collision avoidance studies will not be used. Thus, the values of driver sensitivities (α) will be limited by a maximum possible deceleration value of $3.4\ m/s^2$.

In order to determine the range of possible values of driver sensitivities, one must solve the ODE for the GM fourth model for different values of α. In this manner, one would be able to determine the values of α for which the deceleration does not exceed $3.4\ m/s^2$ at any time in the cluster joining process. The ODE is solved using the simplest numerical integration scheme, viz. the Euler method, for a range of α values (Strogatz, 2000). The time step used in the solution is 0.01 seconds. The typical traffic flow conditions that have been used as the initial conditions in the numerical simulation are:

(a) Free flow velocity, $v_{free} = \dot{x}_{n+1}(t = 0) = 25 m/s \approx 55\ miles/hr$

(b) Free headway, $h_{free} = [x_{n+1}(t = 0) - x_n(t = 0)] = 100\ m$. The free headway is actually the approximate interaction distance at which a following vehicle may begin to brake to avoid a collision (Helbing, et al., 1998).

(c) Cluster velocity, $v_c = \dot{x}_n(t = 0) = 0\ to\ 2\ m/s$. A very small value of cluster velocity is taken instead of $v_c = 0$ to avoid irregularities that may be caused in the numerical solution when the vehicle entering the cluster reaches very close to $v_c = 0$.

This set of initial conditions completes the requirements for performing the numerical solution. The MATLAB code used for the simulation is presented in Appendix 3. The numerical solutions are presented here for two cases with $\alpha = 0.3$ and with $\alpha = 0.7$ (Figure 19 and Figure 20). The cluster velocity v_c is taken to be $2\ m/s \approx 4\ miles/hr$, in order to provide a meaningful comparison. The results are discussed below.

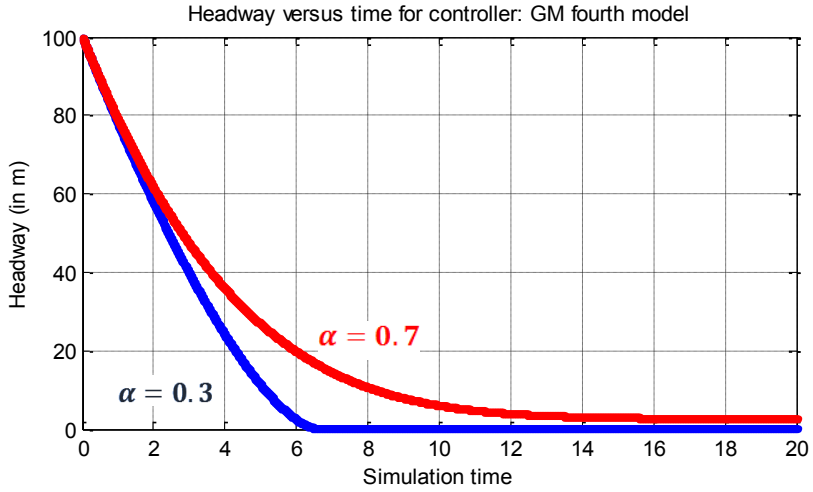

(a) Vehicle headway versus time. The vehicle joins the cluster faster for lower values of driver sensitivity α

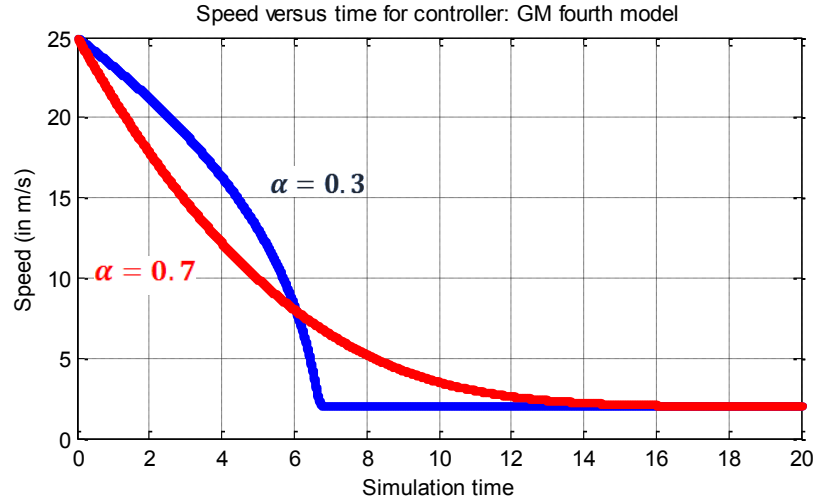

(b) Vehicle velocity versus time. The vehicle appears to have a higher mean velocity for lower values of driver sensitivity α.

Figure 19: Vehicle headway and vehicle velocity versus time. Simulations have been performed for driver sensitivities $\alpha = 0.3$ and $\alpha = 0.7$

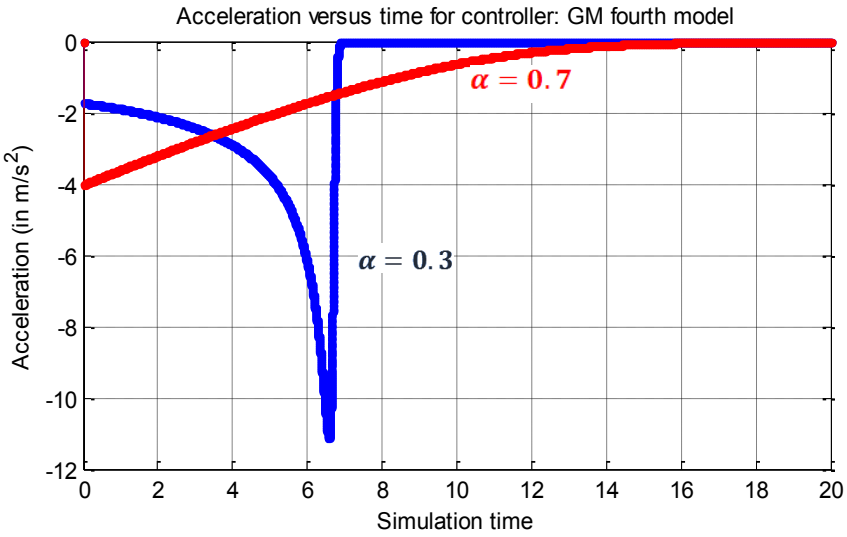

(a) Vehicle acceleration versus time. Drivers with low sensitivities apply a control effort later than drivers who are sensitive to the situation.

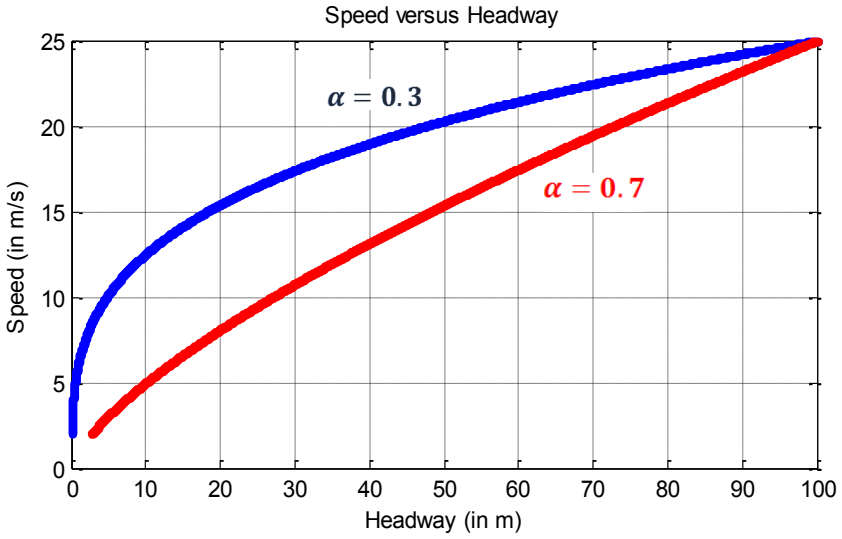

(b) Vehicle speed versus vehicle headway

Figure 20: Vehicle acceleration versus time and vehicle speed versus vehicle headway for driver sensitivity value $\alpha = 0.3$ and $\alpha = 0.7$

Effect of driver sensitivity on time to join a cluster

The impact of driver sensitivity on time to join a cluster is now discussed. Specifically, the effect on the deceleration as a vehicle approaches a cluster is observed. Figure 19 describes how the headway and velocity vary as a vehicle joins the cluster. For low driver sensitivities, it observed that the vehicle maintains a higher velocity throughout the cluster joining process, and as a result reaches the cluster faster than when higher driver sensitivities are involved. Specific to the simulation, it is observed that for the vehicle which is driven by a driver with sensitivity $\alpha = 0.3$, the

vehicle joins the cluster (reaches cluster headway) in just 6 seconds. On the other hand, a vehicle driven by a driver who is aware of the situation ($\alpha = 0.7$) joins the cluster in 15 seconds. In fact, the aware or "alert" driver reaches the cluster headway asymptotically, unlike the "sleepy" driver, who reacts slowly and joins the cluster quickly.

The difference in "alertness" level of the drivers is made evident in Figure 20(a). The "sleepy" driver does not decelerate enough initially, and consequently, has to apply an extremely large deceleration effort of the order of $10\ m/s^2$ later to avoid a collision with the cluster. On the other hand, the "alert" driver applies a deceleration effort as soon as he/she detects that a cluster is forming ahead. As a result, the largest deceleration effort that the "alert" driver ever applies is the one he/she applies initially. It will be shown later in Chapter 5, that low driver sensitivities (corresponding to "sleepy" drivers) are indicative of true human driving behavior, based on observations from German highways. It is reasonable to expect that human drivers have lower sensitivities because humans perform numerous activities simultaneously, and are not solely dedicated to the task of driving a vehicle, or following another car. On the other hand, it is also reasonable to expect that driver models for computer-based ACC vehicles have high sensitivities because they are dedicated to the task of driving alone. Further, the driver sensitivity in an ACC vehicle is a controllable quantity, and may be adjusted by the manufacturer. Further, it is useful to utilize the worst-case human drivers (with the lowest permissible driver sensitivities) as a basis for deciding the improvement in traffic flow offered by inclusion of ACC vehicles (with higher driver sensitivities). In the remainder of this thesis, human drivers are considered to have low driver sensitivities, while ACC vehicles are considered to have high driver sensitivities.

Driver sensitivities under consideration

The numerical solution for the nonlinear ODE is repeated for various driver sensitivities. The plot for the maximum deceleration versus driver sensitivity (α) is included in Figure 21. The maximum deceleration values indicate that values of driver sensitivities in the range $[0.4, 0.65]$ form an adequate interval for consideration according to AASHTO standards.

Thus, the range of sensitivity values for which the GM fourth model is applicable on a highway with the typical traffic conditions is $[0.4, 0.65]$. Next, the expression for time to join a cluster is obtained and the effect of sensitivity values on the quantity is identified analytically.

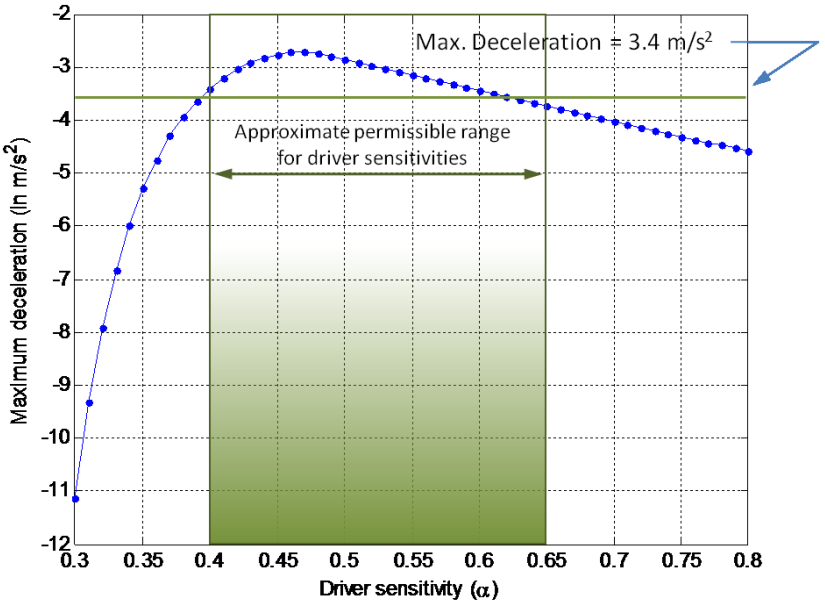

Figure 21: Maximum deceleration values indicate the range of permissible driver sensitivities

4.2.2 Proposed transition rates

In the previous sub-section the permissible range of driver sensitivities was obtained. In this sub-section, the time to join a cluster is obtained as a closed form expression in terms of the driver sensitivity and other pertinent variables. The expression for the transition rate $w_+(n)$ is then determined.

Simplified GM fourth model

As a first step, the nonlinear ODE that describes the GM fourth model is solved to obtain an analytical expression for vehicle headway as a function of time. This step is followed by determining the time taken to proceed from free flow (with headway h_{free}) to a clustered state (with headway $h_{clust} = 1m$). The GM fourth model ODE is first modified to ease analysis by neglecting the reaction time, i.e. assuming $\Delta t = 0$. The modified model equation is included below:

$$\ddot{x}_{n+1}(t) = \frac{\alpha\,[\dot{x}_{n+1}(t)]}{[x_n(t) - x_{n+1}(t)]}\left(\dot{x}_n(t) - \dot{x}_{n+1}(t)\right) \tag{4.9}$$

It is further realized that the term, $x_n(t) - x_{n+1}(t)$, in the denominator represents the vehicle headway at time t. Since the primary variable of interest is the headway, $h(t) = x_n(t) - x_{n+1}(t)$, the remaining variables in the equation are also expressed in terms of $h(t)$. Thus, the terms in the above equation can be re-written as follows:

(a) $x_n(t) - x_{n+1}(t) = h(t)$,

(b) $\dot{x}_n(t) - \dot{x}_{n+1}(t) = \dot{h}(t)$. Assuming that the cluster velocity $\dot{x}_n(t) = v_c$ is constant, this term translates to $v_c - v(t) = \dot{h}(t)$, where $v(t) = \dot{x}_{n+1}(t)$ is the velocity of the vehicle joining the cluster.

(c) $\ddot{x}_{n+1}(t) = \ddot{x}_n(t) - \ddot{h}(t)$. However, $\dot{x}_n(t) = v_c$ is constant, therefore $\ddot{x}_n(t) = 0$ and this term reduces to $\ddot{x}_{n+1}(t) = -\ddot{h}(t)$.

Thus, equation (4.9) can now be expressed in terms of the headway to the preceding vehicle, or the headway to the cluster. Suppressing the explicit dependence on time, the equation reduces to:

$$h\ddot{h} = \alpha(\dot{h} - v_c)\dot{h} \tag{4.10}$$

The above equation is then solved to determine the time taken for a vehicle to reach a certain headway. While solving the differential equation, one also reaches an intermediate result of importance, which is the relationship between the headway and the velocity. The relationship is presented below and its derivation is included as an intermediate result in Appendix 4.

$$v(t) = k[h(t)]^{\alpha}, \ where\ k = v_{max}/h_{br}^{\alpha} \tag{4.11}$$

where, $v(t)$ = Vehicle velocity at time t

$h(t)$ = Vehicle headway at time t

v_{max} = Maximum vehicle velocity

h_{br} = Free headway, or headway at which braking interaction becomes significant

It may be observed that the constant k is dependent on the driver sensitivity α. Specifically, as the driver sensitivity increases, the constant k decreases. This inverse relationship indicates that given two drivers traveling at the same velocity, the alert driver will tend to maintain a larger headway as compared to the "sleepy" driver. This inference provides a glimpse of why alert ACC-driven vehicles may turn out to be better than "sleepy" drivers. Next, the expression for time taken to reach headway h is calculated.

Time taken to join a cluster

The solution to the GM fourth model, with the initial condition $h(0) = h_{free}$, yields the following expression for the time taken to reach a particular headway. The intermediate steps between equation (4.10) and equation (4.12) are included in Appendix 4.

$$t(h) = \frac{1}{v_c} \sum_{m=1}^{\infty} \left\{ \frac{1}{1 - m\alpha} \left(\frac{v_c}{k} \right)^m \left(h_{free}^{1-m\alpha} - h^{1-m\alpha} \right) \right\} \quad (4.12)$$

where, $t(h)$ = Time taken by following vehicle to reach headway h

h_{free} = Headway of following vehicle in free flow = h_{br}

v_c = Constant cluster velocity

k = Driver dependent constant, ($= v_{max} / h_{free}^{\alpha}$)

Since the obtained expression is an infinite series, it is desirable to know the behavior of the series. For this reason, the time taken to reach a particular headway is plotted for various number of terms included in the calculation of time. In other words, in the first run, the time is calculated using only the first term; in the second run, it is calculated using two terms and so on. Further, in order to verify the expression, the time obtained from the above expression is plotted over the headway versus time plot obtained from the numerical simulation. The plots are included as Figure 22. It is evident that as the number of terms used in calculating the time is increased, the value from the expression approaches that from the numerical simulation. The MATLAB code for calculating the time taken to join the cluster is included in Appendix 5.

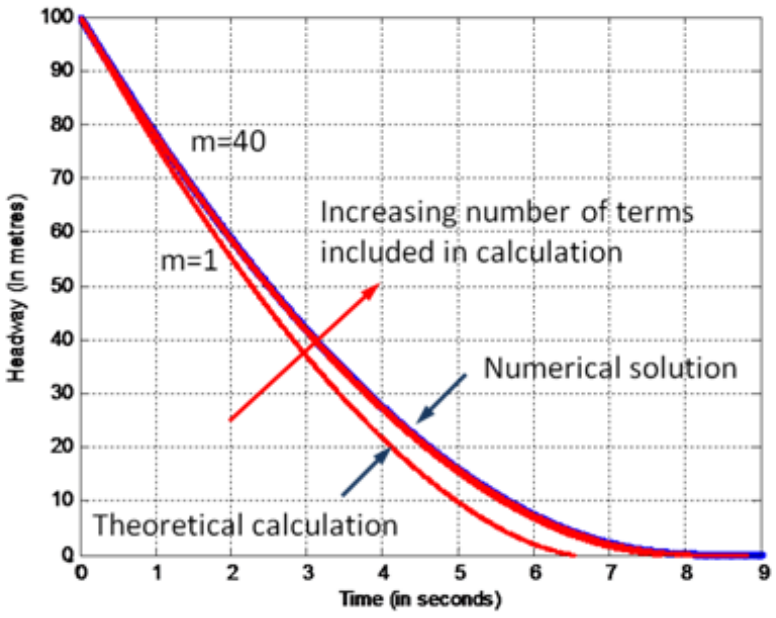

Figure 22: Time to join cluster – verification of theoretical expression using numerical solution. As number of terms included (m) increases from 1 to 40, the theoretical expression converges quickly to the numerical solution.

It may be observed that the expression in equation (4.12) describes a *hypergeometric* series. A hypergeometric series is essentially a power series for which the coefficients of the power terms are themselves a rational function of the power index. A general form of the hypergeometric series is as follows:

$$F(a,b;c;z) = 1 + \frac{ab}{c}z + \frac{a(a+1)b(b+1)}{c(c+1)}z^2 + \cdots \tag{4.13}$$

As can be seen the coefficients of the terms are rational functions of the degree of the variable term. In the above expression for hypergeometric series, one observes that the numerator is a polynomial whose degree is dependent on the power of the variable term. For example the coefficient of z^2 is the polynomial $(a^2b^2 + a^2b + ab^2 + ab)$, which is dependent on the power of the variable term (z), which is 2. Similarly the denominator is also a polynomial whose degree is dependent on the power of the variable term. Thus the coefficients are rational functions of the power or degree of the variable terms. In the present context and with reference to equation (4.12), the coefficient $1/(1 - m\alpha)$ is the rational coefficient dependent on the degree m of the variable term. The hypergeometric series are usually studied as infinite sums or infinite products, and a closed form for the infinite sum may not exist, like it does for an infinite geometric progression (Gasper, et al., 2004). Certain hypergeometric series may result in special functions such as the Bessel function, whose sum at various parameter values may be well known. For example, if $\alpha = 1$, the solution to the simplified GM fourth model results in a logarithmic series. However, in general, a closed form for the infinite sum of a hypergeometric series is extremely hard to find.

In such a scenario, it may seem that the time taken to reach a particular headway, such as the cluster headway h_{clust}, cannot be calculated. However, it may be observed that the series shown in equation (4.12) is convergent as long as $(v_c/k)h^{-\alpha} < 1$.[1] Since it is known that the series is convergent for the said values, it is possible that an approximate total time taken to reach a cluster may be obtained. Successively larger number of terms in the infinite hypergeometric series may be taken in order to determine the total time taken to join a cluster.

[1] On a related note, the convergence condition may be re-written as $v_c h_{br}^{\alpha} < v_{max} h^{\alpha}$. The condition reveals the ***critical headway***, or the smallest headway the vehicle may reach based on the driver sensitivity. The critical headway, is given by $h_{cr} = h_{br}(v_c/v_{max})^{1/\alpha}$. The vehicle cannot travel to beyond h_{cr} because beyond that point the expression for the time taken to reach a smaller headway is divergent, and it will take an infinite amount of time to get to the smaller headway. One may notice that as $v_c \to 0, h_{cr} \to 0$.

Approximate time taken to join a cluster

As was mentioned above, it is inconvenient that the total time taken to join a cluster is represented by the sum of an infinite series. It is desirable instead to have a simpler expression to represent the time taken to join a cluster. In the following analysis, the focus is on obtaining a simplified expression to pursue an analytical development of cluster dynamics.

As a first step in determining the approximate total time taken to join a cluster, the first term alone is considered. The first term, say t_1, is compared against the total time or sum to infinity, say t_∞. The first term of the hypergeometric series in equation (4.12) may be written as:

$$t_1 = \frac{h_{free}^{1-\alpha} - h^{1-\alpha}}{k(1-\alpha)} \tag{4.14}$$

Since an exact measure for the total time is unavailable, it is approximated by the sum to n terms, say t_n. The number of terms n used to calculate the sum t_n is found by using successively more terms to calculate the required time, till the contribution of the following term falls below a specific value (say 3%). For example, if the sum to n terms is calculated to be 100 seconds, and the contribution of the $(n+1)^{th}$ term is less than 3 seconds, the sum to infinity is approximated by t_n, i.e. the time taken to join a cluster is considered to be 100 seconds. It is hoped that a relationship between t_1 and t_n can be established, so that the approximate time taken to join the cluster can be expressed in terms of t_1 alone. Since the framework for calculating the time taken to join the cluster with increasing number of terms has already been demonstrated in Figure 22, the same setup is used to determine t_1 and t_n for the range of permissible values of driver sensitivities (α). The ratio t_n/t_1 will henceforth be referred to as the *truncation ratio* (T_R). The plot for truncation ratio (t_n/t_1) versus driver sensitivity (α) is included in Figure 23.

Observing the scale on the y-axis, it is realized that there is limited variation in the truncation ratio. Specifically, the standard deviation of truncation ratio across the range of driver sensitivities is 0.038 for typical traffic conditions. Thus, the average truncation ratio may adequately represent the ratio t_n/t_1 across all α values. The mean truncation ratio value is 1.4, and consequently the total time taken to join the cluster may be approximated by:

$$t_n \approx \bar{T}_R\, t_1 = \frac{\bar{T}_R}{k(1-\alpha)}\left(h_{free}^{1-\alpha} - h^{1-\alpha}\right) \tag{4.15}$$

$where\ \bar{T}_R\ = mean\ truncation\ ratio = 1.4$

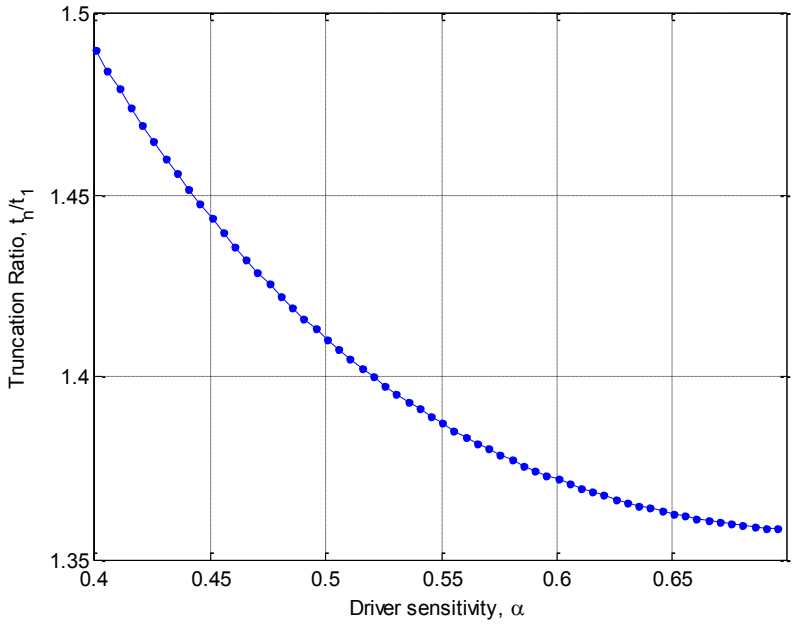

Figure 23: Plot of truncation ratio versus driver sensitivity

Now that an expression for the total time taken to join a cluster has been obtained, one can proceed towards calculating an expression for the transition probability rate.

Transition probability rates, $w_+(n)$ and $w_-(n)$

It has been determined that the total time taken to join a cluster may be estimated as a product of a constant truncation ratio and the first term in the hypergeometric series $t(h)$. It has already been demonstrated in section 4.1 that the transition probability rate for joining a cluster may be calculated as the inverse of the time taken to join the cluster. In other words, the transition probability rate $w_+(n)$ may be determined using the following expression:

$$\boldsymbol{w_+(n) = \frac{1}{t_{join}} = \frac{1}{t_n} = \frac{1}{\overline{T}_R\, t_1} = \frac{k(1-\alpha)}{\overline{T}_R}\left(\frac{1}{h_{free}^{1-\alpha} - h^{1-\alpha}}\right)} \qquad (4.16)$$

On the other hand, the transition probability rate for leaving the cluster as proposed by Mahnke was found to be reasonable, so the same transition rate is employed in the following analysis. Thus, the transition probability rate for leaving a cluster is given by:

$$\boldsymbol{w_-(n) = \frac{1}{t_{leave}} = \frac{1}{\tau_{rel}}} \qquad (4.17)$$

In (Mahnke, et al., 1999), the value of time taken to leave a cluster is obtained from the velocity of the collective backward motion of a cluster. In other words, the transition probability rate of a vehicle leaving the cluster is determined by the collective movement of a cluster, which in turn is also dependent on the rate at which vehicles join the cluster. The value for τ_{rel} used is 1.5 seconds, and is obtained by fitting the optimal velocity model to specific data from German highways. On the other hand, in this thesis, the vehicle is considered to be in one of two states. The vehicle can either be in free flow, or it can be stuck inside a cluster. For the purposes of this thesis, the transition probability rate is considered as the rate at which a vehicle transitions from one of these states to the other. Thus, in this thesis, the time taken to leave a cluster is determined by the time taken for a vehicle to accelerate from a stationary state inside a cluster to near free flow velocity outside a cluster. This time is calculated to be in the range of 5-7 seconds using typical traffic conditions.

In this chapter, the limitations of transition rates proposed by Mahnke and Pieret were discussed, and an alternative set of transition rates was proposed. In the next chapter, the steady state analysis of the vehicle cluster dynamics is performed, and the newly proposed transition rates are employed to determine the steady state vehicle cluster size.

CHAPTER 5
VEHICLE CLUSTER DYNAMICS

In the previous chapter the limitations of the transition rates proposed by Mahnke and Pieret were discussed, and new transition rates that better described the driver-dependent vehicle behavior in traffic flow were proposed. In this chapter, the new expressions for transition rates are used to determine the steady state cluster size from vehicle cluster dynamics.

5.1 Steady state analysis for single species environment

In this section, traffic is considered as consisting of a single species, or a single set of drivers with a fixed value of driver sensitivity. The approach followed in this section resembles the one presented by Mahnke in (Mahnke, et al., 1997) to an extent, with the difference that new transition probability rates are used in the analysis. In the next section, Mahnke's approach is developed into a novel methodology to analyze the impact of multiple species on the formation of self-organizing traffic jams. Specifically, the problem of the impact of ACC vehicles on traffic jam dynamics is discussed. The present research unveils new insights into the effects on ACC vehicles on the cluster formation process.

In section 3.3 it was mentioned that the cluster formation process may be modeled as a one-dimensional random walk. Further, the rate of change of probability of system states was described and expressed as a discrete master equation in equation (3.17). In other words, the equation provides a description of the manner in which the probability that the vehicle cluster contains n vehicles changes with time. The next logical step is to use the probability rate change equation to determine the dynamics of the vehicle cluster. This would provide an understanding of how traffic jams grow or diminish in size. Specifically, one would like to know how the formation of traffic jams is dependent on driver behavior as represented by varying driver sensitivities.

5.1.1 Free headway from steady state condition

Since the cluster formation has been considered as a stochastic process, it only make sense to study the dynamics of the **expected cluster size** $\langle n \rangle$. In other words, due to the inherent randomness of the cluster formation process, it is difficult to determine the exact size of the vehicle cluster (or traffic jam) for any single cluster formation process. Instead, it only makes the sense to study the size of the traffic jam one expects to observe when a large number of jam forming

processes are considered over a long period of time. The expected value $\langle n \rangle$ of the cluster size, n, is given by:

$$\langle n \rangle = \sum_{n} nP(n,t) \tag{5.1}$$

where, $P(n,t)$ is the probability that the cluster contains n vehicles at time t. Further, it is desirable to know how the steady state cluster size varies with system parameters such as the density of vehicles on the road. Thus, the quantity of interest is the rate at which the expected cluster size varies, and is described as follows:

$$\frac{d}{dt}\langle n \rangle = \frac{d}{dt}\sum_{n} nP(n,t) = \sum_{n} n\,\frac{dP(n,t)}{dt} \tag{5.2}$$

The above expression for the dynamics of the expected system state can be augmented by the knowledge of the master equation as presented in equation (3.17), and the corresponding boundary conditions presented in equation (3.18), to read as follows:

$$\frac{d}{dt}\langle n \rangle = \sum_{n} n \begin{Bmatrix} w_{+}(n-1)P(n-1,t) + w_{-}(n+1)P(n+1,t) \\ -[w_{+}(n) + w_{-}(n)]P(n,t) \end{Bmatrix}$$

Expanding the expression under the summation sign $\forall\, n \,\epsilon\, [0, N]$, using the boundary conditions for $n = 0, N$ as described in equation (3.18), and through some simple algebraic manipulations, the above equation reduces to the following form:

$$\frac{d}{dt}\langle n \rangle = \sum_{n} w_{+}(n)P(n,t) - w_{-}(n)P(n,t)$$

Further, by the definition of the expected value of a function, the above equation reduces to:

$$\frac{d}{dt}\langle n \rangle = \langle w_{+}(n) \rangle - \langle w_{-}(n) \rangle \tag{5.3}$$

In the above equation, it is known that the transition probability rate of leaving a cluster, $w_{-}(n)$, is defined as a constant $1/\tau_{rel}$. Thus, the expected value of the function is same as the constant value, i.e. $\langle w_{-}(n) \rangle = 1/\tau_{rel}$. On the other hand, the expected value of the function $\langle w_{+}(n) \rangle$ is not known. Consequently, further analysis is difficult without a simplifying assumption. The simplifying assumption comes in the form of the *mean field approach* which assumes that a many-body problem may be replaced with a one-body problem with suitable external field. In the present context, the assumption suggests that expected value of the function $w_{+}(n)$ across all

possible states n may be approximated by the value of the function at the expected state $\langle n \rangle$. In other words, the mean field approximation suggests that:

$$\langle w_+(n) \rangle \approx w_+ \langle n \rangle$$

Thus, the equation for the dynamics of the expected cluster size reduces to:

$$\frac{d}{dt}\langle n \rangle = w_+ \langle n \rangle - \frac{1}{\tau_{rel}} \tag{5.4}$$

At steady state, the cluster size remains constant, and the expected cluster size tends towards this constant value. Consequently, the rate of change of the steady state cluster size equals zero and the rate of change of the expected cluster size tends to zero. Thus from equation (5.4), the condition for steady state is obtained as:

$$w_+(n) = \frac{1}{\tau_{rel}} \tag{5.5}$$

Further, substituting the expression for $w_+(n)$ from equation (4.16), the following expression for the free headway when a steady state vehicle cluster size exists on the road is obtained:

$$h_{free}(n) = \left\{ h_{clust}^{1-\alpha} + \frac{\tau_{rel}\, k(1-\alpha)}{\bar{T}_R} \right\}^{1/1-\alpha} \tag{5.6}$$

5.1.2 Free headway from physical constraints

In the previous subsection, an expression for the free headway was obtained from the steady state condition. In this subsection the free headway expression is obtained from physical constraints of operating on a fixed length of road. The free headway expression obtained is directly dependent on the number of vehicles present in the cluster. Equating the sum of various headways and lengths of vehicles to the total length of the road, one obtains the following equation:

$$L = Nl + (N - n + 1)h_{free} + (n-1)h_{cluster} \tag{5.7}$$

where, L = Total length of road (= 1000 m, in subsequent simulations)

N = Total number of vehicle on the road

l = Effective length of a vehicle (= 5 m in simulations)

n = Total number of vehicles present in cluster

h_{free} = Free headway

$h_{cluster}$ = Headway inside the cluster (≈ 1 m in simulations)

Thus, the expression of free headway as obtained from physical constraints reads as:

$$h_{free}(n) = \frac{L - Nl - (n-1)h_{cluster}}{(N - n + 1)} \tag{5.8}$$

5.1.3 Relationship between density and steady state cluster size

The previous two subsections derived the free headway (headway outside a cluster) using two different approaches, one involving the steady state condition, and the other involving physical constraints due to fixed road length. These two expressions are now equated to obtain a relationship between the density of vehicles on the road and the steady state cluster size. Equations (5.6) and (5.8) are used to obtain the following for a steady state condition:

$$\left\{h_{clust}^{1-\alpha} + \frac{\tau_{rel}\, k(1-\alpha)}{\bar{T}_R}\right\}^{1/1-\alpha} = \frac{L - Nl - (\langle n\rangle - 1)h_{cluster}}{(N - \langle n\rangle + 1)} \tag{5.9}$$

After rearrangement and expressing Nl/L as ρ^* (dimensionless density) and $\langle n\rangle l/L$ as $\langle n\rangle^*$ (normalized cluster size), the above equation may be expressed as follows to explicitly illustrate the relationship between steady state cluster size and vehicle density on the road:

$$\langle n\rangle^* = \frac{\rho^*(h_{free} + l) + (h_{free} - h_{cluster})l/L - l}{(h_{free} - h_{cluster})} \tag{5.10}$$

where $h_{free} = \left\{h_{clust}^{1-\alpha} + \frac{\tau_{rel}\, k(1-\alpha)}{\bar{T}_R}\right\}^{1/1-\alpha}$. Under the simplifying assumption that for large cluster sizes $n - 1 \approx n$, the above equation reduces to:

$$\boldsymbol{\langle n\rangle^* = \frac{\rho^*(h_{free} + l) - l}{(h_{free} - h_{cluster})}} \tag{5.11}$$

The equation indicates that the relationship between density and steady state vehicle cluster size is linear in nature. Further, since the value of the cluster size cannot be less than zero, the range of validity of the above equation is restricted to values of ρ^* for which $\langle n\rangle^*$ is greater

than zero. For values of $\langle n \rangle^*$ less than zero, the steady state cluster size is considered to be zero. At this point, one may observe that there is a particular density at which cluster formation is initiated, and this density is referred to as the **critical density**, ρ_c^*. In other words, the smallest density at which a cluster begins to form is defined as the critical density. The expression for the critical density may be obtained by substituting the value of $\langle n \rangle^*$ by zero:

$$\rho_c^* = \frac{l}{(h_{free} + l)} \tag{5.12}$$

Figure 24 describes the phase portrait for vehicular density versus the corresponding stable cluster size, using typical values for traffic flow conditions (as described in section 4.2) and driver sensitivity (α) = 0.4. The phase portrait also provides an insight as to how the cluster size proceeds to the steady state. The arrows indicate the direction of progression to the stable cluster size. For example, when the density of the vehicles on the road is less than the critical density, the stable cluster size is zero. In such conditions if any vehicle cluster is formed it quickly dissipates and traffic flow returns to free flow. On the other hand, for densities above the critical density, the stable cluster size is given by the linear relationship presented in equation (5.11). If the existing vehicle cluster contains a different number of vehicles, either more or less, it is expected that the cluster will either diminish or grow, respectively, to reach the steady state cluster size.

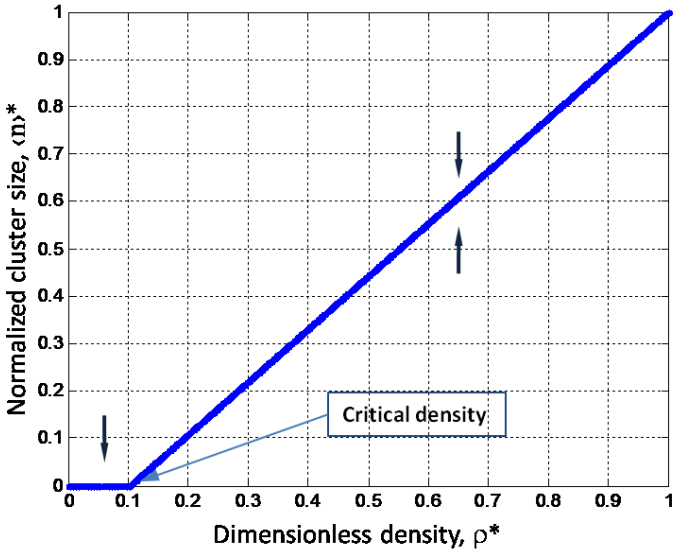

Figure 24: Phase portrait for density versus cluster size for human drivers with α = 0.4. Solid line indicates stable cluster size.

At this point it would be informative to compare the critical density obtained from the above analysis with actual critical densities observed in highway data, with the goal to determine if the choice of α in the model reasonably agrees with data. It may be observed from Figure 24 that

for driver sensitivity (α) = 0.4, and with typical traffic conditions described in section 4.2, the dimensionless critical density is close to 0.1. Further, equations (5.6) and (5.12) indicate that the relation between critical density and driver sensitivity is a one-to-one mapping. Thus, it may be concluded from Figure 24 that an observed critical density of 0.1 corresponds uniquely to a driver sensitivity value of 0.4. Next, Mahnke and Kaupužs (Mahnke, et al., 1999) have presented the fundamental diagram of traffic flow in terms of dimensionless density, which has been included as Figure 25. The figure includes the data for flow (or flux) versus density obtained for human drivers on German highways, and indicates that the dimensionless critical density is indeed close to 0.1. This observation indicates that it is justified to use a lower bound driver sensitivity value of 0.4 for the worst-case human drivers.

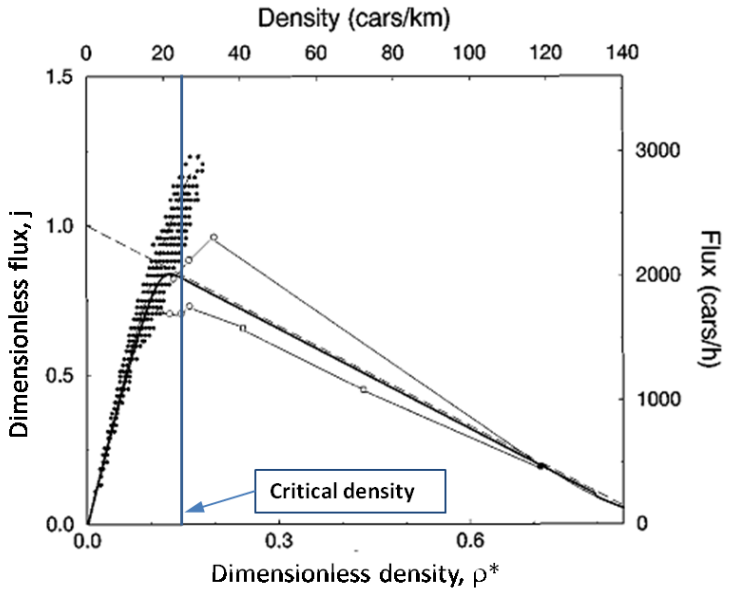

Figure 25: Fundamental diagram indicating the critical density for traffic consisting solely of human drivers. Separate dots indicate observed values of flow, or flux. [Modified from (Mahnke, et al., 1999), using data from (Kerner, et al., 1993)]

While the above analysis provides an insight into how the steady state cluster size varies as the vehicular density varies, it does not provide a description as to how the introduction of ACC vehicles into traffic flow consisting primarily of human-driven vehicles affects the traffic flow. The concept of mixed traffic or multiple species is covered in the next section.

5.2 Steady state analysis for multi-species environment

In the previous section it was observed how the steady state cluster size varies with changing vehicular density. However, the issue of a mix of human-driven and ACC vehicles was not

addressed. In this section the scenario of having mixed human-driven and ACC vehicles on the road is assessed and its impact on formation of self-organizing traffic jams studied. Further, Monte Carlo simulations are performed to validate the results obtained from this methodology.

5.2.1 System description and transition rates

For the multi-species analysis, i.e. the analysis of mixed traffic with both human-driven and ACC vehicles, the same closed ring system is used as presented in Figure 14. The number of vehicles on the road is assumed to be large enough so that the proportion of ACC vehicles both inside and outside the cluster may be considered to be equal. This assumption is necessary to enable a probabilistic development of a multi-species framework.

Since the system now consists of two types of drivers, their respective behaviors pertaining to joining and leaving a cluster must be considered. For purposes of simplicity, it is assumed that the rate at which both types of vehicles leave the cluster is the same. This is a reasonable assumption because, as mentioned before, the manner in which the vehicles leave the cluster may be considered to be independent of their car-following behavior. On the other hand, the manner in which they join the cluster is different for different types of drivers because the transition probability rate for joining the cluster is dependent on the driver sensitivity. Thus, the following two transition probability rates are obtained for human-driven and ACC vehicles using equation (4.16):

$$\boldsymbol{w_+^H(n)} = \frac{k_H(1-\alpha_H)}{\bar{T}_R}\left(\frac{1}{h_{free}^{1-\alpha_H} - h_{cluster}^{1-\alpha_H}}\right);$$
$$\boldsymbol{w_+^{ACC}(n)} = \frac{k_{ACC}(1-\alpha_{ACC})}{\bar{T}_R}\left(\frac{1}{h_{free}^{1-\alpha_{ACC}} - h_{cluster}^{1-\alpha_{ACC}}}\right) \quad (5.13)$$

where the script H indicates that the transition probability rate is for human-driven vehicles and the script ACC indicates that the transition probability rate is for ACC vehicles. Let the percentage of ACC vehicles on the road be represented by p. Further, using the assumption that the number of vehicles both inside and outside the cluster is large enough, one may infer that the probability that the vehicle joining a cluster is an ACC vehicle is given by p. Similarly the probability that the vehicle joining the cluster is driven by a human is $(1-p)$. Then the *effective transition rates* for the multi-species system may be written as:

$$w_+^{eff}(n) = (1-p)w_+^H(n) + pw_+^{ACC}(n); \text{ and } w_-^{eff}(n) = 1/\tau_{rel} \quad (5.14)$$

The effective transition rates may be employed to draw conclusions about the steady state cluster size in a multi-species environment.

5.2.2 Steady state analysis for multi-species system

Prior to determining the system behavior for a multi-species environment, it would be informative to know the behavior when the system is populated with human-driven vehicles alone or ACC vehicles alone. In other words, it is desirable to know the variation in critical density as the driver sensitivity is varied. With an additional simplifying assumption that the cluster headway tends to vanish or is negligible compared to free headway, on may obtain the relationship between vehicular density and steady state cluster size for varying driver sensitivities as shown in Figure 26.

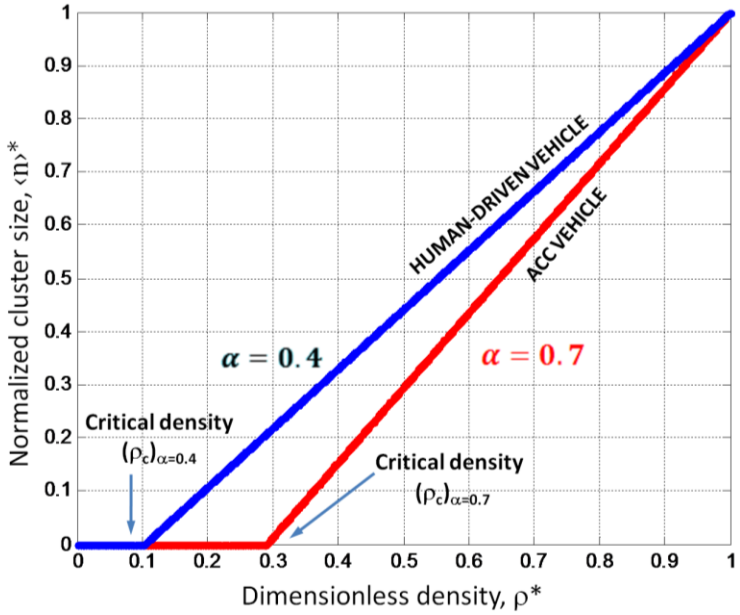

Figure 26: Phase portrait for relationship between density and cluster size for different driver sensitivities. Solid lines indicate stable cluster sizes.

As is evident, if the traffic flow consists solely of "sleepy" drivers with low driver sensitivities, the cluster formation process is initiated at lower densities. On the other hand, if the drivers in the traffic flow are "alert", as is considered to be the case with ACC vehicles, the cluster formation process is initiated at higher densities. Thus, one may conclude that in a comparison of traffic scenarios which consist either of human-driven vehicles alone or ACC vehicles alone, the ACC vehicles will perform better. Better performance is considered in the sense that the traffic flow will be able to proceed to higher densities and consequently higher traffic flows before self-organizing traffic jams or vehicle clusters begin to form.

CONCLUSION: If traffic flow consists solely of ACC vehicles (with high driver sensitivities), self-organizing traffic jams will begin to form at higher densities. In fact, with only ACC vehicles on the road the critical density increases by a factor of 3.

Steady state condition

The steady state condition for the multi-species system is similar to the condition for the single-species system, with the difference that the transition probability rate in the single-species system is replaced by an effective transition probability rate for the multi-species system. Thus the steady state condition is given by the following equation:

$$w_+^{eff}(n) = (1-p)w_+^{H}(n) + pw_+^{ACC}(n) = \frac{1}{\tau_{rel}} \tag{5.15}$$

Substituting the expressions for the individual transition probabilities into the above equation and performing some algebraic manipulations, one obtains the following equation in terms of the free headway:

$$h_{free}^{1-\alpha_H} h_{free}^{1-\alpha_{ACC}} - bh_{free}^{1-\alpha_H} - ch_{free}^{1-\alpha_{ACC}} + d = 0 \tag{5.16}$$

where, $b = h_{cluster}^{1-\alpha_{ACC}} + \tau pk_{ACC}(1-\alpha_{ACC})/\bar{T}_R$

$c = h_{cluster}^{1-\alpha_H} + \tau(1-p)k_H(1-\alpha_H)/\bar{T}_R$

$d = h_{cluster}^{1-\alpha_H} h_{cluster}^{1-\alpha_{ACC}} + (\tau pk_{ACC}(1-\alpha_{ACC})/\bar{T}_R)h_{cluster}^{1-\alpha_H} + (\tau k_H(1-p)(1-\alpha_H)/\bar{T}_R)h_{cluster}^{1-\alpha_{ACC}}$

The above equation is a transcendental equation, and in its present form it can only be solved either numerically or graphically. However, it is desirable to obtain a closed form solution for the free headway in order to continue with the current path of analysis. A closed form solution may be obtained if a relation is enforced between α_H and α_{ACC}. The intent of enforcing such a relation is to transform the transcendental equation into an algebraic one. Such a transformation can be brought about by a relation that reduces equation (5.16) into a quadratic, cubic, bi-quadratic or similar functional form. One such relation that reduces equation (5.16) into a cubic equation and thus allows a closed form solution is $(1-\alpha_H) = 2(1-\alpha_{ACC})$, $i.e.\, \alpha_{ACC} = 0.5(1+\alpha_H)$. It may be observed that, once this substitution is made, arbitrary choices of driver sensitivities cannot be made in this analysis. This is due to the fact that the choices are restricted by two constraints, viz. the maximum acceptable deceleration (as discussed in section 4.2), and the need to obtain a closed

form solution. A number of values of driver sensitivities (α_H, α_{ACC}) such as (0.35, 0.675), (0.4, 0.7) etc. which satisfy the relation $(1-\alpha_H) = 2(1-\alpha_{ACC})$ also lie approximately in the range defined by maximum acceptable deceleration. Thus, the relation $(1-\alpha_H) = 2(1-\alpha_{ACC})$ may be used as an approximation, together with this restricted set of values, to reduce equation (5.16) into a cubic form as follows:

$$\left(h_{free}^{1-\alpha_{ACC}}\right)^3 - b\left(h_{free}^{1-\alpha_{ACC}}\right)^2 - c\left(h_{free}^{1-\alpha_{ACC}}\right) + d = 0 \tag{5.17}$$

whereby a closed form expression for h_{free} can be obtained as follows:

$$h_{free} = \frac{1}{6}\left\{-2b + 2\cdot 2^{\frac{1}{3}}\frac{(b^2-3ac)}{D} + 2^{\frac{2}{3}}D\right\} \tag{5.18}$$

where $D = \left\{-2b^3 + 9abc - 27a^2d + \sqrt{-4(b^2-3ac)^2 + (2b^3 - 9abc + 27a^2d)}\right\}^{\frac{1}{3}}$

The expression for h_{free} obtained from the steady state condition may then be equated to the expression for free headway obtained from physical constraints. The relationship between steady state cluster size and vehicular density is obtained in the same manner to be:

$$\langle n\rangle^* = \frac{\rho^*(h_{free}+l) - l}{(h_{free} - h_{cluster})}$$

where h_{free} is given by the expression in equation (5.18). It is now of interest to know how the addition of ACC vehicles to the traffic affects the tendency of the traffic flow to self-organize into jams. Specifically, it is of interest to know the impact of ACC penetration on the critical density, or the density at which vehicle clusters first begin to appear.

5.2.3 Behavior prediction

Since the quantity of interest is the critical density, the impact of increased ACC penetration on the critical density is analyzed. One would like to know if the presence of larger number of ACC vehicles on the road results in an increase in critical density, i.e. higher traffic flow before a self-organized traffic jam begins to restrict flow. There is already an inkling of this happening from the analysis in the previous subsection. In this subsection the impact of increased ACC penetration is analyzed.

It is known that the critical density is a function of the free headway. Further, the solution for the free headway, h_{free}, obtained in the previous subsection is a function of the percentage of ACC vehicles on the road. Thus there exists a relation between the critical density and the percentage of ACC vehicles. This relation is plotted in Figure 27. The figure indicates that the critical density increases as the proportion of ACC vehicles on the road increases. The driver sensitivity values used for the analysis are $\alpha_H = 0.4$, which is the lower bound for the permissible range of driver sensitivities, and $\alpha_{ACC} = 0.7$, which is obtained from the relation enforced to enable an analytical solution to the transcendental equation (5.16). It is understood that the value for α_{ACC} lies outside the permissible range of driver sensitivities, but one may also observe that the maximum deceleration value corresponding to α_{ACC} is only 4 m/s^2. Since this deceleration value is close to the prescribed AASHTO standards, it is assumed to be permissible for the sake of obtaining an analytical solution to the problem at hand.

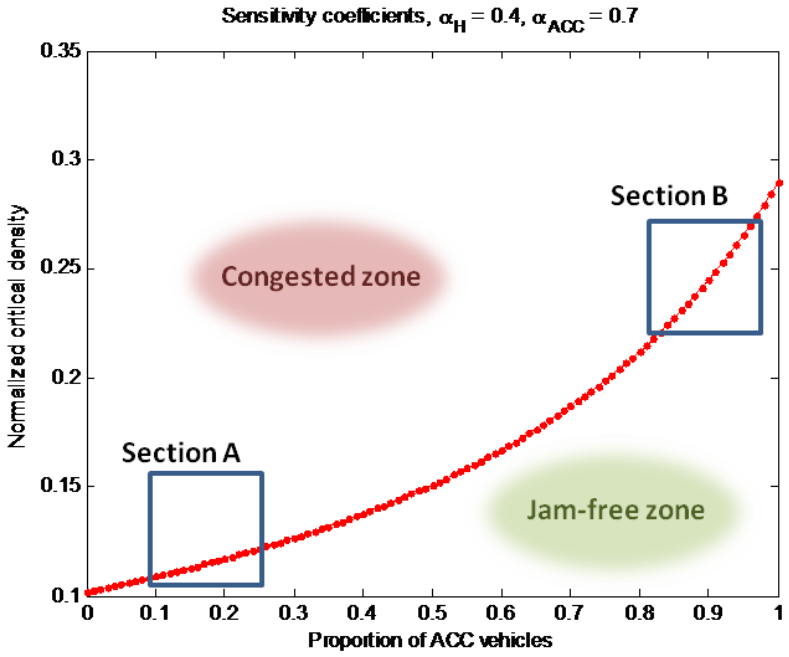

Figure 27: Normalized critical density versus ACC penetration in highway traffic

The above figure may be interpreted as follows. Consider a traffic system consisting of a fixed proportion of ACC vehicles, say 50%. Further, consider the corresponding critical density, which from the figure, is approximately 0.15. Now, if the density of vehicles on the road is greater than 0.15, i.e. greater than the critical density, self-organized traffic jams will emerge in the system, and the system will exist in a congested state. However, if the density of vehicles on the road is less

than the critical density, self-organized traffic jams will not emerge and traffic will exist in a free flow state. The distinction between these two phases of the system is made by means of the critical density line. For a fixed density, as the proportion of ACC vehicles in the traffic system increases, the system goes from congested state to free flow, and vice versa. Alternatively, for a fixed proportion of ACC vehicles in the system, as the density increases, the system goes from free flow to congested state, and vice versa.

One may observe that the slope of the curve described in Figure 27 increases as the percentage of ACC vehicles on the road increases. In the context of analyzing a potential control mechanism for the dynamics of self-organizing systems, one may consider the percentage of ACC vehicles (p) as the independent or controllable variable, and the normalized critical density (ρ_c^*) as the dependent variable. Then the sensitivity of the dependent variable may be expressed as:

$$Sensitivity, s(p_0) = \left(\frac{d\rho_c^*}{dp}\right)_{p=p_0} \tag{5.19}$$

The sensitivity describes the effect of a small change in the percentage of ACC vehicles on the normalized critical density. Determining the slope of the curve from Figure 27, the sensitivity of the normalized critical density to the proportion of ACC vehicles may be obtained. Figure 28 indicates how the sensitivity of the normalized critical density to ACC penetration varies with ACC penetration.

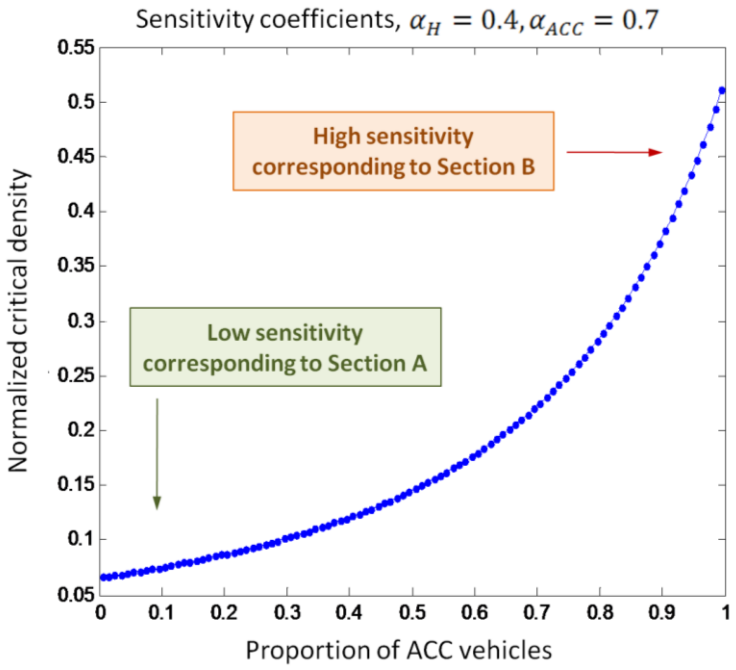

Figure 28: Sensitivity of normalized critical density to the proportion of ACC vehicles on the road.

It may be observed that as the proportion of ACC vehicles on the road increases, the normalized critical density becomes increasingly sensitive to small changes in the ACC penetration. For example, consider section A in Figure 27, which depicts the behavior of a system consisting predominantly of only human-driven vehicles. This system is characterized by small values of p. If a small percentage, say 5%, of ACC vehicles is added to this system, the critical density at which clusters begin to form does not change much. Thus, addition of ACC vehicles to a predominantly human-driver system does not produce any significant changes. This behavior corresponds to a low sensitivity. The implications of low sensitivity are that the system behavior is independent of any small changes made to the vehicle proportions. In other words, the analysis suggests that adding a group of "alert" ACC vehicles to the traffic will not improve the traffic flow, and that self-organizing traffic jams will continue to form at relatively low densities.

On the other hand, consider section B in Figure 27, which depicts the behavior of a system consisting predominantly of ACC vehicles. This system is characterized by large values of p. If a small percentage, say 5%, of human-driven vehicles with low driver sensitivities is added to this system, the critical density at which clusters begin to form drops sharply. This suggests that addition of a few human-driven vehicles to traffic consisting predominantly of ACC vehicles has the potential to suddenly reduce the critical density at which traffic jams form. Thus, if the traffic system is operating at a certain density that is just below the critical density for predominantly ACC traffic, addition of human-driven vehicles will reduce the critical density. The rapid reduction in critical density will cause the formation of self-organizing traffic jams, even though no major changes in actual vehicular density have occurred. This behavior corresponds to high sensitivity. The implications of high sensitivity are that the system behavior is greatly impacted by small changes in vehicle proportions. In other words, the analysis suggests that addition of a group of "sleepy" (human) drivers to a predominantly ACC vehicular traffic will result in a sudden reduction in critical density and will quickly lead to self-organized traffic jams. Specifically, it can be seen from Figure 28 that with typical driving conditions the traffic system is 10 times as sensitive to changes in vehicle proportion when it consists of predominantly ACC vehicular traffic than when it consists predominantly of human-driven vehicular traffic.

CONCLUSION: Higher ACC penetration makes the traffic system more sensitive to perturbations. In other words, more ACC vehicles on the road leave the traffic flow more prone to formation of self-organizing traffic jams.

5.3 Monte-Carlo simulations

The entire development up to this point has been analytical in nature. In this section the cluster formation is simulated as a one-dimensional random walk. The only inputs to the simulation are the transition probability rates, $w_+(n)$ and $w_-(n)$, and none of the simplifying assumptions used for analysis in this chapter have been included in the simulations. The removal of assumptions from the simulation process ensures that the simulation models the true cluster formation process as closely as possible. The simulations can thus be used to validate the analytical development.

The simulation methodology used for simulating the cluster formation process is known as Monte-Carlo method (Robert, 2004). In the present context, the Monte Carlo method simulates the cluster formation process a large number of times and determines the expected steady state cluster size from the mean cluster size observed in the long term limit. Figure 29 describes the schematic for the simulation. The MATLAB code for the Monte Carlo simulation is included in Appendix 6.

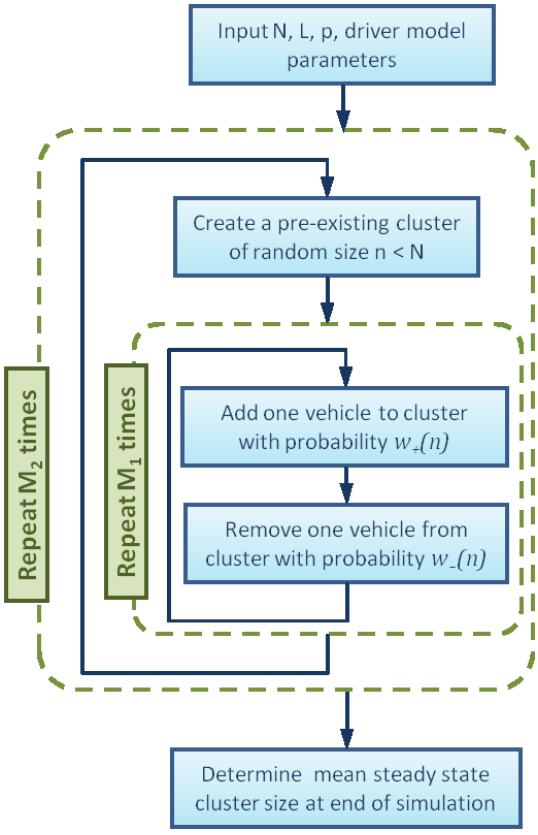

Figure 29: Schematic for Monte Carlo simulation

The schematic indicates that the simulation is first initialized with a set of parameters. These parameters include the total number of vehicles on the road, the total length of track, the percentage of ACC vehicles on the road, the driver sensitivities for both human-driven and ACC vehicles, and other typical traffic conditions. At the next step, the simulation randomly creates a cluster of size n. The simulation is then allowed to run for M_1 time steps indicative of progression in time. As the simulation progresses in time, vehicles may join the cluster or leave the cluster till a steady state cluster size is achieved. M_1 should be long enough so that the cluster is allowed to reach a steady state. After a number of test simulations with varying parameter values, it was found that the cluster size generally reached a steady state within 10,000 iterations. Thus, in the simulation, M_1 has been taken as 10,000 time steps. Once the steady state cluster size is achieved, the process is repeated with a new cluster of a randomly chosen size. The complete process is repeated M_2 times allowing one to obtain an expected cluster size as the mean of all steady state cluster sizes obtained from the simulation with the same set of initialization parameters. In the simulation, M_2 has been taken as 1000 iterations. The results from the simulations are discussed next.

5.3.1 Simulation results

As a first step in validating the analytical development, one would like to see how the simulation fares for the single-species environment. Then, one would like to see the system behavior simulated for the multiple-species environment. Simulation results for both environments are included below.

Single-species environment

For the single-species environment the quantity of interest is the steady state cluster size, and its variations with changes in density. The results shown below are for the simulations performed with human drivers, i.e. drivers with low sensitivities. The specific simulation shown here is for the scenario when the entire road is populated by human-driven vehicles with each driver having the sensitivity value (α) equal to 0.4. The simulation is first presented below in Figure 30 for a representative set of densities to demonstrate that the simulated behavior of the cluster at certain vehicular densities matches the analytically derived behavior. Specifically one notices that for the simulation where the dimensionless density is 0.1, no traffic jams are formed and the

corresponding analytical solution also yields a cluster size of zero. Similar observations are made for simulations with other densities as well.

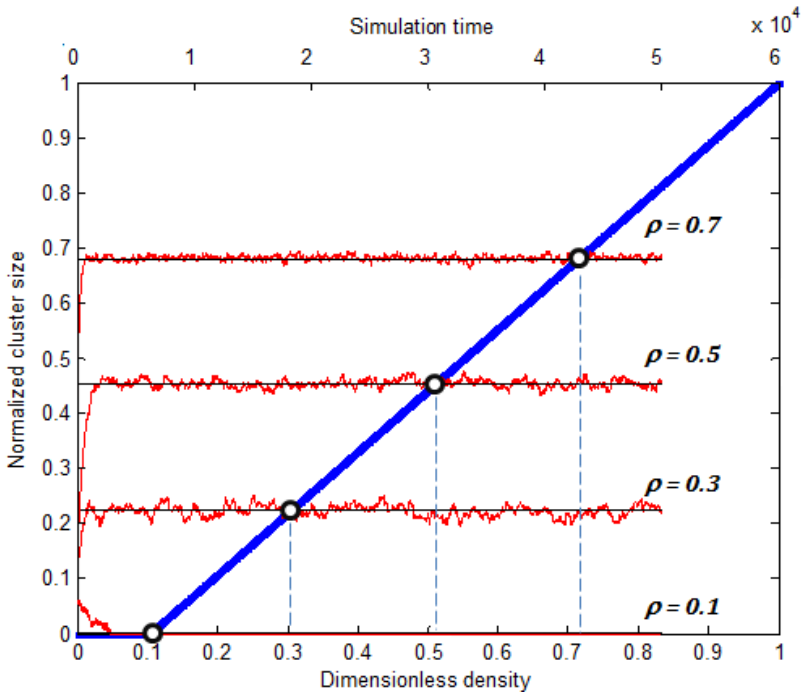

Figure 30: Monte Carlo simulation for single species environment performed for a small set of densities. Solid black lines indicate mean cluster size.

The Monte Carlo simulation is then performed for all densities and the results are presented in Figure 31. It can be seen that the simulation matches the analytical solution quite well. The simulation is performed only up to a dimensionless density of about 0.8, because beyond this point the calculation of free headway from physical constraints yields incorrect solutions. The expression of free headway from equation (5.8) is presented below:

$$h_{free}(n) = \frac{L - Nl - (n-1)h_{cluster}}{(N - n + 1)}$$

It is evident that as $N \to L/l$, the numerator becomes smaller, and represents the limit of bumper-to-bumper traffic. Any further subtractions due to the presence of the cluster headway term, $(n-1)h_{cluster}$, will cause the free headway to become negative. Thus, the simulation indicates that present form of the analysis may not be applicable for extremely high density traffic. However, it may also be observed that situations in which the traffic flow reaches extremely high densities are not expected to be observed too often, and the analysis remains valid in a majority of cases.

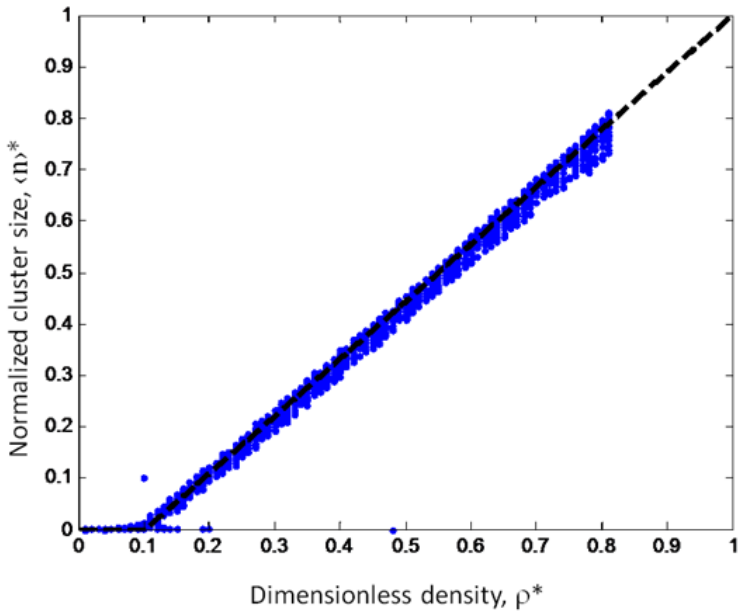

Figure 31: Monte Carlo simulation for single species environment describing dependence of cluster size on density. Thick dashed line denotes analytical solution. Solid dots indicate the mean steady state cluster sizes obtained from the simulation

Multi-species environment

In the single-species environment it was shown that the simulation matched the analytical solution quite well. This indicates that the critical density for a given driver sensitivity is also correctly calculated. In this subsection, the simulation is extended to encompass the multi-species case, in order to verify the theoretical development regarding the variation of critical density with the proportion of ACC vehicles in the traffic flow. Since the quantity of interest in the multi-species case is the critical density, the simulation determines the densities at which cluster formation is initiated. The results from the simulation are included in Figure 32 on the following page.

The red line (with solid dots) in Figure 32 indicates the analytical solution obtained for the variation of critical density with changes in ACC penetration. The results from the Monte Carlo simulation are included as the mesh in the background. The mesh and the corresponding colormap indicate the number of runs out of 1000 that resulted in the formation of a cluster in steady state. In other words, the mesh represents the number of instances in the simulation when a self-organized traffic jam formed with the given input parameter values. The region between pale blue, representing absence of cluster formation, and pale red, representing high frequency of cluster formation, indicates the phase transition from a free state to congested state of traffic flow. Thus, the lower bound of this intermediate region is representative of the critical density at which cluster

formation is initiated. It may also be observed that the analytical solution also yields the lower bound, or the critical density at which clusters begin to form. As is evident, these simulation results appear to agree with the analytical solution.

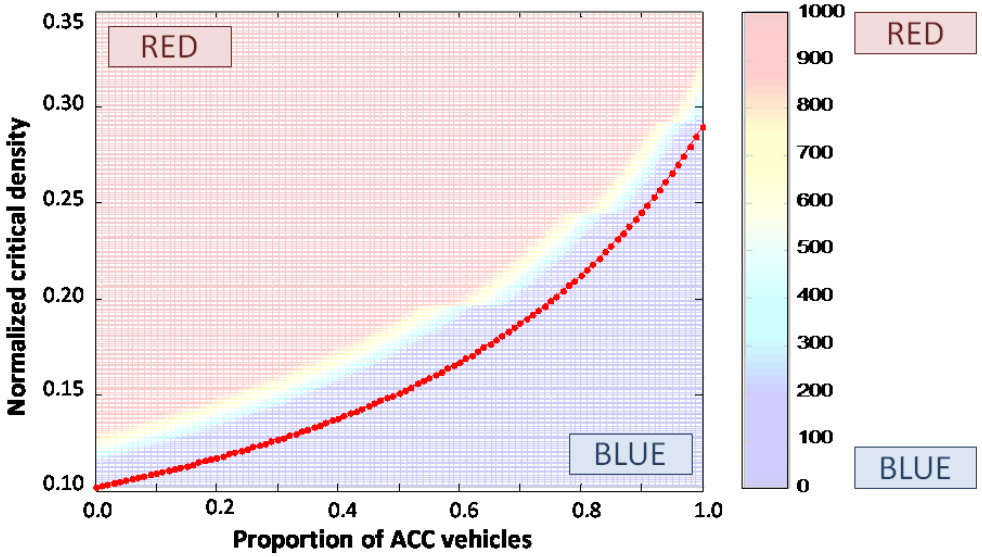

Figure 32: Monte Carlo simulation for multi-species environment. Colormap indicates the number of runs out of 1000 runs (for a given parameter set of density and proportion of ACC vehicles) that resulted in the formation of a steady state cluster (or self-organized traffic jam).

CHAPTER 6
CONCLUSIONS

The goal of the present study was to develop a methodology to analyze the effects of introduction of ACC vehicles on the formation of self-organizing traffic jams. The effect of introduction of ACC vehicles into a closed ring road traffic system was analyzed. Another aim of the study was to provide a starting point for attaining a more wide-ranging goal of developing a methodology for controlling the behavior of self-organizing systems in general. A stochastic master equation based approach was considered and adapted to provide a framework for modifying the dynamics of self-organizing systems by introduction of similar agents with slightly differing interaction properties. This chapter contains a summary of conclusions obtained from the study and provides recommendations for future work.

6.1 Summary of conclusions

The study on the effect of introduction of ACC vehicles on the formation of self-organizing traffic jams in highway traffic has yielded the following conclusions:

- **Increased ACC penetration results in higher traffic flows without self-organizing traffic jams:** The study has shown that as the percentage of ACC vehicles in the traffic system is increased the critical density also increases correspondingly. The increase in critical density implies that the density at which vehicle clusters begin to appear is increased. This indicates that the traffic flow can operate at higher densities and consequently higher flow rates, since it is known from the fundamental diagram of traffic flow that, in the free flow regime, the flow increases as the density increases.
- **Increased ACC penetration results in the traffic system being more susceptible to formation of self-organizing traffic jams:** While increased ACC penetration may allow the traffic system to operate at increased densities and flows, it comes at a cost. As ACC penetration increases, a small percentage of drivers with low sensitivities are enough to cause a self-organized traffic jam. In other words, in a predominantly ACC traffic system, introduction of a small percentage of human drivers may cause a rapid reduction of critical density, resulting in a self-organized traffic jam.

- **Self-organizing systems may be controlled by introduction of a small percentage of similar agents with slightly different interaction effects:** As was mentioned in the previous bullet, it appears to be possible to control or modify the behavior of self-organizing systems. The system behavior control is made possible by introduction of a small set of agents that react according to the same set of laws that govern agents already existing in the system, but whose interaction effects differ from the existing population. The difference in interaction effects causes a change in system behavior.

6.2 Recommendations for future work

The present study has provided a proof of concept that the dynamics of self-organized systems may be modified (and hence controlled) by introduction of a small percentage of agents with slightly different interaction effects. Further, the study has applied the concept to a practical problem and analyzed the effects of such modifications on the system behavior. Some of the possible thrust areas of research to follow up on the present study are discussed below:

- **Experimental validation**: The present study has addressed the problem from a theoretical viewpoint and justified the analysis using Monte Carlo simulation. As a logical next step, experiments should be performed to validate the results from the study. An experiment may be performed using actual vehicles with a certain percentage being driven by humans and the remaining being driven using ACC algorithms. Alternatively, the experiment may be performed using robots with a certain percentage being run by comparable human driver models and the remaining being run by ACC algorithms.
- **Analyze traffic flow with additional driver models**: The scope of the problem may be expanded by including variability in the driver sensitivities, or using altogether different models to represent driver behavior. The multi-species approach will then have to be expanded to included a large number of species against the two (human and ACC) used in the current analysis.
- **Extension to other self-organizing systems**: It would be appropriate at this point to note that for the system under consideration, the agents in the system have a relatively low degree of interaction, with each vehicle interacting only with the next neighbor. Further, the system is one-dimensional. These two facts together produce an environment where the introduction of similar agents with slightly different interaction behavior does not

dramatically alter the self-organizing behavior of the collective traffic system. However, self-organizing systems may be high-dimensional with large degree of interactions between agents, and introduction of new agents may cause different behavior in the system. Thus, the present approach may be applied to other self-organizing systems, such as flocks of birds, to observe the range of its applicability. Specifically, it would be interesting to analyze how 'different' the interaction effects of the agents being added must be to completely alter the self-organizing behavior of the system.

- **Development of a rigorous control framework:** The present analysis may be used as a stepping stone to develop a more rigorous framework for controlling the behavior of a self-organizing system. Specifically, the number of additional agents added to the system may be varied to produce a desired effect. In other words, one may add or remove agents with desired properties according to a feedback from an error signal (behavioral or otherwise) to guide the system evolution to a desired state. A rigorous framework may be developed starting from the master equation and corresponding transition rates.

Appendix 1: Derivation of the Chapman-Kolmogorov equation

Consider the joint probability distribution for the states (x_1, t_1), (x_2, t_2) and (x_3, t_3), where $t_1 < t_2 < t_3$. The joint probability distribution, $P_3(x_3, t_3; x_2, t_2; x_1, t_1)$, is given by –

$$P_3(x_3, t_3; x_2, t_2; x_1, t_1) = P_{1|1}(x_3, t_3|x_2, t_2) \cdot P_{1|1}(x_2, t_2|x_1, t_1) \cdot P_1(x_1, t_1) \tag{A1.1}$$

Integrating over x_2, we have –

$$\int P_3(x_3, t_3; x_2, t_2; x_1, t_1)\, dx_2 = \int P_{1|1}(x_3, t_3|x_2, t_2) \cdot P_{1|1}(x_2, t_2|x_1, t_1) \cdot P_1(x_1, t_1)\, dx_2 \tag{A1.2}$$

Since $P_1(x_1, t_1)$ is independent of x_2, it can be taken out of the integral sign on the right hand side. Further, the integral on the left hand side represents the integral of joint probability of states (x_1, t_1), (x_2, t_2) and (x_3, t_3), over all possible states x_2. Consequently, the integral reduces to the joint probability $P_2(x_3, t_3; x_1, t_1)$. Thus, we have –

$$P_2(x_3, t_3; x_1, t_1) = P_1(x_1, t_1) \int P_{1|1}(x_3, t_3|x_2, t_2) \cdot P_{1|1}(x_2, t_2|x_1, t_1)\, dx_2 \tag{A1.3}$$

The joint probability $P_2(x_3, t_3; x_1, t_1)$ can now be expressed as the product of the conditional probability $P_{1|1}(x_3, t_3|x_1, t_1)$ and $P_1(x_1, t_1)$, yielding –

$$P_{1|1}(x_3, t_3|x_1, t_1) P_1(x_1, t_1) = P_1(x_1, t_1) \int P_{1|1}(x_3, t_3|x_2, t_2) \cdot P_{1|1}(x_2, t_2|x_1, t_1)\, dx_2 \tag{A1.4}$$

which further results in the Chapman-Kolmogorov equation.

$$\boldsymbol{P_{1|1}(x_3, t_3|x_1, t_1) = \int P_{1|1}(x_3, t_3|x_2, t_2) \cdot P_{1|1}(x_2, t_2|x_1, t_1)\, dx_2} \tag{A1.5}$$

Appendix 2: Differential form of the Chapman-Kolmogorov equation

The Chapman-Kolmogorov equation for a two-step transition is (from equation (3.6)):

$$T_{\tau+\tau'}(x_3|x_1) = \int T_{\tau'}(x_3|x_2) \cdot T_{\tau}(x_2|x_1)\, dx_2 \tag{A2.1}$$

And the Taylor series expansion of the transition probability yields (from equation (3.11)):

$$T_{\tau'}(x_3|x_2) = (1 - \alpha_0\tau')\delta(x_2 - x_3) + \tau' W(x_3|x_2) \tag{A2.2}$$

Substituting equation(3.11) into equation (3.6), we get:

$$T_{\tau+\tau'}(x_3|x_1) = \int [(1 - \alpha_0\tau')\delta(x_2 - x_3) + \tau' W(x_3|x_2)] \cdot T_{\tau}(x_2|x_1)\, dx_2$$

$$\text{or,}\quad T_{\tau+\tau'}(x_3|x_1) = \int T_{\tau}(x_2|x_1)\delta(x_2 - x_3)\, dx_2 + \tau' \int \alpha_0(x_2)\delta(x_2 - x_3) T_{\tau}(x_2|x_1)\, dx_2 + \tau' \int W(x_3|x_2)\, T_{\tau}(x_2|x_1)\, dx_2$$

$$\text{or,}\quad T_{\tau+\tau'}(x_3|x_1) = T_{\tau}(x_3|x_1) - \tau' \int W(x_2|x_3) T_{\tau}(x_3|x_1)\, dx_2 + \tau' \int W(x_3|x_2) T_{\tau}(x_2|x_1)\, dx_2 \tag{A2.3}$$

Rearranging the terms in equation (A2.3), and dividing be τ' on both sides, one obtains:

$$\frac{T_{\tau+\tau'}(x_3|x_1) - T_{\tau}(x_3|x_1)}{\tau'} = \int [W(x_3|x_2) T_{\tau}(x_2|x_1) - W(x_2|x_3) T_{\tau}(x_3|x_1)]\, dx_2 \tag{A2.4}$$

Now, taking the limit $\tau' \to 0$, we obtain the differential form of the Chapman-Kolmogorov equation, or the Master equation:

$$\frac{\partial}{\partial \tau} T_{\tau}(x_3|x_1) = \int [W(x_3|x_2) T_{\tau}(x_2|x_1) - W(x_2|x_3) T_{\tau}(x_3|x_1)]\, dx_2 \tag{A2.5}$$

Appendix 3: MATLAB code for simulating GM fourth model

```
%% Contender number 6 - GM fourth model

clear all;
close all;

k = 0.7;          % k = alpha = driver sensitivity
hn = 100;         % Free headway
vn = 25;          % Free velocity
vref = 2;         % Cluster/target velocity

endTime = 20;
incrTime = 0.001; % Time step for numerical integration
t = linspace(0,endTime,endTime/incrTime);
iden = ones(1,length(t));
h(1) = hn;
v(1) = vn;

i = 1;
while(i <length(t))
    a(i+1) = (k*v(i)/h(i))*(vref - v(i)); % GM fourth model
    hOld = h(i);
    vOld = v(i);
    alphaOld = a(i+1);
    v(i+1) = vOld + incrTime*alphaOld;
    h(i+1) = hOld + incrTime*(vref - vOld);
    i = i+1;
end
```

Appendix 4: Derivation of expression for time taken to reach headway *h*

The starting point for the derivation is the simplified form of the GM fourth model as described in equation (4.10)

$$h\ddot{h} = \alpha(\dot{h} - v_c)\dot{h} \tag{A 4.1}$$

The equation may be re-written as:

$$\frac{\ddot{h}}{\dot{h}} = \frac{\alpha(\dot{h} - v_c)}{h} \tag{A 4.2}$$

Further, one may realize that:

$$\frac{\ddot{h}}{\dot{h}} = \frac{d\dot{h}/dt}{dh/dt} = \frac{d\dot{h}}{dh}$$

Consequently, the simplified form of equation (A 4.2) may be written as:

$$\frac{d\dot{h}}{dh} = \frac{\alpha(\dot{h} - v_c)}{h}$$

or,
$$\frac{d\dot{h}}{(\dot{h} - v_c)} = \alpha\frac{dh}{h} \tag{A 4.3}$$

Integrating both sides:

$$\int \frac{1}{(\dot{h} - v_c)} d\dot{h} = \alpha \int \frac{1}{h} dh$$

or,
$$ln(\dot{h} - v_c) = \alpha \ln(h) + \ln(c)$$

or,
$$(\dot{h} - v_c) = ch^{\alpha} \tag{A 4.4}$$

The constant of integration can be calculated from the initial conditions when a vehicle is moving at its maximum velocity (v_{max}) in free flow, and first comes within the interaction (or braking) distance (h_{br}). Since $\dot{h} = v_c - v_{max}$, equation (A 4.4) yields the value of $c = -k = -v_{max}/h_{br}^{\alpha}$. Thus, equation (A 4.4) can also be used to describe the relationship between vehicle velocity and vehicle headway as:

$$v(t) = k[h(t)]^{\alpha}, where\ k = v_{max}/h_{br}^{\alpha} \tag{A 4.5}$$

It may be observed that this relation indicates that the vehicle velocity reaches zero when the headway is zero. Typically this is not a desired characteristic, since one would want the velocity to

be zero at a certain safe distance. The safe distance may be considered to be the distance at which vehicles come to a stop in jammed traffic, i.e. the cluster headway $h_{clust} = 1\,m$. Thus the relationship between vehicle velocity and vehicle headway can be expressed as:

$$\boldsymbol{v(t) = k[h(t) - h_{clust}]^{\alpha}}, where\ k = \ v_{max}\ / h_{br}^{\alpha} \qquad \text{(A 4.6)}$$

Meanwhile, continuing with equation (A 4.4), the described differential equation can be re-written as:

$$\frac{dh}{dt} = v_c + ch^{\alpha} = v_c - kh^{\alpha}$$

or,
$$\frac{dh}{v_c - kh^{\alpha}} = dt \qquad \text{(A 4.7)}$$

Integrating on both sides with their respective limits:

$$\int_{h_{free}}^{h} \frac{dh}{v_c - kh^{\alpha}} = \int_0^t dt \qquad \text{(A 4.7)}$$

Performing the integration, the following expression for time taken to reach a particular headway is obtained:

$$\boldsymbol{t(h) = \frac{1}{v_c} \sum_{m=1}^{\infty} \left\{ \frac{1}{1 - m\alpha} \left(\frac{v_c}{k} \right)^m \left(h_{free}^{1-m\alpha} - h^{1-m\alpha} \right) \right\}} \qquad \text{(A 4.8)}$$

Appendix 5: MATLAB code for calculating time taken to join a cluster

```
%% For vehicles joining a cluster

a = 0.4;           % Driver sensitivity
m = 1;             % Number of terms included
sum = 0;
hnterm = 0;
hterm = 0;

vmax = 25;
hbr = 100;
vn = 25;
hn = 100;
vc = 2;
k = vmax/(hbr^a);
vn = k*(hn^a)
hCritical = hbr*(power((vc/vmax),(1/a)));

h = linspace(hn,1.001*hCritical,2000);
iden = ones(1,length(h));

count = 1;

for(i = 1:1:40)
    while(m<=i)
        hnterm = hnterm + (hn)*((1/(1 - m*a))*((vc^(m-
1))/((vmax)^m))*((hbr/hn)^(m*a))).*iden;  %For joining a cluster

        hterm = hterm + ((1/(1 - m*a))*((vc^(m-
1))/((vmax)^m))*((hbr*iden./h).^(m*a))).*h;  %For joining a cluster

        sum = (hnterm - hterm);
        m = m + 1;
    end
    t = sum;

    plot(t, h,'r.-', 'MarkerSize', 4); grid on;
    xlabel('Time (in seconds)');
    ylabel('Headway (in metres)');
    hold on;
end
```

Appendix 6: MATLAB code for Monte Carlo simulation

```
%% Script to simulate formation of self-organizing traffic jams using
Monte Carlo method

clear all;
close all;
clc;

%% Initialize all variables
L = 5000;                % Length of track
l = 5;                   % Effective length of car
vmax = 25;               % Maximum vehicle velocity
hbr = 100;               % Interaction distance
tau = 5;                 % Relaxation time
vc = 0.00;               % Cluster velocity
TR = 1.4;                % Truncation ratio
d0h = 1;
d0r = 1;

ah = 0.4;                % human driver sensitivity
ar = 0.5*(1+ah);         % autonomous vehicle sensitivity

pIND = 1;
cNIND = 1;
iterIND = 1;
maxIter = 1000;
count = 1;

pStart = 0.05;
pIncr = 0.1;
pEnd = pStart;
cNStart = 0.13;
cNIncr = 0.01;
cNEnd = cNStart;


clusterSize(1) = 50;
endTime = 20000;

%% Calculate transition probabilities for different cluster sizes
kh = vmax/(hbr^ah);
kr = vmax/(hbr^ar);
hch = (vc/kh)^(1/ah) + d0h;
hcr = (vc/kr)^(1/ar) + d0r;

for(p = pStart:pIncr:pEnd)
    hc = p*hcr + (1-p)*hch;
    for(cN=cNStart:cNIncr:cNEnd)
        iter = 1;
        N = cN*L/l;
        n = linspace(1,N,N);
        iden = ones(1,length(n));
```

```
        A2h = ((hch.*iden).^(1 - ah));
        while(iter<=maxIter)
            % Time to join a cluster for human driven vehicles
            hnh = ((L)*iden - l*N.*iden - (n-iden).*hc)./(N*iden - n +
iden);
            A1h = hnh.^(1-ah);
            tPlusH = (1/(kh*(1-ah))).*(A1h - A2h);

            % Time to join a cluster for ACC vehicles
            hnr = ((L)*iden - l*N.*iden - (n-iden).*hc)./(N*iden - n +
iden);
            A1r = hnr.^(1-ar);
            A2r = ((hcr.*iden).^(1 - ar));
            tPlusR = (1/(kr*(1-ar))).*(A1r - A2r);

            wPlus = (1-p)./(TR.*tPlusH) + p./(TR.*tPlusR);
            wRatio = tau.*wPlus;

%% Running the simulation - 1-D random walk for cluster size
            Rin(endTime) = 0;
            Rout(endTime) = 0;
            wPlus(endTime) = 0;
            wMinus(endTime) = 0;
            clusterSize(endTime) = 0;
            clusterSize(1) = round(N*rand(1));

            for(time=1:1:endTime)
                if((clusterSize(time) > 0)&&(clusterSize(time) < N))
                    Rin(time) = rand(1);
                    wPlus(time) = wRatio(clusterSize(time))/tau;
                    Rout(time) = rand(1);
                    wMinus(time) = 1/tau;

                    if((Rin(time) <
wPlus(time))&&(Rout(time)<wMinus(time)))
                        clusterSize(time+1) = clusterSize(time);
                    end
                    if((Rin(time) >
wPlus(time))&&(Rout(time)<wMinus(time)))
                        clusterSize(time + 1) = clusterSize(time) - 1;
                    end
                    if((Rin(time) <
wPlus(time))&&(Rout(time)>wMinus(time)))
                        clusterSize(time + 1) = clusterSize(time) + 1;
                    end
                    if((Rin(time) >
wPlus(time))&&(Rout(time)>wMinus(time)))
                        clusterSize(time + 1) = clusterSize(time);
                    end
                else

                    p0 = 0.01;
                    Rin(time) = rand(1);
                    wPlus(time) = p0*N/tau;
                    if((clusterSize(time) == 0)&&(Rin(time) <
wPlus(time)))
```

```
                        clusterSize(time+1) = 1;
                    else
                        clusterSize(time+1) = 1;
                    end

                    Rout(time) = rand(1);
                    wMinus(time) = 1/tau;
                    if((clusterSize(time) == N)&&(Rout(time) <
wMinus(time)))
                        clusterSize(time + 1) = N - 1;
                    else
                        clusterSize(time + 1) = clusterSize(time);
                    end

                end
            end

            store(pIND,cNIND).cluster(iterIND,:) = clusterSize;
            store(pIND,cNIND).mean(iterIND) =
mean(store(pIND,cNIND).cluster(iterIND,endTime - 1000:endTime));

            clear timeVector
            timeVector = linspace(1,time+1, time+1);

            meanClusterSize =
(mean(clusterSize*1/L)).*ones(length(timeVector),1);
            meanClusterSize2 = (mean(clusterSize*1/L));
            MEAN(cNIND,iterIND) = meanClusterSize2;

            figure(3)
            plot(timeVector, clusterSize*1/L);
            title(['Total iteration count = ', num2str(count),' p =
',num2str(p),' cN = ',num2str(cN)]);
            xlabel('Simulation time');
            ylabel('Normalized cluster size');
            ylim([0 1]);

            iter = iter + 1;
            count = count + 1;
            iterIND = iterIND + 1;

        end
        store(pIND,cNIND).meanMean = mean(store(pIND,cNIND).mean(:));
        meanMean = mean(store(pIND,cNIND).mean(:));
        if(meanMean>0.1*N)
            cN = cNEnd + 1;
        end
        cNIND = cNIND + 1;
        iterIND = 1;

    end
    pIND = pIND + 1;
    cNIND = 1;
end
```

BIBLIOGRAPHY

Agarwal G S Master Equation Approach to Spontaneous Emission [Journal] // Physical Review A. - [s.l.] : American Physical Society, 1970. - 5 : Vol. 2. - pp. 2038-2046.

Ashby W Ross Principles of self-organizing dynamic systems [Journal] // Journal of General Psychology. - 1947. - Vol. 37. - pp. 125-128.

Bak P, Tang C and Wiesenfeld K Self-organized criticality [Journal] // Physical Review A. - 1988. - 1 : Vol. 38. - pp. 364-374.

Bando M [et al.] Dynamical Model of Trafffic Congestion and Numerical Simulation [Article] // Physical Review E. - 1995. - 2 : Vol. 51. - pp. 1035-1042.

Bando M [et al.] Phenomenological Study of Dynamical Model of Traffic Flow [Journal] // J. Phys. I France. - 1995. - Vol. 5. - pp. 1389-1399.

Bellomo N., de Angelis E. and Delitala M Lecture Notes on Mathematical Modelling in Applied Sciences [Online] // Marcello Delitala Web site. - 2007. - March 16, 2009. - http://staff.polito.it/marcello.delitala/.

Berg P, Mason A and Woods A Continuum Approach to Car-following Models [Article] // Physical Review E. - 2000. - 2 : Vol. 61. - pp. 1056-1066.

Birkeland K W and Landry C C Power-laws and snow avalanches [Journal] // Geophysical Research Letters. - 2002. - 11 : Vol. 29. - pp. 49.1-49.3.

Brackstone M and McDonald M Car-following: a historical review [Journal] // Transportation Reseach Part F: Traffic Psychology and Behavior. - 1999. - 4 : Vol. 2.

Chandler R E, Herman R and Montroll E W Traffic Dynamics: Studies in Car Following [Article] // Operations Research. - 1958. - 2 : Vol. 6. - pp. 165-184.

Chien C C, Zhang Y and Ioannou P Traffic density control for Automated Highway Systems [Journal] // Automatica. - 1997. - 7 : Vol. 33. - pp. 1273-1285.

Cremer M and Ludwig J A Fast Simulation Model for Traffic Flow on the Basis of Boolean Operations [Article] // Mathematics and Computers in Simulation. - 1986. - 4 : Vol. 28. - pp. 297-303.

Darbha Swaroop and Rajagopal K R Intelligent Cruise Control Systems and Traffic Flow Stability [Report]. - [s.l.] : California Partners for Advanced Transit and Highways, 1998.

De Wolf Tom and Holvoet Tom Emergence and Self-Organisation: A statement of similarities and differences [Book Section] // Lecture Notes in Artificial Intelligence. - 2004.

Del Castillo J M, Pintado P and Benitez F G The Reaction Time of Drivers and the Stability of Traffic Flows [Article] // Transportation Research, Part B. - 1994. - 1 : Vol. 28B. - pp. 35-60.

Dempster M B L Self-organizing systems perspective on planning for sustainability. - [s.l.] : University of Waterloo, School of Urban and Regional Planning, 1998.

Descartes R In: The philosophical writings of Descartes, 1985 [Book]. - [s.l.] : Cambridge University Press, 1637. - Vol. I.

Doraiswamy L K and Kulkarni B D The analysis of chemically reacting systems: a stochastic approach [Book]. - [s.l.] : Taylor and Francis, 1987.

Ebeling Werner and Sokolov Igor M Statistical thermodynamics and stochastic theory of nonequilibrium systems [Book]. - [s.l.] : World Scientific, 2005.

Evans R M L Detailed balance has a counterpart in non-equilibrium states [Journal] // Journal of Physics A: Mathematical and General. - [s.l.] : Institue of Phsyics Publishing, 2005. - Vol. 38. - pp. 293-313.

FHWA Our nation's highways 2008 [Report]. - Washington D.C. : US DoT, 2008.

Garber N J and Hoel L A Traffic and Highway Engineering [Book]. - : Cenage Learning, 2009. - 4th.

Gasper G and Rahman M Basic Hypergeometric Series [Book]. - [s.l.] : Cambridge University Press, 2004.

Gazis D C, R Herman and B Potts R Car-following Theory of Steady-state Traffic Flow [Article] // Operations Research. - 1959. - 4 : Vol. 7. - pp. 499-505.

Gershenson Carlos Design and Control of Self-organizing Systems // PhD. Dissertation. - [s.l.] : Center Leo Apostel for Interdisciplinary Studies, Vrije Universitiet Brussel, 2007.

Greenberg H An Analysis of Traffic Flow [Article] // Operations Research. - 1959. - 1 : Vol. 7. - pp. 79-85.

Greenshields B D [et al.] A study of traffic capacity [Article] // Highway Research Board Proceedings. - 1935. - 1 : Vol. 14. - pp. 448-477.

Haken Herman Self-organization [Online] // Scholarpedia. - 2008. - November 1, 2009. - http://www.scholarpedia.org/article/Self-organization.

Haken Hermann Synergetics [Online] // Scholarpedia. - 2007. - November 3, 2009. - http://www.scholarpedia.org/article/Synergetics.

Hansen T Collective animal behavior [Online]. - 2006. - November 3, 2009. - http://en.wikipedia.org/wiki/Collective_animal_behavior.

Helbing D and Tilch B Generalized force model of traffic dynamics [Journal] // Physical Review E. - 1998. - 1 : Vol. 58. - pp. 133-138.

Helbing D Traffic and Related Self-driven Many-particle Systems [Article] // Reviews of Modern Physics. - 2001. - 4 : Vol. 73. - pp. 1067-1141.

Helbing Dirk Survival Analysis, Master Equation, Efficient Simulation of Path-Related Quantities, and Hidden State Concept of Transitions [Book Section] // Social Science Microsimulation. - [s.l.] : Springer- Verlag, 1995.

Herman R [et al.] Traffic Dynamics: Analysis of Stability in Car Following [Article] // Operations Research. - 1958. - 1 : Vol. 7. - pp. 86-106.

Ilachinski Andrew Cellular Automata: A Discrete Universe [Book]. - [s.l.] : World Scientific, 2001.

Ioannou P A and Chien C C Autonomous intelligent cruise control [Journal] // IEEE Transactions on Vehicular Technology. - 1993. - 4 : Vol. 42. - pp. 657-672.

Jensen H J Self-Organized Criticality: Emergent Complex Behavior in Physical and Biological Systems [Book]. - [s.l.] : Cambridge Lecture Notes in Physics, 1998.

Johnson Steven Emergence: The connected lives of ants, brains, cities and software [Book]. - [s.l.] : Scribner, 2001.

Kerner B S and Konhauser P Cluster effect in initially homogeneous traffic flow [Journal] // Physical Review E. - 1993. - 4 : Vol. 48. - pp. 2335-2338.

Kesting A [et al.] Jam-avoiding adaptive cruise control (ACC) and its impact on traffic dynamics [Book Section] // Traffic and Granular Flow / ed. Schadschneider A [et al.]. - Berlin : Springer, 2005.

Koshi M, Iwasaki M and Ohkura I Some Findings and an Overview of Vehicular Flow Characteristics [Conference] // 8th International Symposium on Transportation and Traffic Theory. - Toronto : [s.n.], 1983.

Kraaslan U, Varaiya P and Walrand J Two proposals to improve freeway traffic flow [Conference] // American Control Conference. - 1991.

Kuhne Reinhart Foundations of Traffic Flow Theory I: Greenshields' Legacy - Highway Traffic [Conference] // AHB45 Committee on Traffic Flow Theory & Characteristics. - [s.l.] : Transportation Research Board, 2008.

Lee H Y, Lee H-W and Kim D Dynamic States of a Continuum Traffic Equation with On-ramp [Article] // Physical Review E. - 1999. - 5 : Vol. 59. - pp. 5101-5111.

Lighthill M J and Whitham G B On Kinematic Waves II: A Theory of Traffic Flow on Long Crowded Roads [Article] // Proceedings of the Royal Society of London. Series A, Mathematical and Physical Sciences. - 1955. - 1178 : Vol. 229. - pp. 317-345.

Ludmann J Der 'Intelligente Tempomat'- eine Analyse mit dem Simulationsprogramm PELOPS [Conference]. - 1995.

Mahnke R and Kaupuzs J Stochastic theory of freeway traffic [Journal] // Physical Review E. - 1999. - 1 : Vol. 59. - pp. 117-125.

Mahnke R and Pieret N Stochastic master-equation approach to aggregation in freeway traffic [Journal] // Physical Review E. - 1997. - 3 : Vol. 56. - pp. 2666-2671.

Mahnke R, Kaupuzs J and Frishfelds V Nucleation in physical and nonphysical systems [Journal] // Atmospheric Research. - 2003. - Vol. 65. - pp. 261-284.

Malamud B D, Morein G and Turcotte D L Forest Fires: An Example of Self-Organized Critical behavior [Journal] // Science. - 1998. - 5384 : Vol. 281. - pp. 1840-1842.

Mason A D and Woods A W Car-following Model of Multispecies systems of Road Traffic [Article] // Physical Review E. - 1997. - 3 : Vol. 55. - pp. 2203-2214.

May Adolf D Traffic Flow Fundamentals [Book]. - [s.l.] : Prentice-Hall, Inc., 1990.

Miller M A, Doye J P K and J Wales D Structural relaztaion in atomic cluster: Master equation dynamics [Journal] // Physical Review E. - 1999. - 4 : Vol. 60. - pp. 3701-3718.

Morell E, Benz Th and Ludmann J AICC Assessment [Conference] // 1st World Congress on Intelligent Transportation Systems. - Paris : [s.n.], 1994.

Nagatani T The Physics of Traffic Jams [Article] // Rep. Prog. Phys.. - 2002. - Vol. 65. - pp. 1331-1386.

Nagel K and M Schreckenberg A Cellular Automaton Model for Freeway Traffic [Article] // Journal de Physique I. - 1992. - 12 : Vol. 2.

Nagel K and Paczuski M Emergent traffic jams [Journal] // Physical Review E. - 1995. - 4 : Vol. 51. - pp. 2909-2918.

Newell G F Nonlinear effects in the Dynamics of Car Following [Article] // Operations Research. - 1961. - 2 : Vol. 9. - pp. 209-229.

Nicolis G and Prigogine I Self-organization in Nonequilibrium Systems [Book]. - New York : John Wiley & Sons, Inc., 1977.

Paczuski M and Nagel K Self-organized Criticality and 1/f Noise in Traffic [Journal]. - [s.l.] : ArXiv Condensed Matter ePrints, 1996.

Paveri-Fontana S.L. On Boltzmann-like Treatments of Traffic Flow: A Critical Review of the Basic Model and an Alternative Proposal for Dilute Traffic Analysis [Article] // Transportation Research. - 1975. - Vol. 9. - pp. 225-235.

Payne H J FREFLO: A macroscopic Simulation Model for Freeway Traffic [Article] // Transportation Research Record. - 1979. - 722. - pp. 68-77.

Philips W F A Kinetic Model for Traffic Flow with Continuum Applications [Article] // Transport Planning and Technology. - 1979. - Vol. 5. - pp. 131-138.

Pipes L A An Operational Analysis of Traffic Dynamics [Article] // Journal of Applied Physics. - 1953. - 3 : Vol. 24. - pp. 274-281.

Prehofer C and Bettstetter C Self-organization in communication networks: principles and design paradigms [Article] // IEEE Communications Magazine. - 2005. - 7 : Vol. 43. - pp. 78-85.

Prigogine I. and Andrews F.C. A Boltzmann-like Approach for Traffic Flow [Article] // Operations Research. - 1960. - 6 : Vol. 8. - pp. 789-797.

Prigogine I. and Herman R. Kinetic Theory of Vehicular Traffic [Book]. - New York : Elsevier, 1971.

Prigogine Ilya Order out of chaos [Book]. - [s.l.] : Bantam, 1984.

Robert C P: Casella, G Monte Carlo statistical methods [Book]. - [s.l.] : Springer, 2004.

Schadschneider A and Schreckenberg M Traffic Flow Models with 'slow-to-start' Rules [Article] // Annalen der Physik. - 1997. - 7 : Vol. 509. - pp. 541-551.

Seiler P, Song B and Hedrick J K Development of a collision avoidance system [Journal] // SAE SPEC PUBL. - 1998. - Vol. 1332. - pp. 97-103.

Seiler Pete, Pant Aniruddha and Hedrick Karl Disturbance Propogation in Vehicle Strings [Journal] // IEEE Transactions on Automatic Control. - 2004. - 10 : Vol. 49.

Shladover S E Potential freeway capacity effects of Advanced Vehicle Control Systems [Conference] // 2nd International Conference on Applications of Advanced Technologies in Transportation Engineering. - Minneapolis, Minnesota : [s.n.], 1991.

Shrank D L and Tomax T J The 2007 Urban Mobility Report [Report]. - [s.l.] : Texas Transportation Institute, 2007.

Strogatz S Nonlinear Dynamics and Chaos: with applications to physics, biology, chemistry and engineering [Book]. - [s.l.] : De Capo Press, 2000.

Sugiyama Y [et al.] Traffic jams without bottlenecks - experimental evidence for the physical mechanism of the formation of a jam [Journal] // New Journal of Physics. - 2008. - Vol. 10.

Treiber M, Hennecke A and Helbing D Microscopic Simulation of Congested Traffic [Book Section] // Traffic and Granular Flow '99. - : Springer, 1999.

Treiterer J and Myers J The hysteresis phenomenon in traffic flow [Conference] // Sixth Symposium on Transportation and Traffic Flow Theory. - [s.l.] : Elsevier, 1974.

Vahidi A and Eskandarian E Research advances in intelligent collision avoidance and adaptive cruise control [Journal] // IEEE Transactions on Intelligent Transportation systems. - 2003. - 3 : Vol. 4. - pp. 143-153.

van Arem B [et al.] An assessment of the impact of Autonomous Intelligent Cruise Control [Report]. - Netherlands : [s.n.], 1995.

Varaiya P Smart cars on smart roads: problems of control [Journal] // IEEE Transactions on Automatic Control. - 1993. - 2 : Vol. 38. - pp. 195-207.

Verlinde E The master equation of string theory [Journal] // Nuclear Physics B. - 1992. - 1-2 : Vol. 381. - pp. 141-157.

Wang J [et al.] Normal Deceleration Behavior of Passenger Vehicles at Stop Sign-Controlled Intersections Evaluated with In-Vehicle Global Positioning System Data [Journal] // Transportation Research Record: Journal of Transportation Research Board. - [s.l.] : Transportation Research Board of the National Academies. - 1937. - pp. 120-127.

Weidlich Wolfgang and Braun Martin The master equation approach to nonlinear eonomics [Journal] // Journal of Evolutionary Economics. - [s.l.] : Springer, 1992. - 3 : Vol. 2. - pp. 233-265.

Whitham G B Exact Solutions for a Discrete System Arising in Traffic Flow [Article] // Proceedings of the Royal Society of London, Series A. - 1990. - 1874 : Vol. 428. - pp. 49-69.

Zhabotinsky Anatol M Bellousov-Zhabotinsky Reaction [Online] // Scholarpedia. - 2007. - November 3, 2009. - http://www.scholarpedia.org/article/Belousov-Zhabotinsky_reaction.

Zhou J and Peng H String Stability Conditions of Adaptive Cruise Control Algorithms [Conference] // IFAC symp.on "Advances in Automotive Control". - 2004.

Zhou Jing and Peng Hui Range Policy for Adaptive Cruise Control Vehicles for Improved Flow Stability andString Stability [Journal] // IEEE Transactions on Intelligent Transportation Systems. - 2004. - 2 : Vol. 6. - pp. 229-237.

Zwaneveld P J and van Arem B Traffic effects of automated vehicle guidance systems [Report]. - [s.l.] : Department of Traffic and transport, 1997.